



foundations

Article

A Fundamental Solution of the Hubble Tension

Hans-Otto Carmesin



<https://doi.org/10.3390/foundations6010007>

A Fundamental Solution of the Hubble Tension

Hans-Otto Carmesin ^{1,2,3} 

¹ Fachbereich 1 for Physics and Electrical Engineering, Bremen University, 28359 Bremen, Germany; carmesil@uni-bremen.de; Tel.: +49-(0)4141-52270

² Studienseminar Stade, Bahnhofstr. 5, 21682 Stade, Germany

³ Gymnasium and Observatory Athenaeum, Harsefelder Straße 40, 21680 Stade, Germany

Abstract

Einstein derived the expansion of space ever since the Big Bang started and introduced the possible cosmological constant Λ . The expansion of space and the present-day expansion rate H_0 , the Hubble constant, has been discovered by Hubble. Perlmutter discovered the positive value of Λ , and Zeldovich showed that Λ corresponds to the energy density u_{DE} of space. Lamb and Retherford as well as Casimir provided evidence for the idea that u_{DE} might be based on quanta, and Riess et al. provided evidence that H_0 is an idealization. In this paper, using the hypothetico-deductive method with very founded hypotheses, these two pieces of evidence are confirmed in a very founded and precise manner. Thereby, neither a fit is executed, nor a postulate, nor an unfounded hypothesis is proposed.

Keywords: relativity; cosmology; dark energy; H_0 + tension; unification; quantum physics; gravity

1. Introduction

The properties of space are essential for theories, see, e.g., Newton [1], Maxwell [2], Einstein [3], Minkowski [4], Einstein [5], Hilbert [6], Einstein [7], Hubble [8], Perlmutter [9], Zeldovich [10], Lamb and Retherford [11], Casimir [12], Riess et al. [13]. Thereby, outer space is a relatively ideal form of space in the universe, as outer space is hardly disturbed by molecules or other objects. Hereby, the universe consists of space and of the objects in space.

Moreover, the properties of space are important for applications such as space navigation, see, for instance, Soffel [14], telecommunication, quantum cryptography or quantum computer networks.

In order to understand space, it is essential to understand that space has a nonzero energy density u_{DE} or u_{Λ} . It has essentially been proposed by [7] with his cosmological constant Λ . Its value has been measured by Perlmutter et al. [9], and later by Riess and others [15], and with a different method by Smoot [16].

Furthermore, space was not given in advance. Instead, space expanded from the Big Bang until today, and space will expand in the future; see Friedmann [17], Wirtz [18], and more completely by Lemaître [19], and with convincing observation by Hubble [8], and in a textbook by Hobson et al. [20], and from an elementary particle point of view by Workman and others [21], and by very precise observation of early universe structures by Planck Collaboration [22]. Thereby, the measurable present-day rate H_0 of increase of the space exhibits a problem, the H_0 -tension: measurements provide different values of H_0 at the 5σ confidence level, for very precise observation of late universe structures, see Riess and others [13].



Academic Editors: Carlo Cafaro and Charalampos Moustakidis

Received: 12 November 2025

Revised: 8 January 2026

Accepted: 26 January 2026

Published: 2 March 2026

Copyright: © 2026 by the authors. Licensee MDPI, Basel, Switzerland. This article is an open access article distributed under the terms and conditions of the [Creative Commons Attribution \(CC BY\) license](https://creativecommons.org/licenses/by/4.0/).

This problem is explained here at the level of first principles and a founded and critically reflected scientific method; see Sections 1.1 and 1.1.1.

Firstly, an idealization of space is identified with help of a paradox. The idealization is that in present-day science space is a single entity. With the help of a founded derivation, this idealization is overcome: homogeneous space is a stochastic average of indivisible volume portions.

Secondly, a volume dynamics is derived for these volume portions.

Thirdly, the quantum postulates, gravity, and the Local Formation of Volume (LFV) are derived from this volume dynamics.

Fourthly, based on these founded and derived dynamical processes, and for the case of the homogeneous universe, the energy density of volume is deduced. For that case, this energy density is called u_{vol} . It is in accurate concordance with the observed value of the early universe, which was very homogeneous. Moreover, for this homogeneous case, the corresponding H_0 value is identified, in precise accordance with observation.

Of course, the universe is heterogeneous. Accordingly, the heterogeneity is analyzed in addition to the homogeneous universe. Consequently, the H_0 value of the late universe, which is very heterogeneous, is derived. This result is in accurate concordance with observation.

These results provide very convincing evidence for the concept that homogeneous space is a stochastic average of indivisible volume portions. Moreover, these results represent a very clear evidence that the H_0 tension is explained by the gradual evolution of heterogeneity in the universe. These two fundamental insights improve the present-day model of cosmology, the Λ CDM model. Additionally, these findings can be applied to space navigation and exploration; see Carmesin [23,24].

1.1. Hypothetico-Deductive Method

In this paper, the results are obtained by the hypothetico-deductive method. That method is very founded and broadly accepted; see original research by Popper [25,26], and see a general epistemological view by Niiniluoto, Sintonen and Wolenski [27]. The used hypotheses have already been tested by many experiments and scientists. This is shown by corresponding citations. Therefore, these very founded hypotheses will not be tested again in the present investigation. These very founded hypotheses are used as a basis for derivations in the hypothetico-deductive method. Moreover, these hypotheses are explained with their mutual logical connections. For these reasons, these hypotheses are explained in paragraphs, and these hypotheses are not expressed as usual hypotheses that have to be tested in the future. Hereby, the following very founded hypotheses are used:

1.1.1. Used Very Founded Hypotheses

In this section, the hypotheses are presented that are used in the hypothetico-deductive method. Thereby, these hypotheses are very founded. Therefore, the risk of failure is very small.

(1) The space that can be observed in the whole volume V , ranging from Earth to the light horizon, is isotropic and homogeneous at this universal scale. Local heterogeneities are possible, for instance near a mass M ; see Schwarzschild [28], see observation of space by Dyson, Eddington and Davidson [29], and see observation at Earth's ground by [30]. This has been observed in a very precise manner; see Planck Collaboration [22].

(1.1) Moreover, there is natural space that is very homogeneous and isotropic at small scales. For instance, natural space is very homogeneous and isotropic in a void; see Zeldovich, Einasto and Shandarin [31], Contarini et al. [32], and

natural space was very homogeneous and isotropic in the early universe; see Planck Collaboration [22].

(1.2) Furthermore, in the heterogeneous universe, natural space can exhibit slight heterogeneity, additionally. For instance, in the heterogeneous universe, Abbott et al. [33] observed the process of merging of two black holes. For that observation, gravitational waves had been utilized. These gravitational waves can be interpreted as coherent states that cannot be emitted in a natural homogeneous universe without heterogeneity, as only an appropriate heterogeneity can emit coherent states.

(2) Additionally, the space in (1) has a positive energy density u_{DE} . Hereby, the subscript *DE* abbreviates dark energy. It describes the energy E of a respective volume V in part (1), divided by this volume:

$$u_{DE} = \frac{E}{V}. \tag{1}$$

This energy density u_{DE} has been discovered by Perlmutter et al. [9], later by Riess and others [15], and with help of the CMB by Smoot [16].

(3) In general, for each object, including the space in (1), the energy-speed relation of special relativity theory (SRT) holds, see Einstein [3], Hobson et al. [20]: In general, a body that has an energy E , can have a velocity \vec{v} relative to a mass m_{ref} , which is used as a reference. Its absolute value is called speed $v = |\vec{v}|$. In particular, at $v = 0$, the energy is called rest energy E_0 . The energy speed relation of SRT is as follows:

$$E_0^2 = E^2 \cdot \left(1 - \frac{v^2}{c^2}\right) \tag{2}$$

In the case $v < c$, the relation has the following equivalent form:

$$E^2 = \frac{E_0^2}{1 - \frac{v^2}{c^2}} \tag{3}$$

Hereby, and in the following, the velocity is determined relative to an adequate coordinate system of relativity theory, for details, see Section 1.1.5.

(4) Moreover, each volume or volume portion ΔV of space in (1) has zero rest energy E_0 , and it has zero rest mass $m_0 = E_0/c^2$.

$$m_0(V) = 0 = E_0(V). \tag{4}$$

This is shown in Section 1.1.2.

(5) In a process of increase in volume or space in (1), the dark energy density u_{DE} in (2) is a nonzero constant, whereby only very small variations might occur. This approximate constancy has been observed for the expansion of the universe, see an early universe observation by Planck Collaboration [22], and a late universe observation by Riess et al. [13]. Additionally, that constancy has been proposed by general relativity theory and cosmology, see a first analysis by Einstein [7], a follow-up theoretical study by Friedmann [17], a more general theory by Lemaître [19], and a textbook by Hobson et al. [20]. Furthermore, the value of u_{DE} is derived here, and the results are additional evidence for this approximate constancy.

The above very founded hypotheses (1)–(5) will be used for deductions in this paper.

1.1.2. Why Volume Has No Rest Mass

In this section, it is shown that volume has zero rest mass m_0 .

Near a mass M , there occurs additional volume δV , see Section 1.1.4 or Figure 1. If that additional volume would have a rest energy $m_0(\delta V) > 0$, then there would be an additional rest mass m_0 near each mass M . Such an additional m_0 has never been observed. This can be confirmed in a textbook by Landau and Lifschitz [34], or by reported research Workman et al. [21], Planck Collaboration [22], Zogg [35]. For instance, if there were such an additional rest mass m_0 , then this m_0 would modify the orbits of the GPS satellites, and this would have been observed, but this has not been observed. Consequently, additional volume δV has no rest mass.

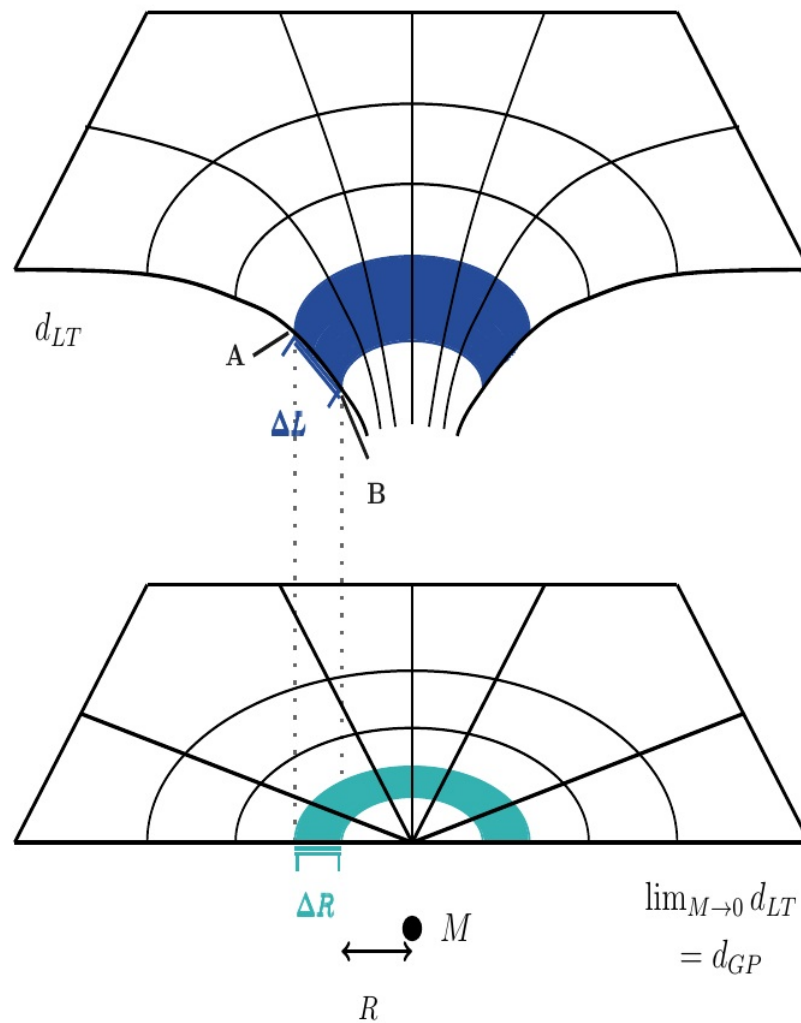


Figure 1. Nearby a mass M , the radial difference ΔL is enhanced relative to the difference ΔR . The latter corresponds to the case $M = 0$. Note that the difference ΔL is measured as a light travel distance d_{LT} , and the difference ΔR is measured as a gravitational parallax distance d_{GP} , see Carmesin [23,36]. Each event is represented in a d_{LT} based map and in a d_{GP} based map, and the two representations of the event are connected by a dotted line. Similarly, each shell can be represented in a d_{LT} based map (blue) and in a d_{GP} based map (green).

Moreover, the additional volume near a mass is the same type of volume as common volume that occurs without any mass. This is confirmed by the observation that only one type of volume exists, it is documented in Workman et al. [21], or also in Planck Collaboration [22], Casimir [12], Zeldovich [10], Perlmutter et al. [9]. Therefore, in general, volume has no rest mass.

1.1.3. Mass Causes an Increase in Radial Light Travel Distance

In this section, it is shown that a mass M causes an increase in the radial distance R to M . This increase occurs at each radial difference ΔR ; see Figure 1.

For instance, near a mass M , an original (for the case of $M = 0$) radial difference ΔR is increased by $\sqrt{g_{RR}}$. Note that it is the root of the tensor element g_{RR} . The increased value is ΔL , see Figure 1,

$$\Delta L = \Delta R \cdot \sqrt{g_{RR}}. \tag{5}$$

Hereby, the value ΔL can be measured as a light travel distance d_{LT} . It is described by Hobson et al. [20]. Similarly, the original value ΔR is measurable. For it, a pair of hand leads can be used. That distance measure is named *gravitational parallax distance (in the context of two hand leads)*, see Carmesin [23,36].

As a consequence of general relativity, see Einstein [5], Hilbert [6], Hobson et al. [20], at each radial coordinate (or gravitational parallax distance) R , the radial element g_{RR} of the metric tensor is a function of the Schwarzschild [28] radius R_S :

$$g_{RR} = \frac{1}{1 - \frac{R_S}{R}}, \quad \text{with} \quad R_S = \frac{2G \cdot M}{c^2} \tag{6}$$

These relations are in accurate concordance with observed values. This is documented by Dyson, Eddington and Davidson [29], and for the case of an observation on Earth’s ground by Pound and Rebka [30], or in an overview by Will [37].

According to the Hacking [38] criterion of reality, this increase in radial light travel distance ΔL is real, as it can be manipulated as follows: The mass M can be increased, and this causes an increase in radial light travel distance ΔL , see Equations (5) and (6).

Moreover, the gravitational parallax distance ΔR is real, as it can be manipulated as well: For instance, in Figure 1, ΔR is the spatial shortest difference between two locations A and B . If B moves towards A , then ΔR decreases. Next, the corresponding volume is analyzed:

1.1.4. Mass Causes an Increase in Volume

In this section, the following is shown: Nearby a mass M , the increase in a radial length ΔL causes an enhanced volume.

Without loss of generality, a portion of volume $\Delta V_R = \Delta R \cdot \Delta x \cdot \Delta y$ is used with $|\Delta R| = |\Delta x|$ and $|\Delta R| = |\Delta y|$.

Near a mass M , ΔR (radial distance) is enhanced to the respective light travel distance ΔL by the factor $\sqrt{g_{RR}}$, while Δx and Δy are not changed by M . Consequently, the volume ΔV_R is increased to the respective volume ΔV_L by a factor $\sqrt{g_{RR}}$, see Equation (5):

$$\Delta V_L = \Delta L \cdot \Delta x \cdot \Delta y = \Delta R \cdot \Delta x \cdot \Delta y \cdot \sqrt{g_{RR}} = \Delta V_R \cdot \sqrt{g_{RR}}. \tag{7}$$

The difference of the volume ΔV_R measured with the gravitational parallax distance and the volume ΔV_L measured with the light travel distance is called *additional volume* δV :

$$\delta V := \Delta V_L - \Delta V_R. \tag{8}$$

The ratio $\delta V / \Delta V_L$ is called *relative additional volume* ε_L :

$$\varepsilon_L := \frac{\delta V}{\Delta V_L}. \tag{9}$$

1.1.5. On the Adequate Coordinate Systems

In the theory of relativity, a time interval t_{sat_E} of a clock onboard a satellite E and a time interval t_{sat_F} of a clock onboard a satellite F exhibit the phenomenon of kinematic time dilation. Relativity theory states: Between two events A and B , a clock in a laboratory coordinate system exhibits a time t_{lab} , a clock onboard the satellite E exhibits a time t_{sat_E} , and a clock onboard the satellite F exhibits a time t_{sat_F} as follows:

$$t_{lab} = t_{sat_E} \cdot \frac{1}{\sqrt{1 - v_{E,lab}^2/c^2}} \quad \text{and} \quad t_{lab} = t_{sat_F} \cdot \frac{1}{\sqrt{1 - v_{F,lab}^2/c^2}}. \quad (10)$$

Hereby, $v_{E,lab} = |\vec{v}_{E,lab}|$ is the absolute value of the velocity (speed) of the satellite E with respect to the laboratory coordinate system (CS), and $v_{F,lab} = |\vec{v}_{F,lab}|$ is the absolute value of the velocity (speed) of the satellite F with respect to the CS. However, the International Astronomical Union (IAU) realized that relativity theory does not provide information about the choice of an adequate laboratory coordinate system or laboratory frame. Such information about the frame is essential for predicting the times shown by the above clocks, and it is important for space navigation. The IAU called this lack of information the problem of finding an adequate coordinate system (ACS), see Soffel [14].

The problem of finding an adequate coordinate system (ACS) has been solved [23,24,39]. Thereby, for each point P in the universe, the *adequate coordinate system* (ACS) is characterized by the following derived properties:

- (1) An ACS exists.
- (2) The ACS has a uniquely determined velocity $\vec{v}_{ACS,CS}$, relative to an arbitrarily chosen coordinate system CS .
- (3) $\vec{v}_{ACS,CS}$ can be measured, and procedures of measurement are provided.
- (4) $\vec{v}_{ACS,CS}$ can be predicted and calculated, and procedures for it are provided.
- (5) The equations of time dilation in Equation (10), as well as the energy speed relation in Equations (2) and (3) hold, when the ACS is used. Moreover, the typical results of relativity hold, when the ACS is used.
- (6) There exists a universal null of the fractional kinematic difference of time

$$\delta t_{kin,frac} := \frac{t_{sat_E} - t_{lab}}{t_{lab}} \leq 0, \quad (11)$$

whereby the chosen laboratory coordinate system is equal to the ACS.

In this paper, the ACS is used. Therefore, the derived results have clearly defined conditions.

1.2. Observed Energy Density of Volume

In astrophysical space, Perlmutter et al. [9], and later Riess et al. [15] observed the acceleration of the universe's expansion rate. As a consequence of the Friedmann Lemaître equation (FLE), empty space has a positive energy density. This is documented in Friedmann [17], together with Lemaître [19], and in the textbook Hobson et al. [20], and with a detailed analysis in Carmesin [40]. It is called density u_Λ , corresponding to the cosmological constant Λ , or to the density u_{DE} of the dark energy density [7,10,20,41]. An actual value has been observed on the basis of the CMB (Cosmic Microwave Background), documented by [22,23,40]:

$$u_{\Lambda,obs} = 5.133^{+0.2432}_{-0.2432} \cdot 10^{-10} \frac{\text{J}}{\text{m}^3} = u_{DE,obs}. \quad (12)$$

2. Problem of the Hubble Tension

Here, we summarize a very interesting problem of modern physics. In particular, this problem is a discrepancy between two observed values that should be equal according to the Λ CDM model of present-day physics, see, e.g., Hobson et al. [20]. Consequently, this discrepancy falsifies the Λ CDM model. In general, according to the hypothetico-deductive method, a solution to such a falsification problem provides the chance to improve concepts of physics [25,26]. In this paper, we will use this problem in order to develop founded and essential improvements of present-day physics.

Hubble [8] discovered the present-day expansion rate of space, the Hubble constant H_0 . In general, the Hubble constant is measured by utilizing signals emitted at an instant of time t_{em} or a respective redshift z_{em} , documented in Hobson et al. [20].

Penzias and Wilson [42] observed the CMB (Cosmic Microwave Background). It has been emitted at $t_{em} = 380,000$ years (after the Big Bang). Utilizing that radiation, the Planck Collaboration [22] observed the following:

$$H_{0,obs,CMB} = 66.88^{+0.92}_{-0.92} \frac{\text{km}}{\text{s} \cdot \text{Mpc}} \tag{13}$$

Hereby, the redshift of emission is $z_{em} = z_{CMB} = 1090.3 \pm 0.41$. In the measurement, the so-called T-T correlation (T abbreviates temperature) is utilized [22] ([table 2, column 1]).

As another example, Riess et al. [13] utilized signals from nearby galaxies (with Ia supernovae) emitted at ca. $z = 0.055$. and observed

$$H_{0,obs,near,Ia} = 73.04^{+1.01}_{-1.01} \frac{\text{km}}{\text{s} \cdot \text{Mpc}}. \tag{14}$$

Thereby, many galaxies with different redshift values z_{em} have been observed. Accordingly, the redshift z_{em} of emission is described by the average of the redshift values of the observed [13] galaxies, $\langle z \rangle$ is equal to $= 0.055$.

Riess et al. [13] discovered a difference $H_{0,obs,near,Ia} - H_{0,obs,CMB}$. It is named Hubble tension or H_0 tension, documented in Planck Collaboration [22]. That discrepancy is at the five σ confidence level. Consequently, that discrepancy can be regarded and named as a scientific result [13]. This result falsifies the Λ CDM model, as this model states that the value of H_0 should not depend on the redshift value of observed objects. Based on such a falsification of a model, that model can be interpreted as an idealization, see Shech [43], Song et al. [44]. Consequently, the idealization of the Λ CDM model is identified:

The Hubble tension falsifies the Λ CDM model. Accordingly, the Λ CDM model is an idealization.

Therefore, the Hubble tension or H_0 tension is a founded scientific problem. A fundamental solution to this problem is derived in this paper. Hereby, no fit is executed, no unfounded hypothesis is proposed, and a precise accordance with observation is achieved, and predictions are derived.

Moreover, the value $H_{0,obs,CMB}$ describes a nearly homogeneous universe, since the early universe was nearly homogeneous [22]. In contrast, $H_{0,obs,near,Ia}$ is a H_0 -value of the late universe, as the observed supernovae occurred in the late universe. Additionally, $H_{0,obs,near,Ia}$ is a value of the heterogeneous and late universe [22,45,46].

As the Hubble constant describes the expansion rate, we analyze the properties of space in more detail. For this, in Section 3, we show that the present-day view of space includes a paradox, the so-called space paradox. Moreover, we derive a solution to that space paradox. With it, we will explain and derive the H_0 tension. This solves the respective H_0 -tension problem.

3. Space Paradox

In general, a paradox provides the chance to develop a deep insight [47]. In this section, we will derive a paradox, and we will use it in order to develop a deep insight.

In the following, the space, that can be observed in the whole volume V ranging from Earth to the light horizon, is considered. For instance, this space has been observed [22].

In physical concepts that are commonly used in the present-day, the space with its volume V is considered as a single entity, see, e.g., Newton [1], Maxwell [2], Einstein [5,17], Lemaître [19] and Planck Collaboration [22].

That space has a positive energy density u_{DE} , see Equation (1):

$$u_{DE} = \frac{E}{V}. \tag{15}$$

As a consequence of time dilation, the volume V with its energy E of space, velocity \vec{v} and speed $|\vec{v}| = v$, obey the energy–speed relationship, see Equations (2) and (3)

$$E^2 = \frac{E_0^2}{1 - \frac{v^2}{c^2}} \quad \text{or} \quad E^2 \cdot \left(1 - \frac{v^2}{c^2}\right) = E_0^2. \tag{16}$$

As the energy density is nonzero, the energy E is nonzero. Thus, the above relationship can be divided by E^2 . Therefore, the following form of the energy–momentum relationship holds:

$$1 - \frac{v^2}{c^2} = \frac{E_0^2}{E^2}. \tag{17}$$

As a consequence of the zero rest energy E_0 of V , see Equation (4), the term $\frac{E_0^2}{E^2}$ in Equation (17) is zero. Consequently, the volume V with the energy E has velocity c .

$$v = c = v(V) = v(E). \tag{18}$$

3.1. The Paradox

In physical concepts that are commonly used in present-day, the volume is considered as a single entity, see, e.g., Newton [1], Maxwell [2], Einstein [5], Friedmann [17], Lemaître [19], Hobson et al. [20], Planck Collaboration [22]. In such a concept of volume, the whole volume would move parallel to some unit direction vector \vec{e}_v and with the speed of light, $\vec{v} = c \cdot \vec{e}_v$, see Equation (18).

However, that velocity \vec{v} would break the isotropy of space observed at a universal scale [22]. This is a contradiction. In general, a paradox is a contradiction, whereby the solution creates a fundamental insight [47]. The above contradiction is called the *space paradox*. It is solved next:

3.2. A Solution of the Space Paradox in Natural Homogeneous Space

In this section, the paradox is solved in three separate steps: The source of the paradox is identified in item (1). Therefrom, a solution of the paradox is developed in item (2). And the validity of the solution is confirmed in item (3).

(1) The space paradox has five premises: There are four founded premises about space and its volume V , see Section 1.1, parts (1)–(4), part (5) is not used here: isotropy, the positive dark energy density, the energy–speed relation of SRT (which is correct in the used ACS, see Section 1.1.5), and the zero rest energy E_0 . In addition, there is one hardly founded premise (see the beginning of Section 3.1): the concept of space as a single entity. Therefore, space is not a single entity.

As space is not a single object, it must consist of many parts of the volume V . These parts δV are analyzed next. Thereby, a part of the space with its volume V is called a *volume portion (VP)*.

Hereby, parts of the volume with at least one local maximum of volume are analyzed. For each part, one such maximum is used in order to localize that part δV . Such a part is called a localized VP.

Since the energy and volume of space have the speed $v = c$, the above parts δV must have the same speed. For instance, each part δV_j has its speed

$$v_j = c. \tag{19}$$

In general, a part of volume is called volume portion.

(2) Next, the following question is analyzed (for a homogeneous universe and common density ρ_{hom} : Can such a part δV_j with $v_j = c$ consist of smaller parts δV_k ? Hereby, a usual density ρ_{hom} is a density below an ultrahigh critical density $\rho_{cr., symmetry\ breaking}$ at which the symmetry of space breaks in a phase transition. This can occur in a phase transition from space to matter in the Higgs [48] mechanism. Moreover, this can take place in a dimensional phase transition [36,40,49,50]. If such a part δV_j with $v_j = c$ of space would consist of smaller parts δV_k , then the following would be implied:

- (2.1) Each smaller part δV_k would have the speed $v_k = c$, as the energy and volume of space have the speed $v = c$.
- (2.2) Consequently, each part δV_k would have a velocity $\vec{v}_k = c \cdot \vec{e}_k$, with a direction vector \vec{e}_k of norm one.
- (2.3) As the considered universe is homogeneous (see, part (2)), there is no source that could provide a uniform direction for the direction vectors \vec{e}_k .
- (2.4) Hence, the velocity \vec{v}_j of the considered part δV_j with $v_j = c$ would be an average of the velocities \vec{v}_k . Thereby, as a consequence of the different direction vectors \vec{e}_k in part (2.3), the velocity \vec{v}_j would have an absolute value smaller than c , i.e., $|\vec{v}_j| = v_j < c$. This would contradict the speed $v_j = c$ in Equation (19).
- (2.5) Therefore, the parts δV_j with speeds $v_j = c$ cannot consist of smaller parts. This is the answer to the question in (2). This implies that the parts δV_j with $v_j = c$ are indivisible. Such a part δV_j with its speed $v_j = c$ is called *indivisible volume portion*, indivisible VP.

(3) Next, it is shown how the indivisible VPs solve the space paradox:

- (3.1) The energy and volume of space have the speed c , and the energy of space obeys $E^2 \cdot \left(1 - \frac{v^2}{c^2}\right) = E_0^2 = 0$, as space consists of indivisible VPs δV_j with the speed $v_j = c$.
- (3.2) Moreover, the velocities $\vec{v}_j = c \cdot \vec{e}_j$ of the indivisible VPs have stochastic direction vectors \vec{e}_j , that are distributed isotropically. Hence, these velocities average to zero.
- (3.3) As a consequence, space is isotropic at a universal scale, see Figure 2. In this manner, the space paradox is solved.

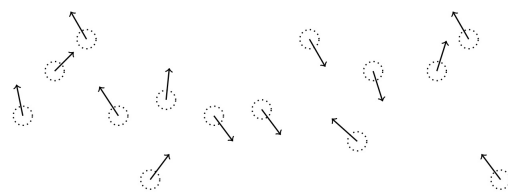


Figure 2. Volume portions δV_j (dotted) with speed $v_j = c$ (arrows with same length) of homogeneous space with different random (arrows with random directions) normalized direction vectors \vec{e}_j of the velocity $\vec{v}_j = c \cdot \vec{e}_j$. The average of the velocities \vec{v}_j is zero. This causes global isotropy of space consisting of rapidly moving volume portions. As a consequence, this solves the space paradox.

Therefore, we obtain the following deep insight, the stochastic property of space: In an isotropic homogeneous universe, space represents a stochastic average of many indivisible volume portions δV_j , each with the speed $v_j = c$. Hereby, the velocity vectors \vec{v}_j of the δV_j average to zero.

(4) Next, the solution is generalized to heterogeneous space: The early universe was very homogeneous and isotropic [22]. In the universe, the heterogeneity of the locations of mass increased gradually, and thereby the heterogeneity of space evolved gradually [23,36,46,51,52]. Therefore, the natural heterogeneous space is a slight variation of the natural homogeneous and isotropic space. Details of that variation will be derived in the solution of the Hubble tension below.

3.3. Examples of Parts of Space

In this section, the essential parts of natural space with volume V are analyzed.

- (1) Additional volume near a mass M : Near a mass M , there occurs additional volume δV , see Section 1.1.4. It is at rest relative to M . Moreover, in the vicinity of M , the ACS (see Section 1.1.5) [23,24,39] is nearly at rest at M . Consequently, the speed of the additional volume nearby a mass is clearly smaller than c , i.e., $v < c$. Each additional volume with a speed $v < c$ must be a stochastic average of the indivisible VPs δV_j with their speeds $v_j = c$, as space with its volume V consists of indivisible VPs δV_j with their speeds $v_j = c$. This is the case for homogeneous and isotropic space and for the case of heterogeneous space which is a slight variation of homogeneous and isotropic space.

Altogether, additional volume that is at rest in the vicinity of a mass M is a stochastic average of indivisible VPs.

- (2) Relative additional volume ϵ_L : In general, a VP δV is located within an underlying VP ΔV_L . The relative additional volume ϵ_L is the ratio of the VP δV with respect to its underlying VP ΔV_L , see Section 1.1.4:

$$\epsilon_L := \frac{\delta V}{\Delta V_L} = \frac{(\Delta L - \Delta R) \cdot \Delta x \cdot \Delta y}{\Delta L \cdot (\Delta x \cdot \Delta y)} = \frac{\Delta L - \Delta R}{\Delta L} = \frac{\delta L}{\Delta L} \tag{20}$$

with $\delta L := \Delta L - \Delta R$.

Thereby, the ratio $\frac{\delta L}{\Delta L}$ is usually interpreted as a tensor element, whereby the L -direction is the z -direction or the 3-direction:

$$\epsilon_{zz} := \frac{\delta z}{\Delta z} = \epsilon_{jj}, \quad \text{with } j = 3. \tag{21}$$

In general, a volume portion VP δV represents a change in an underlying VP ΔV , and this change represents a tensor element or tensor. Thereby, typically, the change in each VP ΔV has a quadrupolar structure. A dipolar structure is excluded, as volume cannot be negative. Therefore, each change in an underlying VP ΔV can be described by a tensor of rank two. It is called *change tensor* [23,36] ϵ_{ij} . In general, an element ϵ_{ij} of a change tensor is the ratio of the change δL_i and underlying length ΔL_j :

$$\epsilon_{ij} := \frac{\delta L_i}{\Delta L_j}. \tag{22}$$

Hereby, for each normalized direction vector \vec{e}_j , the underlying length ΔL_j is the sum of the original length ΔR_j and the change δL_j :

$$\Delta L_j := \Delta R_j + \delta L_j. \tag{23}$$

In general, indivisible VPs can have the structure of a change tensor as well, see Figure 3.

- (3) Gravitational wave: Without loss of generality, a gravitational wave (GW) can be described via [53]: It has an angular frequency ω . At a location, a GW has one propagation unit vector \vec{e}_z , and two transverse unit vectors \vec{e}_x and \vec{e}_y . There are two possible modes. In the first mode, the elongations are $\varepsilon_{xx} \cdot \cos(\omega t)$ and $\varepsilon_{yy} \cdot \cos(\omega t)$, with $\varepsilon_{xx} = -\varepsilon_{yy}$, see Figure 3. The second mode is equal to the first mode rotated by 45° around \vec{e}_z .

The elongations and the velocity of the gravitational wave can be measured with the help of a Michelson interferometer. For instance, Abbott et al. [33] measured the amplitude $\varepsilon_{xx,max} = 1 \cdot 10^{-21}$.

In the theory of waves, the above-observed gravitational wave is a wave with a coherence length that amounts to several wavelengths. Accordingly, a gravitational wave could be interpreted as a coherent state in the framework of quantum physics, if quantum physics is applicable.

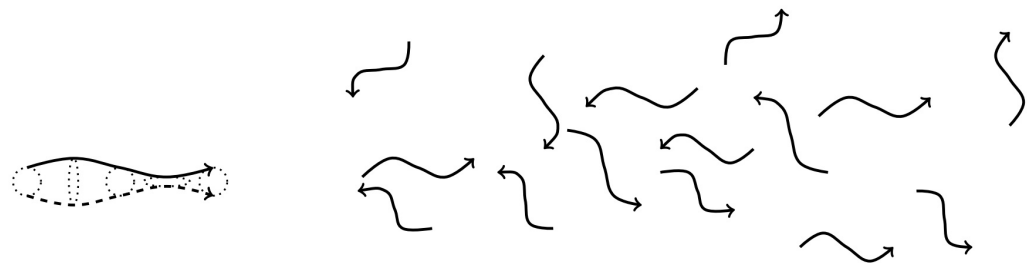


Figure 3. Volume portions (VPs) δV_j (marked by dotted lines or by wiggly lines with arrow) with speed $v_j = c$ with different velocities $\vec{v}_j = c \cdot \vec{e}_j$; In general, each VP can include a change as marked on the left. In principle, each VP δV_j can be characterized very precisely by that change. For instance, the change in a VP δV_j moves with its velocity \vec{v}_j , and typically, it has a quadrupolar structure (dotted lines). A dipolar structure is excluded, as volume cannot be negative. On the right, these changes are indicated by wiggly lines, for simplicity. The average of the velocities $\vec{v}_j = c \cdot \vec{e}_j$ is zero. This causes global isotropy of space consisting of volume portions with speeds $v_j = c$. Therefore, this solves the space paradox.

3.4. On Quantum Properties of an Indivisible VP

The indivisible VP in homogeneous space is very founded. According to this indivisibility, a minimal extension of an indivisible VP is estimated with the help of the Heisenberg [54] uncertainty relation in quantum physics:

In general, an indivisible VP can have very different forms, and matter or radiation can be placed in the VP. As an example, and as a very simple model, an indivisible VP is analyzed, that has the form of a ball with a radius ΔL , and contains no radiation or matter.

Consequently, the volume is

$$\Delta V_L = \frac{4\pi}{3} \Delta L^3. \tag{24}$$

Thus, the VP has the following energy:

$$\Delta E_L = \frac{4\pi}{3} \Delta L^3 \cdot u_{DE}. \tag{25}$$

As the VP has the speed $v = c$, the energy momentum relation of special relativity theory (SRT) provides the following momentum:

$$\Delta p_L = \frac{\Delta E_L}{c} = \frac{4\pi}{3} \Delta L^3 \cdot \frac{u_{DE}}{c}. \tag{26}$$

In the rest system of the VP, the momentum is zero, so that the standard deviation alias uncertainty of momentum is estimated by Δp_L . Similarly, the spatial standard deviation alias uncertainty of the indivisible VP is estimated by

$$\sigma_L = \Delta L. \tag{27}$$

The Heisenberg [54] uncertainty relation for these standard deviations is as follows:

$$\Delta p_L \cdot \Delta L \geq \frac{\hbar}{2}. \tag{28}$$

The estimated standard deviations in Equations (26) and (27) are inserted into the above uncertainty relation:

$$\frac{4\pi}{3} \Delta L^4 \cdot \frac{u_{DE}}{c} \geq \frac{\hbar}{2}. \tag{29}$$

This uncertainty relation is solved for the spatial uncertainty ΔL :

$$\Delta L \geq \sqrt[4]{\frac{3\hbar \cdot c}{8\pi \cdot u_{DE}}} = 3.957 \cdot 10^{-5} \text{ m}. \tag{30}$$

Altogether, the very particularly considered indivisible VP, which does not contain any matter or radiation, has a minimal spatial uncertainty of $\Delta L \approx 0.03957 \text{ mm}$.

3.5. Empirical Evidence for Indivisible Volume Portions

The derivation of indivisible VPs is based on isotropy at small scales. Accordingly, empirical evidence for indivisible VPs is of interest. Such evidence is presented in this section.

3.5.1. Estimated Time Uncertainty of Indivisible Volume Portions

In four-dimensional spacetime, the length ΔL of an indivisible VP is estimated by Equation (30). It is the standard deviation according to the Heisenberg [54] uncertainty relation. In four-dimensional spacetime, the corresponding time uncertainty Δt of an indivisible volume portion is estimated by the ratio of ΔL to c :

$$\Delta t_{\text{indivisible VP}} = \frac{\Delta L}{c} \geq \frac{3.957 \cdot 10^{-5} \text{ m}}{c} = 1.319 \cdot 10^{-13} \text{ s}. \tag{31}$$

For instance, for the case of an average time of one second, $\tau_{av} = 1 \text{ s}$, the fractional uncertainty is estimated as follows:

$$\Delta t_{\text{indivisible VP, frac}} \geq \approx 1.319 \cdot 10^{-13}. \tag{32}$$

3.5.2. Time Uncertainty of an Atomic Clock Using Gas

Many atomic clocks use gas atoms [55,56]. As these atoms move in natural space, and as an atom is extremely small relative to the estimated extension of an indivisible VP, the clock's uncertainty is greater than or equal to the uncertainty of an indivisible VP in homogeneous natural space, in general. Similarly, if an object moves within a ship, then the object's uncertainty is larger or equal to the ship's uncertainty, in general.

For the case of natural space consisting of indivisible VPs, the uncertainty of space is estimated by $\Delta t_{indivisible VP, frac}$ in Equation (32). Therefore, in the case of averaging one second,

$$\Delta t_{atomic gas clock, frac} \geq \Delta t_{indivisible VP, frac} \geq \approx 1.319 \cdot 10^{-13} \text{ s.} \tag{33}$$

In general, the uncertainty of a clock can be reduced by averaging during time τ_{av} . Thereby, according to statistics and according to observation, the uncertainty decreases by the factor $1/\sqrt{\tau_{av}}$ [55,57]. Empirical data show the following [55]: Atomic clocks that use gas atoms, which are not confined to any particular location or trajectory, and are averaged at most one second, $\tau_{av} \leq 1 \text{ s}$, exhibit time uncertainties larger than the estimated uncertainty of indivisible VPs in Equation (32). This provides evidence for the existence of indivisible VPs. Moreover, a control experiment is available:

3.5.3. Time Uncertainty of an Atomic Lattice Clock

In an atomic lattice clock, the used atoms are confined to the potential minima of a standing wave of laser light. Hereby, the standing wave, and the device that generates that wave, are large compared to the estimated size of an indivisible VP. As a consequence, these atoms do not move freely in an indivisible VP of homogeneous natural space, but in artificially generated potential minima. Therefore, the atomic lattice clock's uncertainty can be smaller than the estimated uncertainty of indivisible VPs in Equation (32). In fact, measurements show that this is clearly the case. There is even a local maximum of the uncertainty depending on the time τ_{av} of averaging [58]:

$$\Delta t_{atomic lattice clock, frac} \leq \Delta t_{maximum atomic lattice clock, frac} \approx 3 \cdot 10^{-16}. \tag{34}$$

This control experiment provides evidence for the following: The independence of the uncertainty of natural space and of indivisible VPs can provide a very small uncertainty of an atomic lattice clock.

$$\Delta t_{atomic lattice clock, frac} \ll \Delta t_{indivisible VP, frac} \tag{35}$$

4. Dynamics of Volume Portions

Here, a very valuable and insightful description of VPs is developed. With it, a very general differential equation (DEQ) of the dynamics of VPs is derived.

Here and in the following, mathematically, a VP could be arbitrarily small. Physically, the Heisenberg [54] relation of uncertainty is a lower limit of the standard deviation of a VP. A particular example is analyzed in Section 3.4.

4.1. Additional Volume

Here, the increase δV of the volume ΔV_R of a VP is analyzed. For it, the difference of the increased volume ΔV_L and the original volume ΔV_R of the VP is used:

$$\delta V := \Delta V_L - \Delta V_R \tag{36}$$

Hereby and in the following, a light travel distance ΔL is greater than or equal to the corresponding gravitational parallax distance ΔR , i.e., $\Delta L \geq \Delta R$, so the particular case without curvature is included. The above difference δV is called additional volume, see Section 1.1.4.

Similarly, as in Section 1.1.3, according to the Hacking [38] criterion, the enlarged volume ΔV_L and the additional volume δV are real, as they can be manipulated. In contrast, the original volume ΔV_R is an idealization corresponding to the idealization of flat space:

Each VP has a real additional volume δV and a real enlarged volume ΔV_L , according to the Hacking [38] criterion. In order to derive general laws of physics, this difference is normalized in the next section:

4.2. Relative Additional Volume

In general, for the purpose of a derivation of general laws of physics, it is valuable to use intensive quantities rather than extensive quantities [59]. In the present case of a VP, it is useful to utilize the ratio of its real additional volume δV to its real enlarged volume ΔV_L . Such ratios are formed and analyzed in detail in this section:

That ratio is called relative additional volume ε_L , see Equation (9):

$$\varepsilon_L := \frac{\delta V}{\Delta V_L}. \tag{37}$$

The relation to the metric tensor is achieved by inserting Equations (7) and (36) into Equation (37):

$$\varepsilon_L := \frac{\Delta V_L - \Delta V_R}{\Delta V_L} = 1 - \frac{\Delta V_R}{\Delta V_L} = 1 - \frac{1}{\sqrt{g_{RR}}}. \tag{38}$$

This is an example of the fact that curvature is describable by a metric tensor or, likewise, by the relative additional volume. Moreover, relative additional volume of a VP is real, as it is a ratio of real quantities of that VP: Each VP has a real relative additional volume ε_L .

Furthermore, the description with the additional volume is compatible with the volume portions that become necessary for the solution of the space paradox. In contrast, the metric tensor does not include the concept of volume portions, and it does not provide the dynamics of the volume portions. As a consequence, the description with the volume portions provides the additional possibility to derive the dynamics of volume portions. Of course, the metric tensor provides the description of time dilation directly. Volume portions can be described with the help of the Schwarzschild [28] metric. Thereby, a tensor element of the time $g_{tt} = \frac{1}{g_{RR}}$ is utilized. With it, an interval of coordinate time dt is transformed to an interval of own time $d\tau = dt \cdot \sqrt{g_{tt}}$ [20]. With help of the volume portions, the dynamics of volume portions is derived next:

4.3. Derivation of the Dynamics of Volume Portions

In this section, the dynamics of an arbitrary VP is described by its relative additional volume. The result is achieved with the help of calculus or standard analysis only. As a consequence, the dynamics of VPs derived here is very general.

Firstly, the applicability of calculus or standard analysis is investigated: Calculus or analysis is a mathematical tool, such as algebra and stochastics. Thereby, calculus or analysis does not include a prejudice about the continuity of space and time. The reason is that, in the present investigation, space is a stochastic average of VPs. Hereby, VPs will be characterized by eigenvalues with a spectrum of eigenvalues. This spectrum can turn out to be discrete, continuous or partially discrete and partially continuous. As calculus or analysis is used in this study, these fields of mathematics do not necessarily include a prejudice about the discreteness or continuity of space.

In contrast, an exclusion of calculus and analysis would include a prejudice about the discreteness or continuity of space.

In fact, the space paradox and the implied structure of space as a stochastic average of VPs already deduce an essential degree of discreteness of space. And it is important to investigate the amount of discreteness and continuity of these VPs in the following.

Moreover, in this paper, the physical reality of the used and deduced concepts is permanently tested with the help of the Hacking [38] criterion.

Secondly, the differential equation, DEQ, of VPs is derived: Each localized VP (see Section 3.2, part (1)) has a local maximum of its relative additional volume ε_L . It depends on the position vector \vec{L} as well as on time τ . An illustration is Figure 4, whereby the three-dimensional position vector is summarized by a position L . Altogether, a localized volume portion is describable by a term $\varepsilon_L(\tau, \vec{L})$ with a local maximum. If there should be several local maxima or a set of local maxima, then one local maximum can be chosen as a convention.

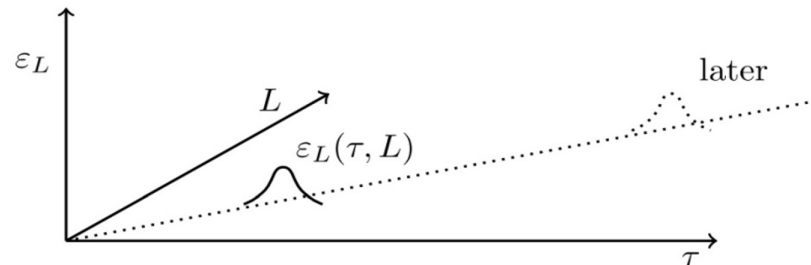


Figure 4. A VP with a relative additional volume $\varepsilon_L(\tau, L)$ with a local maximum is shown, depending on location L , and depending on time τ . Thereby, the location L summarizes the vector \vec{L} (in 3D space), so that the length of the path (dotted, for an indivisible VP, the path is a semiclassical idealization, correspondingly, the path is dotted) of the VP is described by L .

Calculus alias analysis imply: The local maximum of $\varepsilon_L(\tau, \vec{L})$ has zero slope. Consequently,

$$d\varepsilon_L(\tau, \vec{L}(\tau)) = 0. \tag{39}$$

Here, partial derivatives are utilized:

$$d\varepsilon_L(\tau, \vec{L}(\tau)) = \frac{\partial}{\partial \tau} \varepsilon_L(\tau, \vec{L}) \cdot d\tau + \frac{\partial}{\partial \vec{L}} \varepsilon_L(\tau, \vec{L}) \cdot d\vec{L} = 0. \tag{40}$$

The VP moves parallel to a corresponding direction unit vector \vec{e}_v of its velocity $\vec{v} = \frac{\partial \vec{L}}{\partial \tau}$. Therefore, during a time $d\tau$, the vector \vec{L} changes by the amount $d\vec{L} = v \cdot d\tau \cdot \vec{e}_v$. With it, the total derivative in Equation (40) is

$$\frac{\partial}{\partial \tau} \varepsilon_L(\tau, \vec{L}) \cdot d\tau + v \cdot \vec{e}_v \cdot \frac{\partial}{\partial \vec{L}} \varepsilon_L(\tau, \vec{L}) \cdot d\tau = 0. \tag{41}$$

Next, the derived formula is divided by $d\tau$. Then, the formula is solved for $\frac{\partial}{\partial \tau} \varepsilon_L$:

$$\frac{\partial}{\partial \tau} \varepsilon_L(\tau, \vec{L}) = -v \cdot \vec{e}_v \cdot \frac{\partial}{\partial \vec{L}} \varepsilon_L(\tau, \vec{L}), \quad \text{each indivisible VP has } v = c \tag{42}$$

The above expression is the differential Equation, DEQ, of VPs or of *volume dynamics* (VD). Next, the DEQ of VD is transformed to a Lorentz invariant expression. For it, the expression Equation (42) is squared, and the right hand side is subtracted,

$$\left(\frac{\partial \varepsilon_L}{\partial \tau}\right)^2 - v^2 \cdot \left(\frac{\partial \varepsilon_L}{\partial \vec{L}}\right)^2 = 0, \quad \text{each indivisible VP has } v = c \tag{43}$$

Altogether, each localized VP fulfills the volume dynamics in Equation (42) or in the Lorentz-invariant Equation (43). Thereby, for the following reasons, the derived dynamics is very well founded and insightful: The derivation needs only the presence of a local maximum. Only founded observation is used, see Figure 5. For comparison, general relativity postulates the Einstein Hilbert action or the Einstein field equation [5,6]. Also,

quantum physics utilizes postulates [60–62]. In the same manner, gravity is based on postulates, via relativity [5], or via Newton [1], or via the graviton [63].

Indeed, we will show later that the differential Equation of the volume dynamics implies gravity, curved space and quantum postulates.

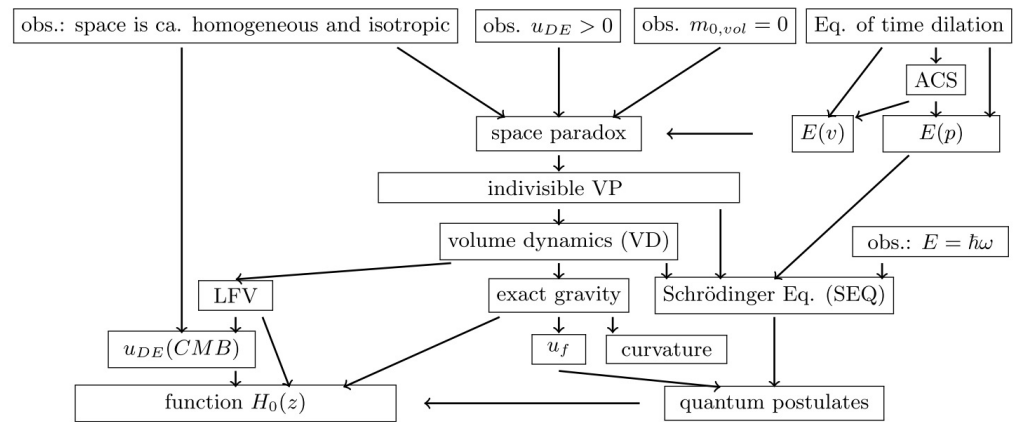


Figure 5. Paths of derivation: Arrows point from premises to implications. Observations (obs.) and the Equation of time dilation are starting points. The Equation of time dilation and the ACS, see [24], are a general basis for the energy-velocity relation, $E(v)$, and the energy momentum relation, $E(p)$. $E(v)$, the nonzero dark energy density u_{DE} , the zero rest mass of volume, and the approximate homogeneity and isotropy of space imply the space paradox. Its solution implies that space is a stochastic average of indivisible VPs. Mathematics implies their dynamics, the VD. The VD implies three important dynamics, the local formation of volume (LFV), exact gravity with the energy density of its field u_f , and the SEQ together with its quantum postulates. Essentially the LFV, and derived quantum correlations, explain and imply the value of the energy density of volume in the homogeneous universe, which is the universe at the CMB. Moreover, the LFV fundamentally explains and implies the value of the Hubble constant H_0 as a function of the redshift z . This explains the Hubble tension and its main source: the time evolution of the rate $H_0(z)$ of formation of new volume. This local formation of new volume is enhanced by the local heterogeneity, as the process of LFV as well as heterogeneity are nonlinear functions of the exact gravity, which is caused by the VD. Altogether, this explanation of the Hubble tension shows how the derived volume dynamics implies and explains relations among LFV, gravity and quanta, which in turn explain the source of the Hubble tension, in precise concordance with observation.

5. Schrödinger Equation: Deduction

Here, we show that each VP fulfills a *generalized Schrödinger equation (GSEQ)*, which implies the usual Schrödinger equation (SEQ), which holds for a slow ($v/c \ll 1$) mass M .

5.1. Volume Dynamics Implies the GSEQ

In this section, it is shown that VPs with their VD imply the GSEQ. The differential equation of volume dynamics is applied to indivisible volume portions with help of three essential steps:

- (1) In a first investigation, the geometry of relative additional volume is analyzed: For each VP, the DEQ (42) of VD is fulfilled. Thereby, the VP moves in the direction \vec{e}_v of its velocity, see Figure 4.

In general, a relative additional volume with an increase δL_3 with the normalized direction vector \vec{e}_3 and with a propagation of indivisible VPs in the same direction, and with an underlying length ΔL_3 , is called unidirectional relative additional volume $\varepsilon_{L,33}$, see Equations (21)–(23). More information about such tensors can be found in the literature [23,36,53,64,65].

- (2) Next, each VP is described by the DEQ of VD. In that DEQ, we utilize v is equal to c . Additionally, we apply the derivative with respect to time, so that the relative additional volume $\varepsilon_{L,jj}$ becomes $\frac{\partial}{\partial \tau} \varepsilon_{L,jj}$, which is usually expressed by $\dot{\varepsilon}_{L,jj}$. The differential Equation of volume dynamics implies

$$\frac{\partial}{\partial \tau} \dot{\varepsilon}_{L,jj} = -c \cdot \vec{e}_v \cdot \frac{\partial}{\partial L} \dot{\varepsilon}_{L,jj}. \tag{44}$$

- (3) Next, the expression is multiplied by $i\hbar$.

$$i\hbar \cdot \frac{\partial}{\partial \tau} \dot{\varepsilon}_{L,jj} = c \cdot \vec{e}_v \cdot \left[-i\hbar \cdot \frac{\partial}{\partial L} \right] \dot{\varepsilon}_{L,jj} \tag{45}$$

Moreover, for the case of an indivisible VP, this indivisibility corresponds to the quantum property with its universal unit of quantization, the Planck [66] constant h or its reduced version $\hbar := \frac{h}{2\pi}$.

Accordingly, the correspondence principle is applicable [67]. Moreover, the momentum operator is derived in the Appendix A. On that basis, that operator is identified; it is the above bracket with right angles:

$$i\hbar \cdot \frac{\partial}{\partial \tau} \dot{\varepsilon}_{L,jj} = \vec{e}_v \cdot c \cdot \hat{p} \cdot \dot{\varepsilon}_{L,jj} \tag{46}$$

In this DEQ, $\dot{\varepsilon}_{L,jj}$ represents a rate. That rate is normalized by a factor t_n . In physics, t_n has the dimension time and the unit second. Consequently, the normalized rate $t_n \cdot \dot{\varepsilon}_{L,jj}$ is dimensionless and has the unit one. It will be shown that the normalized rate has the role of a wave function in the above Equation. Accordingly, $t_n \cdot \dot{\varepsilon}_{L,jj}$ is named wave function Ψ . Of course, this can be regarded as an abbreviation, if desired. Therefore, the differential Equation of volume dynamics implies the following DEQ:

$$i\hbar \cdot \frac{\partial}{\partial \tau} \Psi = c \cdot \vec{e}_v \cdot \hat{p} \cdot \Psi \tag{47}$$

$$\Psi := t_n \cdot \dot{\varepsilon}_{L,jj} \tag{48}$$

The product of the momentum operator and the direction vector of propagation, $(\vec{e}_v \cdot \hat{p})$, is the quantum mechanical operator of the measurable value of the absolute value of the momentum in physics \hat{p} :

$$i\hbar \cdot \frac{\partial}{\partial \tau} \Psi = (c \cdot \hat{p}) \cdot \Psi \tag{49}$$

In the present case of a VP that propagates with the speed c , special relativity implies that the above bracket is equal to the energy E . Consequently, according to the correspondence principle [67], pages 673–674, the bracket is equal to the energy operator:

$$i\hbar \cdot \frac{\partial}{\partial \tau} \Psi = \hat{E} \cdot \Psi \tag{50}$$

The above equation is identified as the Schrödinger equation (SEQ). The SEQ holds for slow ($v/c \ll 1$) objects. This differential Equation holds for fast objects too, and it implies the differential Equation for slow objects, see next Section 5.2. Accordingly, this differential Equation is a generalized SEQ, it is abbreviated with GSEQ. Moreover, $\dot{\varepsilon}_{L,rr}$ is real, as it is the derivative of the real $\varepsilon_{L,rr}$. As a consequence, the wave function Ψ is real, as it is the normalized form of the real $\dot{\varepsilon}_{L,rr}$.

Each VP fulfills the GSEQ (50) and has a physically real wave function $\Psi \propto \dot{\varepsilon}_{L,rr}$ in Equation (48). Thereby, according to the Hacking [38] criterion, a wave function has an

extraordinary physical reality, as it can be manipulated even so that nonlocal phenomena occur [68].

5.2. The Volume Dynamics Implies the SEQ

In this section, it is shown that volume portions and their volume dynamics imply the Schrödinger equation. The following is derived for localizable quantum objects with $v \leq c$. The following derivation steps are essential:

(1) In a first case, entities with $p^2 c^2 \gg m_0^2 c^4$ [21] are analyzed. Accordingly, following (linear) approximation is applied to $E = \sqrt{p^2 c^2 + m_0^2 c^4}$, whereby $\frac{m_0^2 c^4}{p^2 \cdot c^2} \ll 1$ is considered:

$$E \doteq p \cdot c + \frac{m_0^2 c^4}{2 \cdot p \cdot c} \tag{51}$$

As usual, \doteq represents an approximation of order one, for small $\frac{m_0^2 c^4}{p^2 \cdot c^2}$. With it, the GSEQ takes the following form:

$$i\hbar \frac{\partial}{\partial \tau} \Psi \doteq \left(\hat{p} \cdot c + \frac{m_0^2 c^4}{2 \cdot \hat{p} \cdot c} \right) \cdot \Psi \tag{52}$$

(2) A second case is determined by $p^2 c^2 \ll m_0^2 c^4 =: E_0^2$. This implies the items below:

(2a) For each eigenvalue of energy, $E = \sqrt{p^2 c^2 + m_0^2 c^4}$ is approximated with $\frac{p^2 \cdot c^2}{E_0^2} \ll 1$:

$$E \doteq E_0 + \frac{p^2}{2 \cdot m_0} \tag{53}$$

(2b) In the differential equation, each eigenvalue p is substituted by \hat{p} .

$$i\hbar \cdot \frac{\partial}{\partial \tau} \Psi_{E_0} \doteq \left(E_0 + \frac{\hat{p}^2}{2 \cdot m_0} \right) \cdot \Psi_{E_0} \tag{54}$$

In the above Equation, the rest energy E_0 is inherent to Ψ_{E_0} . As a consequence of linear algebra,

$$\hat{p}^2 = \hat{p}^2. \tag{55}$$

(2c) An Ansatz of factorization yields

$$\Psi_{E_0} = \Psi \cdot \exp\left(\frac{E_0 \cdot \tau}{i\hbar}\right). \tag{56}$$

In Equation (54), the derivative yields

$$E_0 \Psi_{E_0} + \exp\left(\frac{E_0 \tau}{i\hbar}\right) i\hbar \frac{\partial \Psi}{\partial \tau} \doteq \left(E_0 + \frac{\hat{p}^2}{2 m_0} \right) \cdot \Psi_{E_0} \tag{57}$$

(2d) In the above DEQ, the terms $E_0 \Psi_{E_0}$ compensate each other. Then, the terms $\exp\left(\frac{E_0 \tau}{i\hbar}\right)$ compensate each other. Therefore, the common Schrödinger [69] Equation is deduced from the VD:

$$i\hbar \cdot \frac{\partial}{\partial \tau} \Psi \doteq \frac{\hat{p}^2}{2 \cdot m_0} \cdot \Psi = \hat{H} \Psi \tag{58}$$

In general, a term E_{pot} is added:

$$i\hbar \cdot \frac{\partial}{\partial \tau} \Psi \doteq \frac{\hat{p}^2}{2 \cdot m_0} \Psi + E_{pot} \Psi = \hat{H} \Psi \tag{59}$$

5.3. Interpretation of VPs and Masses

In this section, the relationship between VPs and masses is elaborated on the basis of the above dynamics of the VD, the GSEQ and the SEQ, and of the Higgs [48] mechanism: Higgs [48] partially deduced and proposed that some elementary particles form their mass from vacuum or from the volume portions by the process of a phase transition [21,70–72]:

In physics [12,67,73], empty space is called vacuum, and its energy density is the density u_{DE} of dark energy [9,41]. In the above phase transition, the vacuum transforms to a mass.

As shown by the space paradox, the vacuum is a stochastic average of indivisible VPs. As a consequence, the above phase transition transforms indivisible volume portions to a mass. Thereby, in a typical phase transition, objects change from one phase to another phase. Thereby, these objects are described by the same fundamental dynamics in both phases of the transition, and in the process of the transition. An example is the phase transition of condensation [74,75].

In particular, in the present case, such fundamental dynamics is derived that holds in both phases, and during transition. It is the differential equation of volume dynamics. It holds for VPs in the first phase, and it implies the SEQ that holds for the masses in the second phase. Phase transitions with vol. portions can explain elementary particles [72]. Hereby, of course, the question remains how a mass can emit its wave function. This will be derived in the next section: In part (Section 6), it is shown that the VPs provide gravitational interaction and curved space as a byproduct. It has already been shown that a mass causes additional volume and VPs, see Sections 1.1.3 and 4.1. In Section 7, the process of *local formation of volume (LFV)* and of VPs is described, and a corresponding DEQ of the LFV is derived. These VPs formed by a mass M represent the wave function of that mass. In part (Section 10), for the homogen. univ., it is shown that this DEQ describing LFV provides an emergence of the volume of our universe and of its u_{vol} (energy density) value. More generally, with matter fluctuations, u_{DE} (energy dens.) and the difference of $u_{DE} - u_{vol}$ increase gradually with the heterogeneity of the universe, and this difference remained relatively small, even at the present-day universe.

Both results are in accurate concordance with empirical records. Therefore, these findings provide clear evidence for this present theory of VPs. Thereby, each mass M fulfills the SEQ, Equation (59) implied by the GSEQ. M can emerge from vol. portions via a phase change [48,50,72].

6. Gravitation and Curved Space

Nearby a mass M , the phenomena of curved space, an exact gravitational potential and field emerge, see Figure 1. These phenomena are explained and implied by the differential equation (DEQ) of volume dynamics

6.1. Exact Generalized and Gravitational Potential and Field

Here, an exact potential and field are deduced from the volume portions.

6.1.1. Generalized Potential and Field

Near a mass M (Figure 6), the unidirectional radial rel. add. vol. $\varepsilon_{L, rr}$ has the following properties. In Figure 6, spherical polar coordinates are utilized, and these are applied in the following.

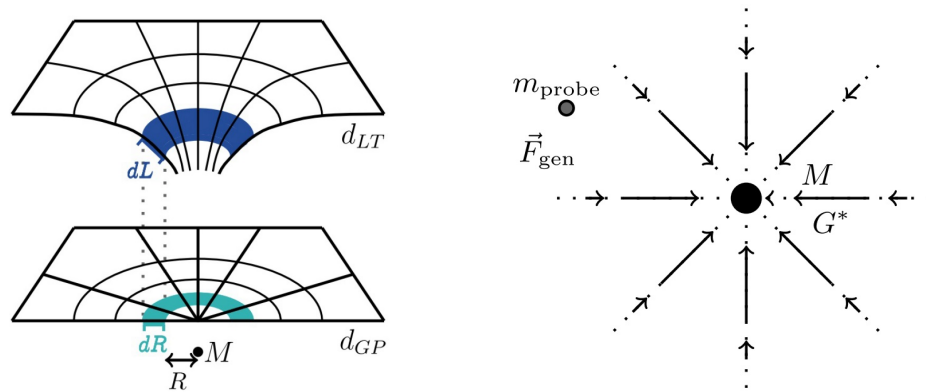


Figure 6. Nearby a mass M , outer space is curved (blue). For $M = 0$ or $M \rightarrow 0$, space is not curved (blue-green), see Figure 1. This physical situation can be expressed with the help of a field in the right part: Thereby, arrows describe vectors of the gravitational field, and dotted lines show respective field lines. The full interaction is achieved with the probe mass.

- (1) For each indivisible VP δV_j , the DEQ of VD describes the relative additional volume $\varepsilon_{L,rr,j}(\tau, \vec{L})$. This is elaborated step by step and progressively in the following paragraphs.

- (1.1) That DEQ is expanded by the factor c :

$$c \cdot \frac{\partial}{\partial \tau} \varepsilon_{L,rr,j}(\tau, \vec{L}) = \vec{e}_v \cdot \frac{\partial}{\partial \vec{L}} \left(-c^2 \cdot \varepsilon_{L,rr,j}(\tau, \vec{L}) \right) \tag{60}$$

- (1.2) At an event (τ, \vec{L}) , including the set \mathcal{S} of its surrounding events in an interval of time $\tau_i \in [\tau - \Delta\tau, \tau + \Delta\tau]$ and in some ball $|\vec{L}_i - \vec{L}| \leq \Delta L$, with \vec{L} near the mass M , the sum of the rel. add. vol. of all indivisible VPs δV_j is applied:

$$c \cdot \frac{\partial}{\partial \tau} \sum_{j \text{ in } \mathcal{S}} \varepsilon_{L,rr,j}(\tau, \vec{L}) = \vec{e}_v \cdot \frac{\partial}{\partial \vec{L}} \left(-c^2 \cdot \sum_{j \text{ in } \mathcal{S}} \varepsilon_{L,rr,j}(\tau, \vec{L}) \right) \tag{61}$$

- (1.3) In the above diff. equation, the gradient is applied to the bracket. The bracket essentially represents the scalar field of rel add. volume. These facts show that the bracket represents a generalized potential $\Phi_{gen}(\tau, \vec{L})$

$$\Phi_{gen}(\tau, \vec{L}) := -c^2 \cdot \sum_{j \text{ in } \mathcal{S}} \varepsilon_{L,rr,j} \tag{62}$$

Moreover, the special potential must be regarded as a generalized potential, as it does not describe a static scalar function. Instead, it describes very fast indivisible volume portions, as $\varepsilon_{L,rr,j}$ describes the rel. add. vol. of indivisible vol. portions that move rapidly in various directions. In fact, an appropriate average of that generalized volume will turn out to be the common gravitational potential.

- (1.4) In principle, in calculus, the gradient (multiplied by minus one) of that generalized potential would be the respective generalized field \vec{G}_{gen} , see Figure 6. In order to apply that gradient, the potential must be a differentiable function. In the present case of VPs, differentiability emerges only in a sufficiently smooth

average. Algebraically, the gradient operator can be applied in principle. Under these conditions, the gradient is applied:

$$\vec{G}_{gen}(\tau, \vec{L}) := -\frac{\partial}{\partial \vec{L}} \left(-c^2 \cdot \sum_{j \text{ in } S} \varepsilon_{L,rr,j} \right) = -\frac{\partial}{\partial \vec{L}} \Phi_{gen}(\tau, \vec{L}) \quad (63)$$

(1.5) Therefore, the DEQ of VD in Equation (60), under the conditions in item (1.4), transforms to the following form of the *rate gravity relation*:

$$c \cdot \frac{\partial}{\partial \tau} \sum_{j \text{ in } S} \varepsilon_{L,rr,j} = \vec{e}_v \cdot \frac{\partial}{\partial \vec{L}} \Phi_{gen}(\tau, \vec{L}) = -\vec{e}_v \vec{G}_{gen}(\tau, \vec{L}) \quad (64)$$

The potential and field in the above equation are generalized to the respective quantities for one indivisible VP δV_j . Thereby, the potential is

$$\Phi_{gen,j}(\tau, \vec{L}) = -c^2 \varepsilon_{L,rr,j}(\tau, \vec{L}), \quad (65)$$

and the field is as follows:

$$\vec{G}_{gen,j}(\tau, \vec{L}) = -\frac{\partial}{\partial \vec{L}} \Phi_{gen,j}(\tau, \vec{L}) = c^2 \frac{\partial}{\partial \vec{L}} \varepsilon_{L,rr,j}. \quad (66)$$

These relations are results of the VD. Formally, these results can be obtained by an application of the above average with one indivisible VP only.

For comparison, expectation values of the field have been derived from the VD as follows: Firstly, a quantum field theory has been derived from the VD. Secondly, the expectation value of a field has been derived from the quantum field theory [23,65].

(2) For these indivisible VPs, and for each event (τ, \vec{L}) , a very essential new scalar is identified and introduced: It is the *rate gravity scalar* RGS_{gen} , and it is equal to zero. This is the rate gravity relation. It can be written in various useful forms:

$$RGS_{gen} := \left(c \cdot \frac{\partial}{\partial \tau} \sum_{j \text{ in } S} \varepsilon_{L,rr,j} \right)^2 - \vec{G}_{gen}^2, \quad \text{thus} \quad (67)$$

$$RGS_{gen} = \left(c \cdot \frac{\partial}{\partial \tau} \sum_{j \text{ in } S} \varepsilon_{L,rr,j} \right)^2 - \sum_{k=1}^{\text{dimension } D} G_{gen,k}^2 \quad \text{and} \quad (68)$$

$$RGS_{gen} = \left(c \cdot \frac{\partial}{\partial \tau} \sum_{j \text{ in } S} \varepsilon_{L,rr,j} \right)^2 - \left(c \frac{\partial}{\partial \vec{L}} \Phi_{gen} \right)^2 \quad \text{and} \quad (69)$$

$$RGS_{gen} = 0 \quad (70)$$

(3) For each underlying volume ΔV_L , and for each event (τ, \vec{L}) , which is at a very useful distance d_{GP} from M (d_{GP} abbreviates the gravit. par. dist.), a respective generalized field is proportional to $\frac{1}{R^2}$:

$$|\vec{G}_{gen}| \propto \frac{1}{R^2}, \quad \text{for } D = 3, \quad \text{and for } \Delta V_L \quad (71)$$

This result is derived as follows:

(3.1) Equation (64) is multiplied by \vec{e}_v . Hence, the field is as follows:

$$\vec{e}_v \cdot c \cdot \frac{\partial}{\partial \tau} \sum_{j \text{ in } S} \varepsilon_{L,rr,j} = -\vec{G}_{gen}(\tau, \vec{L}) \tag{72}$$

(3.2) Integration with respect to τ from zero to a time $\delta\tau$ yields:

$$\vec{e}_v \cdot c \cdot \sum_{j \text{ in } S} \varepsilon_{L,rr,j}(\delta\tau) = - \int_0^{\delta\tau} \vec{G}_{gen}(\tau, \vec{L}) d\tau \tag{73}$$

For it, a very small time $\delta\tau$ is used. In particular, that time is sufficiently small, so that the above integral in the above equation is approximated by $\delta\tau \cdot \vec{G}_{gen}$. Thus, the field is as follows:

$$\vec{e}_v \cdot c \cdot \sum_{j \text{ in } S} \varepsilon_{L,rr,j}(\delta\tau) = -\delta\tau \cdot \vec{G}_{gen} \tag{74}$$

(3.3) The definition $\varepsilon_{L,rr,j} = \frac{\delta V_{L,rr,j}}{dV_L}$ is utilized. In the whole emerging gravity of this theory, it is essential that the energy density u_{vol} of volume is positive. (it is approximately the same as u_{DE} , which is positive [9,15,16]). Therefore, the indivisible VP $\delta V_{L,rr,j}$ is proportional to the corresponding energy δE_j . The latter is proportional to the momentum $\delta p_j = \delta E_j/c$, as each VP propagates with the speed c , that is: $\delta V_{L,rr,j} = \frac{\delta E_j}{u_{vol}} = \frac{c \cdot \delta p_j}{u_{vol}}$.

(3.4) An underlying volume dV_L is considered. It is very useful to apply the shell that has its center at the field generating mass M . That volume is $dV_L = A_D \cdot R^{D-1} \cdot dL$. Consequently, for $D = 3$, the field is as follows:

$$-\vec{e}_v \cdot \frac{c^2}{u_{vol} \cdot A_D \cdot dL} \cdot \frac{\sum_{j \text{ in } S} \delta p_j}{\delta\tau} \cdot \frac{1}{R^2} = \vec{G}_{gen} \tag{75}$$

Hereby, the thickness dL of each shell is chosen constant, so that it does not depend on R . In that case, in the above equation the left ratio is constant. The middle ratio is identified with the momentum current, which propagates through each of the shells. This momentum current does not change, since none of the shells causes any momentum. Consequently, $\frac{1}{R^2} \propto |\vec{G}_{gen}|$. Thus, it is proved. A version of the corresponding result for a dimension $D > 3$ is shown in Carmesin [65] ([THM 9]).

(4) Moreover, according to the Galileo equivalence principle, the mass M is proportional to the field (the mass may be interpreted as the source of the field) $\vec{G}_{gen}(R)$: $|\vec{G}_{gen}(R)| \propto \frac{M}{R^2}$. Consequently, there is a proportionality factor (it is interpreted as a universal constant) G_{gen} :

$$|\vec{G}_{gen}(|R|)| = \frac{G_{gen}M}{R^2}, \text{ for } D = 3. \tag{76}$$

In general, the value of a universal constant, such as G_{gen} , must be obtained from observation. Accordingly, G_{gen} is obtained in the next section. Additionally, the curvature of space is analyzed:

6.1.2. Spin, Statistics and the Additive Structure of VPs, Potentials and Fields

In general, a VP has the tensor property of a quadrupolar structure, see Section 3. Consequently, it is represented by a tensor of rank two.

Therefore, at the level of quantum physics, an indivisible VP has an integer valued spin, see Landau and Lifschitz [76], §58, Carmesin [77]:

$$S = n \cdot \hbar, \quad \text{with a natural number } n. \tag{77}$$

As a consequence, at the level of quantum physics, an indivisible VP is a boson, see Landau and Lifschitz [76], §64, Carmesin [77]. Consequently, at the level of quantum physics, an indivisible VP obeys the Bose [78] statistics, alias Bose-Einstein statistics, see Landau and Lifschitz [76], §64, Sakurai and Napolitano [61], Section 7.2.

The Bose-Einstein statistics imply that several bosons can exist at the same place. Consequently, the additional volumes $\varepsilon_{L,rr,j}$ caused by different masses m_j can exist simultaneously at each point P in the universe, and these $\varepsilon_{L,rr,j}$ add up at P . This, in turn, implies that the potential $\Phi_{gen}(P)$ at P is the sum of these additional volumes $\varepsilon_{L,rr,j}(P)$ multiplied by $-c^2$. This founds Equation (62) at the level of quantum physics. As a consequence of this potential, the generalized field $\vec{G}_{gen}(P) = -\frac{\partial}{\partial \vec{L}}\Phi_{gen}(P)$ has the same additive structure.

6.2. Curvature near a Mass

In fact, the DEQ of VD can be used to deduce the curvature near a mass M . This is done step by step and progressively in the following paragraphs:

- (1) As shown above, a shell is considered, which has its center at M , and has a gravitational parallax radius R , the relative additional volume $\varepsilon_{L,rr}$ is as follows:

$$\varepsilon_{L,rr} = \frac{dV_L - dV_R}{dV_L} = 1 - \frac{dV_R}{dV_L} = 1 - \frac{4\pi R^2 dR}{4\pi R^2 dL} = 1 - \frac{dR}{dL}. \tag{78}$$

The resulting fraction $\frac{dR}{dL}$ is called *position factor* [65]:

$$\varepsilon_E(R) := \frac{dR}{dL} = 1 - \varepsilon_{L,rr} \tag{79}$$

Hereby, the ratio $\frac{dL}{dR}$ is equal to $\sqrt{g_{rr}}$:

$$\sqrt{g_{rr}} := \frac{dL}{dR} = \frac{1}{\varepsilon_E(R)}. \tag{80}$$

More generally, at each R , or at each event (τ, \vec{L}) with $|\vec{L}| \geq R$, the curvature can be generalized for the case of a single indivisible VP δV_j , with the relative additional volume $\varepsilon_{L,rr,j}$, as follows:

$$g_{rr,j} := \frac{1}{\varepsilon_{E,j}^2} := \frac{1}{(1 - \varepsilon_{L,rr,j})^2}. \tag{81}$$

- (2) A DEQ for the position factor is derived: For it, $\frac{\partial}{\partial L}$ is applied to Equation (79). This implies:

$$\frac{\partial}{\partial L}\varepsilon_E = \frac{\partial R}{\partial L} \frac{\partial}{\partial R}\varepsilon_E = \varepsilon_E \frac{\partial}{\partial R}\varepsilon_E = -\frac{\partial \varepsilon_{L,rr}}{\partial L} \tag{82}$$

The potential $\Phi_{gen} = -c^2\varepsilon_{L,rr}$ is solved for $\varepsilon_{L,rr}$, and this is inserted into Equation (82):

$$\varepsilon_E(R) \frac{\partial \varepsilon_E}{\partial R} = \frac{\partial \Phi_{gen} / c^2}{\partial L} \tag{83}$$

The gradient $\frac{\partial}{\partial L} = \vec{e}_v \frac{\partial}{\partial \vec{L}}$ is applied:

$$\varepsilon_E(R) \frac{\partial \varepsilon_E}{\partial R} = \vec{e}_v \frac{\partial \Phi_{gen}/c^2}{\partial \vec{L}} \tag{84}$$

The field $-\frac{\partial \Phi_{gen}}{\partial \vec{L}} = \vec{G}_{gen}$ is identified:

$$-\vec{e}_v \frac{1}{c^2} \vec{G}_{gen} = \varepsilon_E(R) \cdot \frac{\partial \varepsilon_E}{\partial R} \tag{85}$$

\vec{G}_{gen} and \vec{e}_v have opposite directions. Consequently, the field is as follows:

$$\frac{1}{c^2} |\vec{G}_{gen}| = \varepsilon_E(R) \frac{\partial \varepsilon_E}{\partial R} \tag{86}$$

Equation (76) is applied:

$$\frac{G_{gen}M}{R^2 c^2} = \varepsilon_E(R) \frac{\partial \varepsilon_E}{\partial R} \tag{87}$$

(3) The above diff. Equation is solved:

$$\int \frac{G_{gen}M}{R^2 c^2} dR = \int \varepsilon_E(R) d\varepsilon_E \tag{88}$$

Integration and a respective K yield

$$K - \frac{G_{gen}M}{Rc^2} = \frac{1}{2} \varepsilon_E^2. \tag{89}$$

The solution with respect to ε_E provides

$$\varepsilon_E = \sqrt{2K - \frac{2G_{gen}M}{c^2} \frac{1}{R}}. \tag{90}$$

There is zero curvature at $R \rightarrow \infty$. Consequently, $\varepsilon_E = \frac{dR}{dL} = 1.0$. As a consequence, $K = 1/2$:

$$\varepsilon_E = \sqrt{1 - \frac{2G_{gen}M}{c^2} \frac{1}{R}} \tag{91}$$

(4) ε_E in Equation (91) is related to observation:

$$\varepsilon_E = \sqrt{1 - \frac{2G_{gen}M}{c^2} \frac{1}{R}} = \frac{1}{\sqrt{g_{rr}}} \tag{92}$$

Empirical records show [20,79]:

$$\sqrt{1 - \frac{2GM}{c^2} \frac{1}{R}} = \frac{1}{\sqrt{g_{rr}}} = \sqrt{1 - \frac{R_S}{R}}. \tag{93}$$

Next, the Schwarzschild radius $R_S := \frac{2GM}{c^2}$ is related to the two tensor elements in Equations (92) and (93). The result is $G_{gen} = G$ (the universal constant of gravity $G = 6.67430(15) \cdot 10^{-11} \frac{m^3}{kg \cdot s^2}$). Consequently, $\vec{G}_{gen} = \vec{G}^*$. The respective relation holds for the potentials. The derived quantities, terms and relations are exact, since they have been derived exactly. Therefore, in the vicinity of a mass, the indivisible VPs cause a generalized potential, a generalized field, their exact field and potential of the gravitational interaction, and curved space as well as time. The respective Equations are derived exactly.

6.3. A Discussion of Gravity and Curvature

Near a mass M , the volume dyn. determines exact quantities, terms and relations: $\varepsilon_{L,rr}(r)$, which provides $\Phi_{exact} = -c^2 \cdot \varepsilon_{L,rr}(r)$, which provides $\vec{G}_{exact}^* = -\frac{\partial}{\partial L} \Phi_{exact}$. Next, these valuable and insightful properties are analyzed and interpreted:

6.3.1. Transmission of the Potential and Field

The indivisible VPs δV_j with their rel. add. vol. $\varepsilon_{L,rr,j}(r)$ cause a net outward propagation. The indivisible vol. portions transfer momentum, as $u_{vol} > 0$. Consequently, the indivisible vol. portions transfer the interaction of gravity. It confirms the graviton idea proposed by Blokhintsev and Galperin [63].

Additionally, these indivisible vol. portions explain and imply curved space. Thereby, curvature is explained with the help of the sum of indivisible VPs. More generally, the curvature of a single indivisible VP has been generalized, see Equations (80) and (81).

6.3.2. On the Exactness of the Potential and Field

The generalized potential and field derived here are exact. In contrast, the gravitational potential is only an approximation in Newton's theory. For instance, correction terms depending on the gravitational parallax distance R and on the velocity \vec{v} have been elaborated in Post-Newtonian approximations [80] (see Equation (2.49) in [81]). Accordingly, the following question arises: How is the exactness achieved here?

Essentially, this is achieved here by the application of especially useful distance measures and coordinate systems:

Firstly, for each point P in the universe, there is an adequate coordinate system (ACS), so that an object at rest in the ACS has an absolute zero of velocity, see Section 1.1.5 or Carmesin [23,24,39]. This ACS is used here. As a consequence, the velocity terms in the Post-Newtonian approximation are zero.

Secondly, two measurable distance measures are used, see Figure 1: d_{LT} [82] (light travel distance), and d_{GP} [23,36,40] (gravitational parallax distance, it can also be measured as a circumferential distance [83] (see Section (2.6) in [84])).

Hereby, according to the Hacking [38] criterion, the light travel distance d_{LT} to a field-generating mass M is real, as an increase of M can change that distance d_{LT} . In contrast, the d_{GP} of an object to a field generating mass M is idealized, since it represents the limit M to zero of the light travel distance:

$$d_{GP} = \lim_{M \rightarrow 0} d_{LT}. \tag{94}$$

This is a typical idealization based on a limit [44]. Though the gravitational parallax distance d_{GP} is idealized and not real, that distance d_{GP} can be measured, and that distance d_{GP} provides the $\frac{1}{R^2}$ law, see Figure 6.

Thirdly, the exact potential and field are determined as follows: For the case of a point P , the idealized gravitational parallax distance d_{GP} from P to the field-generating mass M is measured or determined by other means. With it, Φ_{exact} and \vec{G}_{exact}^* are functions of $d_{GP} = R$. The result is exact, as no approximation has been used in the derivation of these equations.

But in the theory proposed by Newton, the flatness of space has been introduced as a postulate. Accordingly, a user might use that postulate and the light travel distance $d_{LT} \neq dR$, and the equations for potentials and fields in Newtonian mechanics. In such a postulate-based determination of the potential or field, the result is an approximation only.

6.3.3. Advantage of the Exact Potential and Field

Indivisible vol. portions provide exactly the transmission, potential, and field of gravity, as well as curved space, in an impartible form. Thereby, by using the adequate coordinate system and the measurable idealized gravitational parallax distance, relatively short, highly structured, and clarifying equations can be used. Moreover, the results are part of the unification of relativity, gravity and quanta. This unification uses the relative difference $\varepsilon_{L,rr}$, which is based on both distance measures: the real d_{LT} and the idealized d_{GP} .

7. Local Formation of Volume in Nature

Here, the dynamics of local formation of volume (LFV) is derived.

Near a mass M , add. vol. δV propagates outwards. Hereby, the amount of add. vol. increases. As a consequence, locally formed volume, LFV, emerges δV or δV_{rr} in radial orientation r . Hereby, at the following, an underlined variable marks the formed volume or the process of formation of volume. Such LFV can be caused via a mass M .

In detail, LFV forms at a gradient of rel. add. vol. $\varepsilon_{L,jj}$, or of the potential $\Phi_L = -c^2 \cdot \varepsilon_{L,jj}$, or at a gravitational field \vec{G}^* . Consequently, a gravitational field causes LFV.

7.1. Definition of Locally Formed Volume

Add. vol. δV_{jj} , which emerges in dV_L , in a direction \vec{e}_j , and in a time interval $\delta\tau$, is described by

$$\dot{\varepsilon}_{L,jj} := \frac{\delta V_{jj}}{\delta\tau \cdot dV_L} \tag{95}$$

It is the named normalized rate of unidirectional LFV.

7.2. Law of Locally Formed Volume

Here, the process of LFV is explained and formulated.

Near a mass M (it can also be an effective mass M_{eff}), at a d_{GP} named R from M or M_{eff} , the normalized rate is as derived step by step and progressively in the following paragraphs:

- (1) A far distance approximation, FDA, is introduced, in which $R_S/R \ll 1$. Hereby, at order $(R_S/R)^1$, the normalized rate is

$$\dot{\varepsilon}_{L,rr}^2 \cdot c^2 = G_{gen,r}^2 \tag{96}$$

Thereby, $G_{gen,r}$ denotes the r -component (parallel to \vec{e}_r) of that field. $G_{gen,r}$ causes $\dot{\varepsilon}_{L,rr}$. In general, $\vec{G}_{gen,j}$ causes $\dot{\varepsilon}_{L,jj}$.

$$\dot{\varepsilon}_{L,jj}^2 \cdot c^2 = G_{gen,j}^2 = (\vec{G}_j^*)^2 \text{ with } \vec{G}_{gen} = -G_{gen,j} \cdot \vec{e}_j \tag{97}$$

- (2) Consequently, non-diagonal components $\dot{\varepsilon}_{L,ij,i \neq j}$ cause no LFV.

- (3) The rate $\dot{\varepsilon}_{L,rr}$ has the exact value

$$\dot{\varepsilon}_{L,rr} = c \cdot \frac{2}{R} \cdot \varepsilon_E \cdot \left(1.0 - \varepsilon_E - \frac{1}{4\varepsilon_E^2 \cdot \frac{R}{R_S}} \right) \tag{98}$$

- (4) In general, $\frac{dR}{dL}$ is abbreviated $\varepsilon_F := \frac{dR}{dL}$, it is a function that has to be determined. As a matter of definition, $\dot{\varepsilon}_{L,rr} = \frac{\partial}{\partial V_L} \frac{\delta V \delta\tau}{\delta\tau}$. The substitution $\frac{\partial}{\partial\tau} = \frac{\partial L}{\partial\tau} \cdot \frac{\partial}{\partial L} = c \cdot \frac{\partial}{\partial L}$ provides

$\dot{\varepsilon}_{L,rr} = c \frac{\partial \delta V}{\partial V_L}$. The substitution $\frac{\partial}{\partial L} = \frac{\partial R}{\partial L} \frac{\partial}{\partial R} = \varepsilon_F \cdot \frac{\partial}{\partial R}$ yields $\dot{\varepsilon}_{L,rr} = \varepsilon_F c \frac{\partial \delta V}{\partial V_L}$. Using $dV_L = 4\pi R^2 dL = 4\pi R^2 dR / \varepsilon_F$, and $\delta V = 4\pi R^2 (dL - dR) = 4\pi R^2 dR (1/\varepsilon_F - 1)$ yields: $\dot{\varepsilon}_{L,rr} = \varepsilon_F^2 c \frac{4\pi dR \frac{\partial}{\partial R} R^2 (1/\varepsilon_F - 1)}{4\pi R^2 dR} = \varepsilon_F^2 c \frac{\partial}{\partial R} \frac{R^2 (1/\varepsilon_F - 1)}{R^2}$. Evaluation of the derivative yields $\dot{\varepsilon}_{L,rr} = \varepsilon_F^2 \cdot c \cdot \frac{2R(1/\varepsilon_F - 1) - R^2 \cdot \varepsilon'_F / \varepsilon_F^2}{R^2} = \varepsilon_F \cdot c \cdot \frac{2(1.0 - \varepsilon_F)}{R} - c \cdot \varepsilon'_F \cdot \varepsilon_L = \frac{dL - dR}{dL} = 1 - \varepsilon_F$ and $\varepsilon'_F = -\varepsilon'_L$ imply

$$\dot{\varepsilon}_{L,rr} = \frac{2c}{R} \cdot \varepsilon_L \cdot (1.0 - \varepsilon_L) + c \cdot \varepsilon'_L. \tag{99}$$

- (5) If desired, Equation (99) can be studied in a computer simulation. It provides a metric, typically with rotation symmetry:

$$\frac{dR}{dL} = 1.0 - \varepsilon_L \text{ or } \frac{dL}{dR} = \frac{1.0}{1.0 - \varepsilon_L} = \sqrt{|g_{rr}|} = \frac{1.0}{\sqrt{|g_{tt}|}} \tag{100}$$

7.3. Derivation of the Law of LfV

Here, the process and the law of LfV are deduced.

Part (1): Shells with their center at M and d_{GP} -based radius R are studied: One shell has a thickness dL . It has the investigated volume dV_L . A second shell represents the additional shell-volume δV . It has the thickness δR , and shell-volume $\delta V = 4\pi R^2 \delta R$. A third shell represents the LfV $\underline{\delta V}$. It has the thickness $\underline{\delta R}$, and the shell-volume $\underline{\delta V} = 4\pi R^2 \underline{\delta R}$.

It is sufficient to analyze the LfV at order one (exponent one) of dR . The result is exact, since dR can be chosen arbitrarily small. If the additional shell-volume $\delta V(R)$ increases as a function of R , formed volume $\underline{\delta V}_{rr}$ emerges (and the direction r is radial).

In general, observable additional volume δV is a function of R . Consequently, the LfV is the change in δV as a function of R . Therefore, the change $\underline{\delta V}_{rr}$ of volume in a shell with thickness $\underline{\delta R}$ is equal to the derivative of the observable additional volume $\frac{\partial}{\partial R} \delta V$ multiplied by that thickness $\underline{\delta R}$:

$$\underline{\delta V}_{rr} := \underline{\delta R} \frac{\partial}{\partial R} \delta V \tag{101}$$

Thereby, δV is as follows:

$$\delta V = dV_L - dV_R = 4\pi R^2 \cdot (dL - dR) = 4\pi R^2 dR \cdot (\varepsilon_E^{-1} - 1) \tag{102}$$

The FDA is utilized at order one, $\frac{R_S}{R} \ll 1$, consequently

$$\varepsilon_E^{-1} \doteq 1 + 0.5 \cdot \frac{R_S}{R}. \tag{103}$$

As a consequence,

$$\frac{\partial}{\partial R} \delta V = \frac{\partial}{\partial R} \left(4\pi R^2 dR \cdot \frac{1}{2} \cdot \frac{R_S}{R} \right) = 2\pi \cdot dR \cdot R_S \tag{104}$$

As a consequence, Equation (101) becomes

$$\underline{\delta V}_{rr} \doteq 2 \cdot \pi \cdot dR \cdot R_S \cdot \underline{\delta R}. \tag{105}$$

Using $\underline{\delta \tau} = \varepsilon_E \cdot \underline{\delta t} = \varepsilon_E \cdot \underline{\delta R} / c$, and $dL = dR / \varepsilon_E$, we derive

$$\dot{\varepsilon}_{L,rr} = \frac{\underline{\delta V}_{rr}}{\underline{\delta \tau} \cdot dV_L} = \frac{2\pi \cdot dR \cdot R_S \cdot \underline{\delta R}}{\underline{\delta R} / c \cdot 4\pi R^2 dR} = \frac{R_S \cdot c}{2R^2} \tag{106}$$

Utilizing $R_S = 2GM/c^2$, we deduce

$$c \cdot \dot{\epsilon}_{L,rr} \doteq \frac{G \cdot M}{R^2}. \tag{107}$$

Application of the field yields

$$\vec{G}^* = \vec{G}_{gen} = -\frac{G \cdot M}{R^2} \cdot \vec{e}_r = -G_{gen,r} \cdot \vec{e}_r. \tag{108}$$

Part (2): Application of the square yields Equation (97):

$$\dot{\epsilon}_{L,rr}^2 \cdot c^2 = \vec{G}_{gen,r}^2 \tag{109}$$

In general, near an effective mass, no invariance related to rotation exists. Then, each direction is analyzed [84] ([chapter 9]). Each field \vec{G}_{gen} parallel \vec{e}_j causes the unidirectional rate $\dot{\epsilon}_{L,jj}$, see Equation (97).

Part (3): The rate in Equation (95) is studied:

$$\dot{\epsilon}_{L,rr} = \frac{\delta V_{rr}}{\underline{\delta\tau}} \cdot \frac{1}{dV_L} \tag{110}$$

$\underline{\delta V_{rr}}$ is the difference of two values of δV_{rr}

$$\dot{\epsilon}_{L,rr} = \frac{1}{dV_L} \cdot \frac{\delta V_{rr}(\tau_0 + \underline{\delta\tau}) - \delta V_{rr}(\tau_0)}{\underline{\delta\tau}} \tag{111}$$

Since $\underline{\delta\tau}$ can be chosen arbitrarily small, order one in $\underline{\delta\tau}$ is sufficient:

$$\dot{\epsilon}_{L,rr} = \frac{1}{dV_L} \cdot \frac{\frac{\partial}{\partial\tau} \delta V_{rr} \cdot \underline{\delta\tau}}{\underline{\delta\tau}} = \frac{1}{dV_L} \cdot \frac{\partial}{\partial\tau} \delta V_{rr} = \frac{1}{dV_L} \cdot \underbrace{\frac{\partial L}{\partial\tau}}_c \cdot \frac{\partial}{\partial L} \delta V_{rr} \tag{112}$$

Substitution of L by R yields:

$$\dot{\epsilon}_{L,rr} = \frac{c}{dV_L} \cdot \underbrace{\frac{\partial R}{\partial L}}_{\epsilon_E} \cdot \frac{\partial}{\partial R} \delta V_{rr} = \frac{\epsilon_{EC}}{dV_L} \cdot \frac{\partial}{\partial R} \delta V_{rr} \tag{113}$$

Next, $\delta V_{rr} = 4\pi R^2 \delta R = 4\pi R^2 (dL - dR) = 4\pi R^2 dR (\epsilon_E^{-1} - 1)$ is used, as well as $dV_L = 4\pi R^2 dR / \epsilon_E$:

$$\dot{\epsilon}_{L,rr} = \frac{\epsilon_E \cdot c}{4\pi R^2 dR / \epsilon_E} \cdot 4\pi dR \cdot \frac{\partial}{\partial R} \left[R^2 \cdot (\epsilon_E^{-1} - 1) \right] \tag{114}$$

The derivative is evaluated:

$$\dot{\epsilon}_{L,rr} = \frac{\epsilon_E^2 \cdot c}{R^2} \cdot \left[2R \cdot (\epsilon_E^{-1} - 1) - \epsilon_E^{-3} \cdot \frac{R_S}{2} \right] \text{ or} \tag{115}$$

$$\dot{\epsilon}_{L,rr} = \frac{2 \cdot \epsilon_E \cdot c}{R} \cdot \left[1 - \epsilon_E - \frac{R_S}{4 \cdot \epsilon_E^2 \cdot R} \right]. \tag{116}$$

Therefore, each mass and each effective mass cause a gravitational field. At each location, a gravity field causes LFV. The respective rates are expressed in Equations (96), (98), (99) and (107).

8. Energy Density of a Gravitational Field

Here, a field’s energy density u_f is introduced and derived.

8.1. Measurement of the Energy Density of the Field

u_f can be measured as follows: The process described in Figure 7 is performed: A mass M is lifted by a radial difference ΔR . Thereby, the required energy ΔE_M is measured. This energy is located in the field within the shell with center M , thickness ΔR and radius R , see Figure 7. That shell has the volume

$$\Delta V = 4\pi R^2 \Delta R. \tag{117}$$

Consequently, the absolute value of the measured energy density is

$$|u_f| = \frac{\Delta E_M}{\Delta V}. \tag{118}$$

The positive required energy compensates the field’s energy in the shell, as the field in the shell with volume ΔV is eliminated in the process of lifting the mass. Consequently, the sign of the field is negative:

$$u_f = -\frac{\Delta E_M}{\Delta V} \tag{119}$$

Alternatively, this measured energy can be calculated:

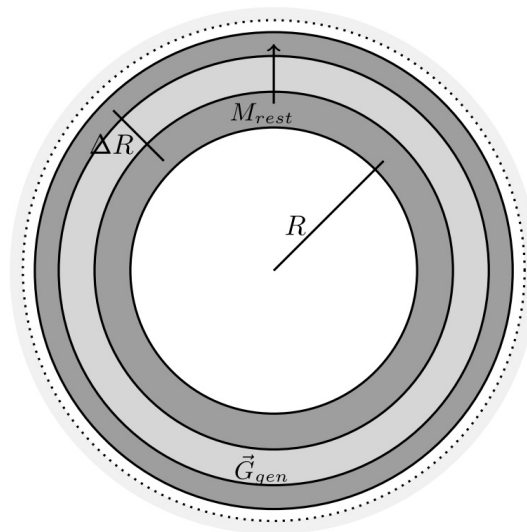


Figure 7. At radii R and $R + \Delta R$, there are two very thin shells with a common center. Initially, in the inner shell, there is a mass M . M is lifted gradually in parts dM to $R + \Delta R$. During that process, at each time, there remains a mass M_{rest} in the inner shell. Between these shells, there is a field $\vec{G}_{gen} = \vec{G}^*$, which gradually becomes zero. The dotted line symbolizes the surroundings, the fields of which add up to zero in a homogeneous universe. This has already been derived by Newton.

8.2. Derivation of the Field’s Energy Density

The required energy ΔE_M can be calculated [65]:

$$\Delta E_M = \frac{G \cdot M^2 \Delta R}{2R^2}. \tag{120}$$

The measured energy density in Equation (119) can be calculated by inserting Equations (120) and (117) into Equation (119):

$$u_f = -\frac{G \cdot M^2}{8\pi R^4} = -\frac{(\vec{G}^*)^2}{8\pi G} \tag{121}$$

For comparison, Peters [85] derived the same formula for the energy density

$$u_f = -\frac{(\vec{G}^*)^2}{8\pi G}. \tag{122}$$

Peters [85] derived this result in a Newtonian approximation.

In contrast, the exact energy density u_f is derived here. This is achieved with help of the exact field, since no approximation is used here. This exactness is achieved here with the help of the distinction between the two distance measures: the d_{GP} distance ΔR and the corresponding d_{LT} distance ΔL .

8.3. Compensation of the Negative Field

The RGS in Equations (67) and (70) is divided by $8\pi G$, and $\vec{G}_{gen} = \vec{G}^*$ is used:

$$0 = \frac{\left(c \cdot \frac{\partial}{\partial \tau} \sum_{j \text{ in } S} \varepsilon_{L,rr,j}\right)^2}{8\pi G} - \frac{(\vec{G}^*)^2}{8\pi G} \tag{123}$$

The sum in Equation (123) is the summed rel. add. vol. of the indivisible VPs:

$$\varepsilon_{L,rr,indivisible \ VPs} := \sum_{j \text{ in } S} \varepsilon_{L,rr,j} \tag{124}$$

With it, the RGS in Equation (123) is

$$0 = \frac{c^2 \cdot \dot{\varepsilon}_{L,rr,indivisible \ VPs}^2}{8\pi G} + \frac{-(\vec{G}^*)^2}{8\pi G}. \tag{125}$$

The second fraction in the above Equation is u_f .

$$0 = \frac{c^2 \cdot \dot{\varepsilon}_{L,rr,indivisible \ VPs}^2}{8\pi G} + u_f \tag{126}$$

As a consequence, the fraction in the above Equation is an energy density u . That fraction describes indivisible VPs δV_j that cause the field. Therefore, that fraction describes the energy density of the indivisible VPs δV_j :

$$u_{indivisible \ VPs} = \frac{c^2 \cdot \dot{\varepsilon}_{L,rr,indivisible \ VPs}^2}{8\pi G}. \tag{127}$$

Consequently, the sum of these two energy densities is

$$u_{indivisible \ VPs} + u_f = 0. \tag{128}$$

The energy density of one indivisible VP is obtained by using $\vec{G}_{gen,j} = \vec{G}_j^*$ and by inserting the field in Equation (66) into Equation (122):

$$u_{f,j} = -\frac{(\vec{G}_j^*)^2}{8\pi G}. \tag{129}$$

Next, the rate gravity relation (see Equations (67) and (70)) is generalized to one indivisible VP:

$$c^2 \dot{\varepsilon}_{L,rr,indivisible \ VP,j} = (\vec{G}_j^*)^2. \tag{130}$$

Similarly, Equation (128) is generalized to one indivisible VP:

$$u_{indivisible VP,j} + u_{f,j} = 0. \tag{131}$$

With these generalizations, the energy density in Equation (129) implies the energy density $u_{indivisible VP,j}$ of one indivisible VP δV_j as follows:

$$u_{indivisible VP,j} = -u_{f,j} = \frac{c^2 \cdot \dot{\epsilon}_{L,rr,indivisible VP,j}^2}{8\pi G}. \tag{132}$$

These relations are results of the VD.

Each indivisible VP has the energy density $u_{indivisible VP,j}$ based on its rate. Moreover, each indivisible VP causes the energy density $u_{f,j}$ based on its gravity. Furthermore, each indivisible VP propagates at the speed c . Accordingly, such an indivisible VP can be called *rate gravity wave, RGW*. In an advanced theory of the VD, expectation values of the field have been derived from the VD as follows, see [23,65].

9. Derivation of the Quantum Postulates

The VD, the dynamics of the indivisible VPs, implies the SEQ, see Section 5.2, the fundamental deterministic dynamics of quantum physics. Accordingly, the following question arises: Does the VD imply the stochastic dynamics of quantum systems and the complete system of quantum postulates?

In order to answer this question, the deterministic time evolution is summarized in a postulate (see Section 9.1), and mathematical consequences (see Sections 9.2 and 9.3) are derived first.

Then, the stochastic dynamics (see Section 9.4) and the complete system (see Section 9.5) of the quantum postulates are derived.

Additional rules about mixed states and about entanglement [62] ([p. 46]) have been derived from the VD [65].

9.1. Postulate About the Deterministic Time Evolution

The VD implies the postulate concerning deterministic time evolution of quanta [86] ([p. 170]):

Postulate about the deterministic time evolution

Kumar writes literally [86] ([p. 170]): ‘The time evolution of the state vector is governed by the time-dependent Schrödinger equation, SEQ [69] ([Equation (4’)]):

$$i\hbar\partial_t|\psi\rangle = \hat{H}|\psi\rangle, \tag{133}$$

where \hat{H} is the Hamilton operator corresponding to the total energy of the system.

More generally, the VD implies the GSEQ, see Section 5.2.

9.2. On Hilbert Space

In this section, the solution spaces of the SEQ and of the GSEQ are analyzed, in order to derive quantum postulates in later sections. In Section 5.2 it is shown, that indivisible VPs can be described by the DEQ of VD, and that indivisible VPs as well as objects at the speed $v = c$ are described by the quantum physical GSEQ. In particular, objects with relatively small momentum, $\frac{p^2}{m_0^2c^2} \ll 1$, in leading order in $\frac{p^2}{m_0^2c^2}$, are described by the SEQ.

In this section, it is shown that the solutions of the SEQ, of the GSEQ and of the DEQ of VD form Hilbert spaces: As usual, Dirac’s notation is used: A wave function (WF) Ψ is expressed by a so-called ket $|\Psi\rangle$. Moreover, for two WFs, there is a scalar product

$$\langle \Psi_1 | \Psi_2 \rangle = \int d^3L \Psi_1^*(\tau, \vec{L}) \cdot \Psi_2(\tau, \vec{L}) \tag{134}$$

The superscript * indicates the complex conjugate [62,86–88]. Based on the scalar product, a normalization factor t_n is as follows:

$$\langle \Psi \cdot t_n | \Psi \cdot t_n \rangle = \int d^3r \Psi^*(\tau, \vec{L}) \cdot \Psi(\tau, \vec{L}) \cdot |t_n|^2 = 1 \tag{135}$$

It is always useful and insightful to analyze the used vector space. It is the space of the solutions of the respective linear differential equation. With the above scalar product, it is a Hilbert space \mathcal{H} [89] ([p. 47]) or Sakurai and Napolitano [61] ([p. 57]).

For the case of the SEQ, the GSEQ, and the VD, the solution space is a Hilbert space. These DEQs and their respective Hilbert spaces, can describe VPs, indivisible VPs, matter, and radiation (the case of radiation is analyzed [65]).

9.3. On Measurements, Operators, and Possible Outcomes

In this section, the modeling of measurements is elaborated, by using respective Hilbert spaces of the solutions of the deterministic dynamics of the GSEQ or of the SEQ. This will be used in later sections in order to derive quantum postulates.

Firstly, the possible outcomes of a single measurement process are derived.

Secondly, the necessity of an additional dynamics is identified.

(1) In physics, in general, a measurement is described as follows:

(1.1) A measurable physical quantity A of an object is a function f of the mathematical description of that object.

(1.2) Thereby, a change in the state should be as small as possible.

(1.3) In general, the function f can be described in linear order by an operator \hat{A} in Hilbert space, and by a Taylor series thereof: $f = \sum_{k=0}^{\infty} c_k \hat{A}^k$. Thereby, the zeroth order is not essential in physics. Thus, $f = \sum_{k=1}^{\infty} c_k \hat{A}^k$. Therefore, a measurable physical quantity A of an object is characterized via a linear operator \hat{A} , which acts upon the states in the respective Hilbert space.

(1.4) In the present case, the mathematical description is a state $|\Psi\rangle$ in a Hilbert space.

(1.5) In linear order in \hat{A} , the function applied to the state is described by

$$f_{linear}(|\Psi\rangle) = \hat{A}|\Psi\rangle, \text{ in linear order.} \tag{136}$$

(1.6) In general, each state $|\Psi\rangle$ is described by a linear combination of eigenvectors $|\Psi_{A,n}\rangle$ with eigenvalues a_n . Here, the case of discrete and different eigenvalues a_n , each with one eigenvector, is analyzed in detail, as other cases can be analyzed analogously:

$$f_{linear}(|\Psi\rangle) = \hat{A} \left| \sum_n \Psi_{A,n} \right\rangle = \sum_n a_n |\Psi_{A,n}\rangle \tag{137}$$

(1.7) In order to keep the state unchanged in a single measurement process, see part (1.2), that process must act upon an eigenvector:

$$f_{linear}(|\Psi_{A,n}\rangle) = \hat{A}|\Psi_{A,n}\rangle = a_n |\Psi_{A,n}\rangle, \text{ single measurement process.} \tag{138}$$

Therefore, a possible result of a single measurement process of a quantity A of an object, is one of the eigenvalues of the operator \hat{A} corresponding to A .

(2) In general, a state is a linear combination of eigenvectors. But a possible result of each single measurement process is an eigenvalue. As a consequence, there must be a second dynamics that provides the choice of the eigenvalue that occurs in the measurement.

(2.1) The derivation of the deterministic dynamics of indivisible VPs is completely general, as only analysis alias calculus has been used in the derivation. As a consequence, if a second dynamics would be deterministic, it would reduce the generality of the deterministic dynamics.

(2.2) Therefore, a general second dynamics must be a stochastic dynamics. This stochastic dynamics is derived next:

9.4. On the Stochastic Dynamics

In this section, the stochastic dynamics is derived from the properties of the indivisible VPs step by step in a progressive manner in the following paragraphs:

(1) For the case of a single indivisible VP δV_j , the probability to measure an indivisible VP at an event (τ, \vec{L}) is proportional to the VP's energy density $u_{indivisible VP,j}$, at that event (τ, \vec{L}) .

(2) The energy density $u_{indivisible VP,j}$ is related to the wave function as follows:

(2.1) For the case of a single indivisible VP δV_j , the WF is the time derivative of its relative additional volume, multiplied by a normalization factor t_n , see Section 5.2:

$$|\Psi_{indivisible VP j}\rangle = t_n \cdot \dot{\epsilon}_{indivisible VP j}. \tag{139}$$

(2.2) The absolute square is applied to the above equation:

$$|\Psi_{indivisible VP j}^2| = \langle \Psi_{indivisible VP j} | \Psi_{indivisible VP j} \rangle = t_n^2 \cdot \dot{\epsilon}_{indivisible VP j}^2. \tag{140}$$

(2.3) The above equation is multiplied by $1 = \frac{8\pi G}{c^2} \cdot \frac{c^2}{8\pi G}$:

$$|\Psi_{indivisible VP j}^2| = \frac{8\pi G}{c^2} t_n^2 \cdot \frac{c^2 \dot{\epsilon}_{indivisible VP j}^2}{8\pi G}. \tag{141}$$

(2.4) In the above equation, the second fraction is the energy density of the indivisible VP δV_j :

$$|\Psi_{indivisible VP j}^2| = \frac{8\pi G}{c^2} t_n^2 \cdot u_{indivisible VP j}. \tag{142}$$

(3) As a consequence, the probability $P_{indivisible VP j}$ to measure an indivisible VP at an event (τ, \vec{L}) is proportional to the WF's absolute square:

$$P_{indivisible VP j} \propto |\Psi_{indivisible VP j}^2|. \tag{143}$$

(4) For each measurable quantity A , and for the corresponding operator \hat{A} , the probability to measure an eigenvalue a_n of an eigenvector $|\Psi_{A,n}\rangle$ has been derived from the result in part (3) or in Equation (143) [65].

Therefore, the result in part (3) or in Equation (143) is the fundamental stochastic dynamics of quantum physics.

(5) As a consequence, the VD implies both, deterministic time evolution as well as the stochastic dynamics of quantum physics. Consequently, the VD implies the full dynamics of quantum physics. This is the case, as for their respective systems, quantum field

theory and the Dirac theory can both be derived with help of the above deterministic and stochastic dynamics [23,61,65,84,90].

Using the above mathematical results as well as the deterministic and stochastic dynamics, the postulates of quantum physics are derived next:

9.5. Derivation of the Postulates

In this section, it is shown how the quantum postulates [86] are implied by the VD:

(1) The postulate about the **deterministic time evolution** has been derived in Sections 5.2 and 9.1.

(2) The postulate about **probabilistic outcomes of measurements** is stated literally by Kumar [86] (pp. 169–170): If a measurement of an observable A is made in a state $|\Psi(t)\rangle$ of the quantum mechanical system, then, the following holds:

[1] The probability of obtaining one of the non-degenerate discrete eigenvalues a_j of the corresponding operator \hat{A} is given by

$$P(a_j) = \frac{|\langle\phi_j|\Psi\rangle|^2}{\langle\P|\Psi\rangle}, \tag{144}$$

where $|\phi_j\rangle$ is the eigenfunction of \hat{A} with the eigenvalue a_j . If the state vector is normalized to unity, $P(a_j) = |\langle\phi_j|\Psi\rangle|^2$.

[2] If the eigenvalue a_j is m_j -fold degenerate, this probability is given by

$$P(a_j) = \frac{\sum_{i=1}^{m_j} |\langle\phi_{j,i}|\Psi\rangle|^2}{\langle\P|\Psi\rangle}, \tag{145}$$

[3] If the operator \hat{A} possesses a continuous eigenspectrum $\{a\}$, the probability that the result of a measurement will yield a value between a and $a + da$ is given by

$$P(a) = \frac{|\langle\phi(a)|\Psi\rangle|^2}{\langle\P|\Psi\rangle} \cdot da = \frac{|\langle\phi(a)|\Psi\rangle|^2}{\int_{-\infty}^{\infty} |\Psi(a')|^2 da'} \cdot da \tag{146}$$

This postulate can be derived from the stochastic dynamics in Section 9.4. The derivation is presented in Carmesin [65,90,91].

(3) The postulate about **Hilbert space** is stated literally by Kumar [86] (p. 168): ‘The state of a quantum mechanical system, at a given instant of time, is described by a vector $|\Psi(t)\rangle$, in the abstract Hilbert space \mathcal{H} of the system.’

For each given quantum state, a respective full dynamics should be determined. It is the deterministic and stochastic dynamics in the above postulates (1) and (2). It has been shown here, that the states of the respective Hilbert space provide the full information to derive the deterministic time evolution (with the SEQ or with the GSEQ, more generally), and to derive the correct probabilities for the probabilistic outcomes. Therefore, for each time, a quantum state is characterized as a state inside a respective Hilbert space.

Moreover, it is insightful to realize that the correct probabilistic outcomes are a consequence of the gravitational properties of the VD. Therefore, it is enlightening to understand that the basis of the quantum postulates is a quantum gravitational foundation. As a consequence, a deep and fundamental understanding of quantum physics without understanding gravity and quantum gravity is hardly possible.

(4) The postulate about the **relation between observables and operators** is stated literally by Kumar [86] (p. 169): ‘A measurable physical quantity A (called an observable or dynamic physical quantity), is represented by a linear and hermitian operator \hat{A} acting in the Hilbert space of state vectors.’

This postulate is founded by the VD, as described in Section 9.3.

(5) The postulate about the relation between **outcomes of a measurement and eigenvalues** is stated literally by Kumar [86] (p. 169): ‘The measurement of an observable A in a given state may be represented formally by the action of an operator \hat{A} on the state vector $|\Psi(t)\rangle$. The only possible outcome of such a measurement is one of the eigenvalues, $\{a_j\}, j = 1, 2, 3, \dots$, of \hat{A} .’

This postulate is founded by the VD, as described in Section 9.3.

10. Emergence of Volume in Nature and of Its Energy Density

Here, the following results are derived: In a homogeneous and empty universe, the process of GFV (global formation of volume) of the universe is elaborated on the basis of LFV (local formation of volume), everywhere in the universe. Moreover, it is shown that this process provides exactly the complete volume of the universe. Furthermore, it is shown that this process provides an energy density of volume, $u_{vol} = \lim_{heterogeneity \rightarrow 0} u_{DE}$. Additionally, it is shown that this u_{vol} is in accurate concordance with empirical values of the dark energy density u_{DE} or u_{Λ} . These results are very insightful, as they show how the complete and global volume of the universe emerges from a local process: LFV.

10.1. On the Development and Improvements of the Lambda-CDM Model

Here, the development of the basic cosmology model (Λ CDM), is summarized and related to the new results derived in this paper.

Einstein [7] realized that general relativity theory (GRT) implies an expansion of space since a Big Bang, in general. Thereby, he introduced the cosmological constant Λ . Zeldovich [10] showed that corresponds to an energy density of space:

$$u_{\Lambda} = \frac{\Lambda c^4}{8\pi G} \tag{147}$$

Hubble [8] discovered the expansion of space and its rate H at the present-day time t_0 (with $t_{Big\ Bang} = 0$). That present-day rate $H(t_0) = H_0$ is called Hubble constant. Thereby, the expansion is modeled by homogeneous and isotropic universe. Hereby, the expansion is described with help of a uniform scaling, characterized by a scale radius R :

$$H := \frac{\dot{R}}{R}. \tag{148}$$

Based on GRT, Friedmann [17] and Lemaître [19] derived the dynamics of that expansion, depending on $\rho = \frac{u}{c^2}$ and a global curvature parameter k in the form of the Friedmann Lemaître equation (FLE):

$$H^2 = \frac{8\pi G}{3} \cdot \rho - \frac{k \cdot c^2}{R^2}. \tag{149}$$

Thereby, $k = 0$, based on empirical data [22], as well as on the basis of derivation [84,92]. A corresponding ρ value is called critical density:

$$H^2 = \frac{8\pi G}{3} \cdot \rho_{cr}, \quad \text{and} \quad H_0^2 = \frac{8\pi G}{3} \cdot \rho_{cr,0}. \tag{150}$$

Hereby and in general, present-day values are marked by a subscript zero. A good approximation of the universe’s age t_0 is the Hubble time $t_{H_0} := 1/H_0$ [20,40] and Equation (150):

$$t_0 \approx t_{H_0} := \frac{1}{H_0} = \sqrt{\frac{3}{8\pi G \cdot \rho_{cr,0}}}. \tag{151}$$

There is a FLE-insight: This Equation shows that t_{H_0} and t_0 cannot be chosen arbitrarily, these are results of the dynamic density ρ and of the dynamics of the FLE.

Therefore, the time evolution and dynamics of the density are essential. For its analysis, the density is a sum of parts with particular dynamical properties, $\rho = \rho_r + \rho_m + \rho_\Lambda$:

- (1) ρ_r is the dynamic density of radiation with $\rho_r \propto (R_0/R)^4$,
- (2) ρ_m describes $\frac{m}{V}$, with CDM [21,22], and with $\rho_m \propto (R_0/R)^3$
- (3) $\rho_\Lambda = \frac{u_\Lambda}{c^2}$ represents a dynamic density, corresponding to Λ , with $\rho_\Lambda \propto (R_0/R)^0$. That density has been discovered [9,15,16].

Therefore, ρ depends on the scale radius R and the density parameters $\Omega_j := \rho_j / \rho_{cr,0}$:

$$\rho = \rho_{r,0} \cdot (R_0/R)^4 + \rho_{m,0} \cdot (R_0/R)^3 + \rho_\Lambda = \rho_{cr,0} \cdot (\Omega_r(R_0/R)^4 + \Omega_m \cdot (R_0/R)^3 + \Omega_\Lambda) \tag{152}$$

There is a Λ CDM-insight: The above components of the density are underlying the model's name Λ CDM, it includes visible densities of radiation and of visible matter, as well as the dark densities that are not visible with help of electromagnetic radiation, cold dark matter and dark energy u_Λ alias u_{DE} . Additionally, the Λ CDM model uses the following idealizations:

- (1) a homogeneous and isotropic space,
- (2) the classical GRT without using the quantum dynamics,
- (3) a space described as one entity without using volume portions.

In this paper, these three idealizations are overcome. Thereby, precise accordance with observation is achieved, and a high predictive power is provided. Hereby, the volume's energy density is deduced from first principles as well as in three-dimensional space for the first time with this method.

Here, VPs are utilized to deduce the dark energy's density u_{DE} . Thereby, as a first step, a homogeneous universe is modeled. Therefore, u_{DE} is derived for the case with zero heterogeneity. The result is an idealized value $u_{vol} = \lim_{heterogeneity \rightarrow 0} u_{DE}$ of the density of space. Accordingly, the derived result is compared with an observation that is based on radiation emitted at a highly homogeneous universe, which is very young. This radiation represents the cosmic microwave background (CMB). The empirical data utilizing the CMB, provides a value of the energy density [22] as follows:

$$u_{\Lambda,obs} = 5.133^{+0.2432}_{-0.2432} \cdot 10^{-10} \frac{J}{m^3} \tag{153}$$

The emergence of the volume of the universe and of its energy density in Equation (153) are derived and explained in this Section 10.

10.2. Process of Local Formation of Volume in the Universe

Here, a fundamental process for the locally emerging volume that provides the complete volume of the universe is described. This description makes possible a test of the completeness of the formed volume. Moreover, this description makes possible a deduction of the volume's energy density u_{vol} . Additionally, the deduced value of u_{vol} is compared with respective empirically based values in Equation (153).

Firstly, that process uses the global flatness of space, the curvature parameter is zero, see Equations (149)–(151): Secondly, the description of that process uses a probe volume: Based on the invariance with respect to shifts (translation), the LFV in the universe is investigated by building up the volume dV_0 in Figure 8. Thereby, dV_0 describes a fixed

amount of three-dimensional extension, which has filled by volume of the universe in the time interval t_{H_0} :

$$dV_0 \text{ has been filled with volume of nature during } t_{H_0} \tag{154}$$

t_{H_0} is named Hubble time.

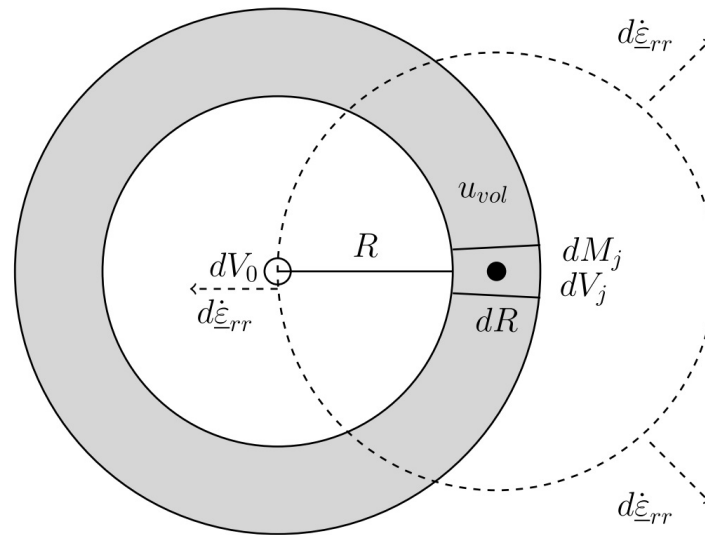


Figure 8. A probe volume dV_0 is in the middle of a shell with radius R . In that shell, there is $dM_j = dE_j/c^2$ (black dot), which causes rates $d\dot{\epsilon}_{rr}$, that propagate (dashed arrows) in the form of VPs or RGWs (freely propagating waves according to the VD) in all directions (dashed circle and dashed arrows) in the same manner.

Thirdly, that process is described step by step in the following paragraphs:

- (1) Local origin of the rate of LFV at dV_0 : Empty space is investigated here. Consequently, LFV is caused at dV_0 by the volume increments or VPs dV_j , see Figure 8. The corresponding energy is described by the energy dE_j or equivalently by the dynamic mass $dM_j = dE_j/c^2$. Each dM_j causes a $\dot{\epsilon}_{L,rr, at dV_0}(dM_j)$ within dV_0 , according to the law of LFV.

$$dM_j \text{ causes the rate } \dot{\epsilon}_{L,rr, at dV_0}(dM_j) \tag{155}$$

- (2) Complete rate of LFV at dV_0 :

(2.1) The complete $\dot{\epsilon}_{L,rr, at dV_0}$ within dV_0 represents the sum of all rates in the above part (1).

(2.2) The complete rate is identified with the Hubble constant H_0 : $\dot{\epsilon}_{L,rr, at dV_0}(t_0)$ within dV_0 is equal to $\dot{\epsilon}_{L,iso, at dV_0}/3$:

$$\dot{\epsilon}_{L, rr, at dV_0} = \frac{1}{3} \cdot \dot{\epsilon}_{L, iso, at dV_0} = \frac{1}{3} \cdot \left(\dot{\epsilon}_{L, xx, at dV_0} + \dot{\epsilon}_{L, yy, at dV_0} + \dot{\epsilon}_{L, zz, at dV_0} \right). \tag{156}$$

As a matter of calculus, H_0 represents the following [65]:

$$H_0 = H(t_0) = \frac{1}{3} \cdot \frac{\dot{V}}{V}. \tag{157}$$

$\frac{\dot{V}}{V}$ as well as $\dot{\epsilon}_{L,iso, at dV_0}$ represent identical emerging isotropic volume within dV_0 [65]:

$$H_0 = \frac{\dot{V}}{3V} = \frac{\dot{\epsilon}_{L, iso, at dV_0}}{3} = \dot{\epsilon}_{L, rr, at dV_0} = \frac{\dot{R}}{R}. \tag{158}$$

- (3) The complete rate provides the complete volume of nature in dV_0 : By definition, $\dot{\underline{\epsilon}}_{L,rr, at dV_0}$ represents the volume $\underline{\delta}V_{rr}$ that forms in a considered volume dV_0 during a time $\underline{\delta}t$:

$$\dot{\underline{\epsilon}}_{L,rr, at dV_0} = \frac{\underline{\delta}V_{rr}}{\underline{\delta}t \cdot dV_0} \tag{159}$$

For the purpose of a deduction of the complete volume formed in dV_0 during the complete Hubble time t_{H_0} , this Equation is solved for the formed volume, the rate $\dot{\underline{\epsilon}}_{L,rr, at dV_0} = H_0$ is used, and the complete time $\underline{\delta}t = t_{H_0}$ is utilized:

$$\underline{\delta}V_{rr} = \underbrace{H_0 \cdot t_{H_0}}_1 \cdot dV_0 = dV_0. \tag{160}$$

Therefore, the complete probe volume dV_0 is filled with LFV. Translation invariance is the basis for the fact that the probe volume represents the complete volume of the universe. Consequently, the complete volume of the universe forms during the Hubble time. Altogether, this is the above introduced first test of the process: The described process shows how the LFV forms exactly the GFV. Thereby, the LFV takes place in the complete space inside the Hubble radius and during the complete Hubble time. This result provides a great additional evidence for the theory of VPs derived above.

10.3. Derivation of the Volume's Energy Density

Here, the formation of LFV in Section 10.2 of volume on the basis of the LFV-dynamics is elaborated in more quantitative detail. Thereby, the energy density $u_{vol} = \lim_{heterogeneity \rightarrow 0} u_{DE}$ of volume is derived, and it is shown that u_{vol} is in precise accordance with observation.

10.3.1. Rate of Formation of Volume by a Volume Portion

A VP dV_j with dM_j in Figure 8 is as follows:

$$dM_j = dV_j \cdot \rho_{vol} \tag{161}$$

Exact gravity provides, see the section about gravity or [65]

$$|d\vec{G}_j^*|(R) = \frac{G \cdot dM_j}{R^2}. \tag{162}$$

The propagation of the above gravity is explained and deduced in the framework of the RGW, see also Figure 8. Hhereby, RGWs caused by dM_j show no destructive interference. This is shown in part eight of Section 10.2.

Equations (96) and (107) imply for each dM_j

$$d\dot{\underline{\epsilon}}_{L, rr, at dV_0}(R, dM_j) = \frac{|d\vec{G}_j^*|(R)}{c} = \frac{G \cdot dM_j}{R^2 \cdot c}. \tag{163}$$

10.3.2. Rate of Formation of Volume by One Shell

dM_j in Figure 8 causes LFV as follows:

Shell with center dV_0 :

The dM_j in Figure 8 cause portions of LFV that add up in a shell as follows

$$dM(R, dR) = \sum_{j, R_j \in \text{shell}} dM_j \tag{164}$$

Rate caused by above shell:

Equations (163) and (164) imply

$$\sum_{j, R_j \in \text{shell}} d\dot{\epsilon}_{L, rr, at dV_0}(R, dM_j) = \frac{G \cdot \sum_{j, R_j \in \text{shell}} dM_j}{R^2 \cdot c} \tag{165}$$

The sum in that Equation is equal to $dM(R, dR)$ in Equation (164):

$$d\dot{\epsilon}_{L, rr, at dV_0}(R, dR) = \frac{G \cdot dM(R, dR)}{R^2 \cdot c} \tag{166}$$

Using ρ_{vol} :

Geometrically, $dM(R, dR) = \rho_{vol} \cdot dV$ with the shell's $dV = 4\pi \cdot R^2 \cdot dR$:

$$dM(R, dR) = \rho_{vol} \cdot 4\pi \cdot R^2 \cdot dR \tag{167}$$

Consequently, the rate in Equation (166) becomes

$$d\dot{\epsilon}_{L, rr, at dV_0}(R, dR) = \frac{4\pi \cdot G \cdot \rho_{vol} \cdot dR \cdot R^2}{R^2 \cdot c} \tag{168}$$

The terms R^2 cancel:

$$d\dot{\epsilon}_{L, rr, at dV_0}(dR) = \frac{4\pi \cdot G \cdot \rho_{vol} \cdot dR}{c} \tag{169}$$

10.3.3. Light-Travel Time of One Shell

Here, indivisible VPs emitted within the shell in Figure 8 are characterized by the time t_{LT} , in which they travel to the probe volume dV_0 .

A VP travels with the speed $v = c$. Therefore, a VP travels through the shell with the thickness dR during the light travel time $dt_{LT} = dR/c$:

$$dt_{LT} = \frac{dR}{c} \tag{170}$$

Accordingly, dR/c in Equation (169) is substituted by dt_{LT} :

$$d\dot{\epsilon}_{L, rr, at dV_0}(dt_{LT}) = 4\pi \cdot G \cdot \rho_{vol} \cdot dt_{LT} \tag{171}$$

Thereby, since the Big Bang until today, the light travel times range from $dt_{LT} = 0$ to the Hubble time $dt_{LT} = t_{H_0}$:

10.3.4. Spatial Integration of the Shells

Here, shells within Figure 8 are integrated: Thereby, all VPs dV_j that emit volume portions that can propagate to the probe volume are included. Therefore, the integration includes exactly the sources in space that provide a rate of LFV at the probe volume dV_0 . Practically, this complete spatial integral is executed by the integration variable time according to the substitution in Section 10.3.3.

Consequently, integration intervals are $[0, t_{H_0}]$, as well as $[0, \dot{\epsilon}_{L, rr, at dV_0}]$. Therefore, Equation (171) implies:

$$\int_0^{\dot{\epsilon}_{L, rr, at dV_0}} d\dot{\epsilon}_{L, rr, at dV_0} = 4\pi \cdot G \cdot \rho_{vol} \cdot \int_0^{t_{H_0}} dt_{LT} \tag{172}$$

The above integral is evaluated:

$$\dot{\epsilon}_{L, rr, at dV_0} = 4 \cdot \pi \cdot G \cdot \rho_{vol} \cdot t_{H_0} \tag{173}$$

That rate represents H_0 , see Equation (158):

$$H_0 = 4\pi \cdot G \cdot \rho_{vol} \cdot t_{H_0} \tag{174}$$

The above Equation is divided by t_{H_0} :

$$\frac{H_0}{t_{H_0}} = \rho_{vol} \cdot 4\pi \cdot G \tag{175}$$

According to the FLE-insight in Section 10.1, the values of H_0 and t_{H_0} are functions of the density. Therefore, the result in Equation (175) is valid and derived in our universe.

Next, Equation (175) is solved for $\rho_{vol} = u_{vol} / c^2$:

$$\rho_{vol} = \frac{H_0}{t_{H_0}} \cdot \frac{1}{4\pi \cdot G} \tag{176}$$

$H_0 = 1/t_{H_0}$ is utilized (Equations (175) and (176)). Moreover, the equality of rates $\dot{\epsilon}_{L, rr, at dV_0} = H_0$ in Equation (158) is used:

$$\rho_{vol} = \frac{H_0^2}{4\pi \cdot G} \quad \text{or} \quad u_{vol} = \frac{H_0^2 c^2}{4\pi \cdot G} \tag{177}$$

10.3.5. Derivation for a Comparison with Observation

Equation (177) shows:

$$u_{vol} = \frac{c^2 \cdot H_{0,empty}^2}{4 \cdot \pi \cdot G} \tag{178}$$

$H_{0,empty}$ represents the respective value for empty space. Empirical data show

$$\begin{aligned} u_{vol} &= \frac{c^2 H_{0,empty}^2}{4\pi G} = 5.034 (\pm 0.1395) \cdot 10^{-10} \frac{\text{J}}{\text{m}^3}, \quad \text{with} \\ H_{0,empty} &= 66.88 (\pm 0.92) \frac{\text{km}}{\text{s} \cdot \text{Mpc}} \end{aligned} \tag{179}$$

For H_0 see [22]. H_0 is related to our universe's age $t_0 \approx 1/H_0$. An accurate Equation is deduced in Carmesin [40]. The empirical quantity $u_{\Lambda,obs}$ is, see [22]:

$$u_{\Lambda,obs} = 5.133_{-0.2432}^{+0.2432} \cdot 10^{-10} \frac{\text{J}}{\text{m}^3} \tag{180}$$

Hereby, it is important that H_0 and $u_{\Lambda,obs}$ are observed in a very homogeneous state of the universe. Such a homogeneous state corresponds to the young universe, observable via the CMB. For it, very accurate data have been obtained by [22].

Discussion of the results of this Section 10.1: The deduced value u_{vol} corresponds accurately to the empirical data $u_{\Lambda,obs}$, within the error of measurement ± 0.2432 . Therefore, the deduced u_{vol} is a second test of the LFV in this Section 10.1. Together with the first test of the exact amount of formed volume, both tests provide a clear evidence for that process of formation of volume and for the theory of VPs. It is a new result that this founded, comprehensive (see Figure 5) and deduced theory based on derived discrete volume portions provides the functional relation for u_{vol} , see Equation (179).

11. Emergence of Volume in a Homogeneous Universe

Here, the above density u_{vol} has been derived for the case of an empty universe. In this Section 11, the density u_{vol} of volume of a homogeneous non-empty univ. is deduced. Therefore, that above model used in Section 10 is supplemented by a homogeneous density ρ_{hom} of radiation and matter, whereby the heterogeneity of radiation and matter is not included. For it, it is essential to summarize the concepts of averaging in cosmology first, see Section 11.1:

11.1. Spatial Averages in Cosmology

Spatial averaging in cosmology uses regions. For instance, Figure 9 shows such regions. Thereby, space is partitioned into boxes with volume L_{box}^3 , and with length L . For each box or window, a density is measured or determined [36,45,93,94]. The following terms are used:

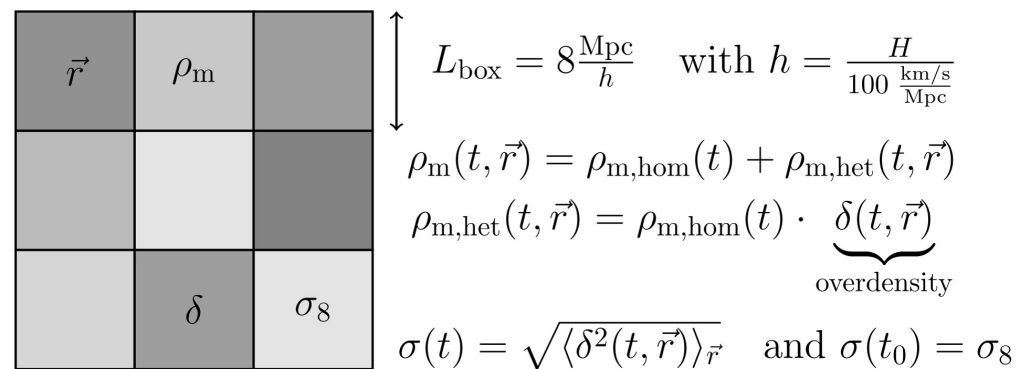


Figure 9. Space is partitioned into boxes or windows. Each box has a vector \vec{r} of location, and a local density ρ_m . The average of these local values $\rho_m(t, \vec{r})$ with respect to space is named $\rho_{m,hom}(t)$ or homogeneous density. At each box, the difference $\rho_m(t, \vec{r}) - \rho_{m,hom}(t)$ is deduced. The ratio $\delta(t, \vec{r}) = \frac{\rho_{m,het}(t, \vec{r})}{\rho_{m,hom}(t)}$ is called relative difference, or overdensity. The squares $\delta^2(t, \vec{r})$ are averaged with respect to the boxes, then the root is applied, in order to obtain the standard deviation of matter fluctuations $\sigma_8(t)$. $\sigma_8(t_0)$ is abbreviated by σ_8 .

Boxes: Each box has a length L_{box} , with a basic length as follows [36,93,95]:

$$L_{box} = 8h^{-1} \text{ Mpc} \quad \text{with} \quad h = H_0 \cdot \frac{1}{100} \frac{\text{km}}{\text{s} \cdot \text{Mpc}} \tag{181}$$

Local density: At each time t , each box is at a place \vec{r} , and has a density

$$\text{local density} \quad \rho_m(t, \vec{r}). \tag{182}$$

Global density: The homogeneous density is the density's global spatial average

$$\text{global density} \quad \rho_{m,hom}(t) = \langle \rho_m(t, \vec{r}) \rangle_{\vec{r}} \tag{183}$$

Density of heterogeneity: The following difference is named density of heterogeneity:

$$\rho_{m,het}(t, \vec{r}) := \rho_m(t, \vec{r}) - \rho_{m,hom}(t). \tag{184}$$

Overdensity: the following fractional difference is named overdensity:

$$\text{overdensity} \quad \delta(t, \vec{r}) := \frac{\rho_m(t, \vec{r}) - \rho_{m,hom}(t)}{\rho_{m,hom}(t)}. \tag{185}$$

The constituents of ρ are

$$\rho = \rho_{m,hom}(t) + \rho_{m,het}(t, \vec{r}) + \rho_r + \rho_\Lambda. \tag{186}$$

Averages of Fluctuations

In cosmology, spatial averages are as follows [36,45,93]. In general, function $f(\vec{r})$ occurs in a volume V_{window} or V_{win} of averaging:

$$\langle f(\vec{r}) \rangle_{V_{win}} = \frac{\int_{V_{win}} f(\vec{r}) \, dr^3}{\int_{V_{win}} 1 \, dr^3} \tag{187}$$

Fluctuations can be described via the standard deviation $\sigma_{V_{win}}$:

$$\sigma_{V_{win}}^2 = \langle [f(\vec{r}) - \langle f(\vec{r}) \rangle_{V_{win}}]^2 \rangle_{V_{win}} = \langle f^2(\vec{r}) \rangle_{V_{win}} - \langle f(\vec{r}) \rangle_{V_{win}}^2 \tag{188}$$

In particular, for the case of the matter, the standard deviation is called standard deviation of matter fluctuations, $\sigma_8(t)$ or $\delta(t)$:

$$\sigma_8(t) = \delta(t) = \sigma_{\delta, V_{win}}(t) \quad \text{with} \quad \sigma_{8,0} = \sigma_8(t_0) \tag{189}$$

11.2. Expectation Values of Fields

In order to observe densities in cosmology, more local observations are averaged as outlined in Section 11.1. The corresponding theoretical values are expectation values. Those expectation values are investigated in this section, which are essential for the LFV at the probe volume dV_0 . That LFV is based on Equation (97):

$$\hat{\xi}_{L,ii}^2 \cdot c^2 = (\vec{G}_i^*)^2 \tag{190}$$

Therefore, for various objects, the important expectation values are derived in respective paragraphs, and an overview is presented in Table 1:

- (1) One separate mass m_j has a gravitational field, which is classical. Consequently, m_j is characterized in terms of a coherent state [62,65,96,97]. Consequently, the field's expectation value $\langle \Psi | \vec{G}_j | \Psi \rangle$ cannot be zero, and the standard deviation $\sigma = \langle \Psi | \vec{G}_j^2 | \Psi \rangle - \langle \Psi | \vec{G}_j | \Psi \rangle^2$ of the field is nearly zero. In this study, the classical expectation values for one mass are not essential (see columns five and six in Table 1):

Table 1. Expectation values of fields and the standard deviation or uncertainty of the field $\sigma := \langle \Psi | \vec{G}_j^2 | \Psi \rangle - \langle \Psi | \vec{G}_j | \Psi \rangle^2$ of the field. Hereby, the expectation value $\langle \Psi | \vec{G}_j | \Psi \rangle$ is abbreviated by $\langle \vec{G}_j \rangle$.

Object	State	$\langle \vec{G}_j \rangle$	σ	$\frac{1}{N} \sum_j^N \langle \vec{G}_j \rangle$	$\frac{1}{N} \sum_j^N \langle \vec{G}_j \rangle^2$	$\langle \hat{\xi}_{L,rr}^2, \text{ at } dV_0 \rangle$
m_j	coherent	$\neq 0$	≈ 0	-	-	$\neq 0$
$VP_{indivisible}$	number	0	$\neq 0$	0	0	$\neq 0$
$\rho_{m,het}$	coherent	$\neq 0$	≈ 0	0	$\neq 0$	$\neq 0$
$\rho_{m,hom}$	coherent	$\neq 0$	≈ 0	0	0	0

- (1.1) In empty space, there is no mass.
- (1.2) In the non-empty homogeneous universe, the fields of masses are completely averaged to zero.
- (1.3) In the case of a heterogeneous density, there are many masses, whereby their fields average to zero, and the standard deviations of the fields remain.

Consequently, the nonzero expectation value of the field is not averaged out to zero. Therefore, such a mass contributes to the LFV at the probe mass (see column seven in Table 1). Such a single mass is not essential at the large scales of several Megaparsecs considered here. This case is included for comparison only.

- (2) For the case of an indivisible VP, the gravitational field is not classical. Accordingly, the VP is characterized in terms of a number state [62,65,96,97]. Thence, the expectation value $\langle \Psi | \vec{G}_j | \Psi \rangle$ of the field is zero, but the standard deviation is nonzero, $\sigma = \langle \Psi | \vec{G}_j^2 | \Psi \rangle - 0 \neq 0$. The classical expectation values are not essential for an indivisible VP, as no classical fields can cancel out. Similarly, the quanta of electromagnetic radiation propagate from our home star to our home planet, without cancellation—otherwise it would be dark at Earth at night and at day. Consequently, the nonzero standard deviation contributes to the LFV at the probe mass (see column seven in Table 1).
- (3) For the case of the heterogeneous density, radiation is not essential. The reason is, that in our universe, heterogeneity developed at a time, at which the density of radiation was already negligible. Accordingly, the heterogeneous density is analyzed for masses only. Similarly, the homogeneous density is analyzed for masses only. In the case of the heterogeneous density, gravitational fields are classical. Consequently, they are described by coherent states [62,65,77,96,97]. Thus, the expectation value $\langle \Psi | \vec{G}_j | \Psi \rangle$ of the field of one mass m_j is nonzero, and the standard deviation is negligible. The classical expectation value of all fields is zero. But the classical expectation value of all squared fields is nonzero. Therefore, the heterogeneous density contributes to the LFV at the probe mass (see column seven in Table 1).
- (4) For the case of the homogeneous density, gravitational fields are classical. Consequently, they are described by coherent states [62,65,77,96,97]. Thus, the expectation value of the field of one mass m_j is nonzero, and the standard deviation is negligible. But the classical expectation values of all fields and of all squared fields is zero. Therefore, the homogeneous density does not contribute to the LFV at the probe mass (see column seven in Table 1).

11.3. Energy Density of Volume

As the homogeneous density $\rho_{m,hom}$ of matter does not contribute to the LFV at dV_0 , the volume’s energy density u_{vol} is equal to that of the empty universe in Equation (179).

In the case of the homogeneous universe, there is sufficient content, that the density parameter can be derived in a meaningful manner:

$$\Omega_{vol} := \frac{u_{vol}}{u_{cr,0}} = \frac{\rho_{vol}}{\rho_{cr,0}} \tag{191}$$

The respective terms in Equations (150) and (177) are inserted:

$$\Omega_{vol} = \frac{\frac{H_0^2}{4\pi \cdot G}}{\frac{3H_0^2}{8\pi \cdot G}} = \frac{2}{3} \tag{192}$$

This is in accurate concordance with empirical data ([22], table 2, column 2), within errors of measurement:

$$\Omega_{\Lambda} = 0.679 \pm 0.013 \tag{193}$$

Therefore, this result of the homogeneous universe provides clear additional evidence for the present mechanism of formation and for the theory of volume portions.

12. Emergence of Volume in a Heterogeneous Universe

In the cases of the empty and of the homogeneous universe, the flatness of space can be used, see Sections 10 and 11. On that basis, and by using adequate coordinate systems (ACS), it is possible to use a regular and constant evolution of time.

$u_{vol} = u_{DE}$, with heterogeneity 0 differs from the corresponding value u_{DE} in the heterogeneous universe. Space's density or volume's density in a heterogeneous universe and in present-day's universe are marked by u_{DE} . The density of space or volume in a homogeneous univ. and in an extremely young univ. is denoted by u_{vol} . The cosm. const. Λ and a corresponding energy density of space u_Λ describe our present-day universe, since Einstein [7] proposed Λ without any specification of the early universe or of a particularly homogeneous universe different from the present-day universe. In each case, a fraction of an energy's density u_j and the critical energy density $u_{cr.} = \rho_{cr.} \cdot c^2$ represents the respective density parameter:

$$\Omega_j = \frac{u_j}{u_{cr.}} \tag{194}$$

Moreover, in the cases of empty and homogeneous universe, u_{DE} is a constant, so that the essential density parameters $\Omega_m := \frac{\rho_m}{\rho_{cr,0}}$ of matter and $\Omega_\Lambda = \frac{\rho_\Lambda}{\rho_{cr,0}}$ of the cosmological constant are essentially constant.

However, in the heterogeneous universe, ρ_Λ and Ω_Λ increase. This causes an increase of H_0 . Indeed, such an increase has been recorded empirically [13,22]. Consequently, the Hubble time t_{H_0} decreases.

For these reasons, the changes of Ω_Λ and of t_{H_0} are analyzed simultaneously in this section.

12.1. VPs Field and Rate Caused by Heterogeneity

In this section, based on the LFV in the homogeneous universe, the additional LFV is derived step by step in respective paragraphs, that additional LFV is caused by heterogeneity.

- (1) Overdensity δ_j of one dM_j : dM_j is in its $dM(R, dR)$ -shell in Figure 8. Its density is dM_j/dV_j . Consequently, its overdensity is

$$\delta_j = \frac{dM_j/dV_j - \rho_{m,hom}}{\rho_{m,hom}} \tag{195}$$

The above fraction is expanded by the shell's volume $dV = 4\pi R^2 \cdot R$:

$$\delta_j = \frac{dM_j \cdot \frac{dV}{dV_j} - dM(R, dR)}{dM(R, dR)} \quad \text{with} \quad dM(R, dR) = 4\pi R^2 dR \cdot \rho_{m, hom} = dV \rho_{m, hom} \tag{196}$$

- (2) δ_j causes a rate: The overdensity δ_j in Equation (196) multiplied by the mass $dM(R, dR)$ is the mass of heterogeneity. The field's $1/R^2$ law ($\vec{G}^* = -\frac{GM}{R^2} \vec{e}_R$) implies

$$d\vec{G}_{gen,j} = -G \frac{dM_j \cdot \frac{dV}{dV_j} - dM(R, dR)}{R^2} \vec{e}_R = -G \frac{\delta_j \cdot dM(R, dR)}{R^2} \vec{e}_R. \tag{197}$$

The shell in Figure 8 provides an average $\langle \dots \rangle_{s,R}$. It is applied to the field's square in Equation (197):

$$\langle d\vec{G}_{gen,j}^2 \rangle_{s,R} = \left(G \frac{dM(R, dR)}{R^2} \right)^2 \cdot \langle \delta_j^2 \rangle_{s,R}, \quad \text{with} \tag{198}$$

$$\langle \delta_j^2 \rangle_{s,R} = \frac{\int_{shell} \delta_j^2 d^3x}{\int_{shell} 1 d^3x} \tag{199}$$

Equation (190) implies that the squared field causes the following squared rate:

$$d\bar{G}_{gen, j}^2 = c^2 d\dot{\xi}_{L, rr}^2 \quad \text{therefore,} \tag{200}$$

$$\left(G \cdot \frac{dM(R, dR)}{R^2} \right)^2 \cdot \langle \delta_j^2 \rangle_{s, R} = c^2 \cdot \langle d\dot{\xi}_{L, rr}^2 \rangle_{s, R} \tag{201}$$

Here, the power with exponent 0.5 is applied. Equation (196) is used. Moreover, $dR = c \cdot dt$ is utilized:

$$4 \cdot \pi \cdot G \cdot dt \rho_{m, hom} \cdot \sqrt{\langle \delta_j^2 \rangle_{s, R}} = \sqrt{\langle d\dot{\xi}_{L, rr}^2 \rangle_{s, R}} \tag{202}$$

Here, standard deviations (or uncertainties such as $\Delta\dot{\xi}_{het}$ or $d\dot{\xi}_{het}$, in the language of physics) are utilized:

$$\sigma_m := \sqrt{\langle \delta_j^2 \rangle_{s, R}} \tag{203}$$

$$d\dot{\xi}_{het} := \sqrt{\langle d\dot{\xi}_{L, rr}^2 \rangle_{s, R}} \tag{204}$$

Rate caused by heterogeneity: The rate in Equations (202) and (204) caused by $\rho_{m,het}$ is the standard deviation $d\dot{\xi}_{het}$. It is written by using usual density parameters of homogeneous densities:

$$\Omega_{vol} = \frac{\rho_{vol}}{\rho_{cr, 0}} \tag{205}$$

$$\Omega_m = \frac{\rho_{m, hom}}{\rho_{cr, 0}} \tag{206}$$

Consequently, $\rho_{m, hom}$ is

$$\rho_{m, hom} = \rho_{vol} \cdot \frac{\Omega_m}{\Omega_{vol}}. \tag{207}$$

With it, Equations (202)–(204) imply

$$4\pi G dt \rho_{vol} \cdot \frac{\Omega_m}{\Omega_{vol}} \sigma_m = d\dot{\xi}_{het}. \tag{208}$$

In the evolution of the universe, gravity accumulated matter. As a consequence, the standard deviation of matter fluctuations σ_m increased as a function of time. This increase is modeled next in part (3):

- (3) Linear growth theory: That theory implies $\sigma(\tilde{a})$ or $\sigma_8(\tilde{a})$ (standard deviation of matter fluctuations) depending on \tilde{a} (scale radius) [36,46,94]:

$$\sigma_m(\tilde{a}) = \sigma_8 \cdot \tilde{a} \tag{209}$$

Essential for the growth of heterogeneity is the matter era. In that era, $\tilde{a} = \tilde{t}^{2/3}$. This is documented in Karttunen et al. [98] ([Equation 19.33]). More details are provided in Carmesin [99] (p. 297):

$$\tilde{a} = \tilde{t}^{q_a} \quad \text{with} \quad q_a = \frac{2}{3} \tag{210}$$

Application of Equation (209) implies

$$\sigma_m = \sigma_8 \cdot \tilde{t}^{2/3}. \tag{211}$$

- (4) Time integral of the rate caused by heterogeneity: The time evolution in Equation (211) is inserted into the rate $d\dot{\epsilon}_{het}$ caused by heterogeneity in Equation (208) is as follows:

$$d\dot{\epsilon}_{het} = 4\pi G\rho_{vol} \cdot \frac{\Omega_m}{\Omega_{vol}} \cdot \sigma_8 \cdot \tilde{t}^{2/3} \cdot dt \tag{212}$$

- (4.1) Different Hubble times: Since $t_{H_0} = 1/H_0$, these times differ in the heterogeneous and homogeneous univ. $t_{H_0,hets} = 1/H_{0,hets} \neq t_{H_0,homs} = 1/H_{0,homs}$. The fraction is introduced:

$$q_t := \frac{t_{H_0,hets}}{t_{H_0,homs}} \tag{213}$$

The value is derived by an iteration. As a first step, the value 0.881 is chosen. That value has to be compared with the values of $t_{H_0,homs}$ and $t_{H_0,hets}$ that will be derived:

$$q_t^{(1)} = 0.881, \text{ as a first step.} \tag{214}$$

- (4.2) Scaled time: t_0 (present-day time) is $t_{H_0} \cdot I_0 = 0.9455$, see ([40], Equation (2.32))

$$t_0 = t_{H_0} \cdot I_0, \text{ with } I_0 = 0.9455. \tag{215}$$

The rate in Equation (212) and in general, the increment of time dt is scaled by the Hubble time. The idealized value is $t_{H_0,homs}$. The realistic value is $t_{H_0,hets}$, which must be multiplied by I_0 . Consequently, the realistic scaled increment is as follows:

$$d\tilde{t} = \frac{dt}{t_{H_0,hets} \cdot I_0} \tag{216}$$

This Equation is solved for dt , and the ratio in Equation (213) is used:

$$dt = d\tilde{t} \cdot t_{H_0,homs} \cdot I_0 \cdot q_1 \tag{217}$$

This realistic scaling is applied to the rate in Equation (212):

$$d\dot{\epsilon}_{het} = [4\pi G t_{H_0,homs} \rho_{vol}] \cdot \frac{\Omega_m \sigma_8}{\Omega_{vol}} \cdot q_1 \cdot I_0 \cdot \tilde{t}^{2/3} \cdot d\tilde{t} \tag{218}$$

Hereby, the rectangular bracket is equal to the rate $\dot{\epsilon}_{L,rr}$, at dV_0 at the homogeneous universe. This rate is abbreviated by $\dot{\epsilon}_{homs}$. Therefore, the rate in the heterogeneous universe in Equation (218) has the following relation to the rate in the homogeneous universe:

$$d\dot{\epsilon}_{het} = \dot{\epsilon}_{homs} \cdot \frac{\Omega_m \sigma_8}{\Omega_{vol}} \cdot q_1 \cdot I_0 \cdot \tilde{t}^{2/3} \cdot d\tilde{t} \tag{219}$$

- (4.3) **Integration:** The integral is applied to the above Equation:

$$\int_0^{\Delta\dot{\epsilon}_{het}} d\dot{\epsilon}_{het} = \dot{\epsilon}_{homs} \cdot \frac{\Omega_m \cdot \sigma_8}{\Omega_{vol}} \cdot q_1 \cdot I_0 \cdot \int_0^{\tilde{t}_{em}} \tilde{t}^{2/3} \cdot d\tilde{t} \tag{220}$$

The integrals are evaluated:

$$\Delta\dot{\epsilon}_{het} = \dot{\epsilon}_{homs} \cdot \frac{\Omega_m \cdot \sigma_8}{\Omega_{vol}} \cdot q_1 \cdot I_0 \cdot \frac{3}{5} \cdot \tilde{t}_{em}^{5/3} \tag{221}$$

The ratio $\frac{\Delta\dot{\xi}_{het}}{\dot{\xi}_{hom}}$ of the rates of the heterogeneous and of the homogeneous universe is formed, and it is named κ_{q_t} . Moreover, the scaled time is expressed by the scaled scale radius with the relation $\tilde{t} = \tilde{a}^{3/2}$ in Equation (210):

$$\kappa_{q_t}(\tilde{t}_{em}) := \frac{\Delta\dot{\xi}_{het}(\tilde{t}_{em})}{\dot{\xi}_{hom}} = \tilde{a}_{em}^{5/2} \cdot \frac{\Omega_m \sigma_8}{2\Omega_{vol}} \cdot \underbrace{\frac{6q_t^{(1)} I_0}{5}}_1 \cdot \frac{q_t^{(n)}}{q_t^{(1)}} \tag{222}$$

Hereby, $q_t^{(n)}$ is determined by an iteration, here a fixed point iteration will be performed. The fixed point iteration is a valid mathematical method to solve the physically based equations of this Section 12 simultaneously. Thereby, the first value for $q_t^{(n)}$ is $q_t^{(1)}$. With it and Equation (213), the Hubble times are obtained, and with these, the new value $q_t^{(2)} \frac{t_{H_0,het}}{t_{H_0,hom}}$ is calculated numerically. This procedure is repeated, until the n -th value $q_t^{(n)}$, at which $q_t^{(n)}$ and the following value $q_t^{(n+1)}$ are equal for the first time, up to an accepted numerical error. Next, the scaled scale radius is expressed by the redshift with the relation $\tilde{a}^{5/2} = \left(\frac{1}{1+z}\right)^{5/2}$:

$$\kappa_{q_t}(z_{em}) = \frac{\Omega_m \cdot \sigma_8}{2\Omega_{vol}(1+z_{em})^{2.5}} \cdot \frac{q_t^{(n)}}{q_t^{(1)}} \tag{223}$$

12.2. Complete Rate in the Heterogeneous Universe

In this section, the rate of the homogeneous and of the heterogeneous univ. are added and studied.

- (1) Addition: The sum of $\Delta\dot{\xi}_{het}(\tilde{t}_{em})$ and $\dot{\xi}_{hom}$ is forms the complete rate:

$$\dot{\xi}_{sum} := \Delta\dot{\xi}_{het} + \dot{\xi}_{hom} = \dot{\xi}_{hom} \cdot (1 + \kappa) \tag{224}$$

Hereby and in the following, the ratio κ_{q_t} is abbreviated by κ , as a short notation.

- (2) Rate of LFV for the sum of rates: The integrated rate $\dot{\xi}_{L,rr}$, at dV_0 , shortly called $\dot{\xi}_{hom}$ in Equation (173) is used:

$$\dot{\xi}_{hom} = 4\pi \cdot G \cdot \rho_{vol} \cdot t_{H_0,hom} \tag{225}$$

The corresponding rate in the heterogeneous universe is the complete rate $\dot{\xi}_{sum}$. The above relation (Equation (225)) is transferred to the complete rate by replacing corresponding terms: The rate $\dot{\xi}_{hom}$ corresponds to $\dot{\xi}_{sum}$. The density $\rho_{vol} = u_{vol}/c^2$ corresponds to $\rho_\Lambda = u_\Lambda/c^2$. The Hubble time $t_{H_0,hom}$ corresponds to $t_{H_0,het}$. Therefore, the above relation is transferred to the following rate:

$$\dot{\xi}_{sum} = 4\pi \cdot G \cdot \rho_\Lambda \cdot t_{H_0,het} \tag{226}$$

- (3) Ratio of rates: The ratio of the rates in Equations (225) and (226) is formed:

$$\frac{\dot{\xi}_{sum}}{\dot{\xi}_{hom}} = \frac{t_{H_0,het}}{t_{H_0,hom}} \cdot \frac{\rho_\Lambda}{\rho_{vol}} \tag{227}$$

$$\frac{1}{1+\kappa} = \frac{H_0,hom}{H_0,het} \cdot (1+\kappa)^{\xi(z)}$$

Hereby, the first fraction is the rate ratio, it is implied by Equation (224). Similarly, the second ratio of Hubble times is equal to the corresponding ratio of Hubble constants, as $t_{H_0} = 1/H_0$. For each redshift z_{em} or z (in a short notation), the third ratio of dynamic densities is an unknown number, which depends on the redshift z :

$$\frac{\rho_{\Lambda}}{\rho_{vol}} = \text{unknown}(z) = (1 + \kappa)^{\xi}, \quad \text{with } \xi = \xi(z) \text{ and } \kappa = \kappa(z). \quad (228)$$

Hereby, without loss of generality and for each z , the unknown is expressed with help of another unknown ξ . In particular, the unknown(z) is replaced by the term $(1 + \kappa(z))^{\xi(z)}$.

- (4) Ratio of Hubble constants: As a consequence of the FLE at $k = 0$ and of Equation (152), the squared Hubble parameter is

$$H^2 = \frac{8 \cdot \pi \cdot G}{3} \cdot \rho_{cr, 0} \cdot \left(\Omega_r \cdot \frac{R_0^4}{R^4} + \Omega_m \cdot \frac{R_0^3}{R^3} + \Omega_{\Lambda} \right). \quad (229)$$

Next, H_0 is represented at $t = t_0$ and $r = r_0$:

$$H_{0,het}^2 = \frac{8 \cdot \pi \cdot G}{3} \cdot \rho_{cr, 0} \cdot \underbrace{(\Omega_r + \Omega_m + \Omega_{\Lambda})}_{H_{0,hom}^2} \quad (230)$$

Hereby, H_0 of a homogeneous univ. in Equation (150) is identified in the underbrace in the above equation. That Equation is solved for the fraction of Hubble constants in the ratio in Equation (227):

$$\frac{H_{0,hom}}{H_{0,het}} = \frac{1}{\sqrt{\Omega_r + \Omega_m + \Omega_{\Lambda}}} \text{ or } H_{0,het} = H_{0,hom} \sqrt{\Omega_r + \Omega_m + \Omega_{\Lambda}} \quad (231)$$

Moreover, the ratio of dynamic densities,

$$\frac{\rho_{\Lambda}}{\rho_{vol}} = (1 + \kappa)^{\xi}, \quad (232)$$

is the same as the respective fraction Ω_j :

$$\frac{\Omega_{\Lambda}}{\Omega_{vol}} = (1 + \kappa)^{\xi}, \quad \text{or } \Omega_{\Lambda} = \Omega_{vol} \cdot (1 + \kappa)^{\xi} \quad (233)$$

These results are inserted in the rate ratio in Equation (227):

$$1 + \kappa = \frac{1}{\sqrt{\Omega_r + \Omega_m + \Omega_{\Lambda}}} \cdot (1 + \kappa)^{\xi}, \quad \text{or} \\ (1 + \kappa) \cdot \sqrt{\Omega_r + \Omega_m + \Omega_{vol} \cdot (1 + \kappa)^{\xi}} = (1 + \kappa)^{\xi} \quad (234)$$

Here, a term for the exponent ξ must be derived:

- (5) Deduction of ξ : In Equation (234), the square is applied. Additionally, the following abbreviations are introduced, $y := 1 + \kappa(z_{em})$ and $w := y^{\xi}$:

$$y^2(\Omega_m + \Omega_{vol} \cdot w) = w^2 \quad \text{or} \quad (235)$$

$$0 = w^2 - w \cdot \Omega_{vol} \cdot y^2 - \Omega_m \cdot y^2 \quad \text{with} \quad (236)$$

$$y = 1 + \kappa(z_{em}) \quad \text{and} \quad w = y^\xi \tag{237}$$

In general, Equation (235) has a pair of solutions:

$$w_\pm = \frac{\Omega_{vol} \cdot y^2}{2} \cdot \left(1 \pm \sqrt{1 + \frac{4\Omega_m}{\Omega_{vol}^2 \cdot y^2}} \right) \tag{238}$$

Since $w_- < 0$, it provides no real exponent in Equation (237). Therefore, it is hardly physical. Consequently, w_+ is used:

$$\rightarrow \xi = \frac{\ln(w_+)}{\ln(y)} \quad \text{with} \quad y = 1 + \kappa(z_{em}) \quad \text{and} \tag{239}$$

$$w_+ = \frac{\Omega_{vol} \cdot y^2}{2} \cdot \left(1 + \sqrt{1 + \frac{4\Omega_m}{\Omega_{vol}^2 \cdot y^2}} \right) \tag{240}$$

12.3. Comparison with Observation

Here, values of $H_{0,h\text{et}}(z)$ corresponding to a heterogeneous universe are studied, depending on the redshift z . Thereby, values deduced with the volume dynamics (VD) are compared with observed values in Figure 10. For a huge range of redshifts, corresponding to time ranging from $t = 380,000$ years (after Big Bang) until t_0 (present-day), derived results are in precise accordance with the observed values. In this section, no fit is executed, no assumption is made, and no new hypothesis is proposed. This provides a clear evidence for the presented theory of volume portions.

Additionally, the numerical study is outlined in detail for the case of the CMB (see part 1) and for the case of the redshift $z = 0.055$ (see part 2). Also in these cases, the values are in precise concordance with empirical data.

- (1) Relation of $H_0(z_{CMB})$ and $H_{0,hom}$ alias $H_{0,\Lambda\text{CDM}}$: At z_{CMB} , heterogeneity was very small. Therefore, $\Omega_{vol} = \frac{2}{3}$ describes volume, and $\Omega_m = 1.0 - \Omega_{vol} = \frac{1}{3}$, and $l\sigma_{8,CMB} = 2.34 \cdot 10^{-4}$ [22] ([table 2]), and $H_0(z_{CMB}) = 66.88^{+0.92}_{-0.92} \frac{\text{km}}{\text{s}\cdot\text{Mpc}}$ [22] ([table 2]). Hereby, a value $q_t = q_t^{(1)}$ is chosen at sufficient accuracy. Consequently, $\kappa(z_{CMB})$ in Equation (222) is

$$\kappa(z_{CMB}) = \frac{0.000234 \cdot 1/3}{2 \cdot 2/3 \cdot (1 + 1090.3)^{2.5}} = 1.5 \cdot 10^{-12} \tag{241}$$

With it, we evaluate ξ , see Equations (239) and (240):

$$\xi_{CMB} = 1.5 \tag{242}$$

Consequently, the Hubble constant $H_{0,h\text{et}}(z_{CMB})$ is deduced by using $\kappa(z_{CMB}) = \mathcal{O}(10^{-12})$, see Equation (241):

$$H_{0,h\text{et}}(z_{CMB}) = H_{0,hom} \cdot (1 + \mathcal{O}(10^{-12})) \approx H_{0,hom} =: H_{0,\Lambda\text{CDM}} \tag{243}$$

That result is insightful: $H_{0,h\text{et}}(z_{CMB}) \approx H_{0,\Lambda\text{CDM}}$. This result confirms that the ΛCDM model is an idealization.

- (2) Hubble constant $H_{0,het}(z_{late})$ at $z_{late} = 0.055$ alias $z_{near} = 0.055$: The redshift $z = 0.055$, corresponds to the late universe, it is already relatively heterogeneous. Therefore, H_0 is deduced by utilizing Equation (231):

$$H_{0,het} = H_{0,\Lambda CDM} \cdot \sqrt{\Omega_m + \Omega_{vol} \cdot (1 + \kappa)^\zeta} \tag{244}$$

Further quantities in Equation (244): Empty space based density parameters: $\Omega_{vol} = \frac{2}{3}$, $\Omega_m = 1 - \Omega_{vol} = \frac{1}{3}$, $\sigma_8 = 0.8118^{+0.0089}_{-0.0089}$ [22] ([table 2]). Therefore, $\kappa(z_{late})$ is:

$$\kappa(z_{late}) = \frac{0.8118 \cdot 1/3}{2 \cdot 2/3 \cdot (1 + 0.055)^{2.5}} \cdot \frac{q_t^{(n)}}{q_t^{(1)}} = 0.1842^{+0.003}_{-0.003} \tag{245}$$

Hereby, the numerical investigation provides the following values of $q_t^{(n)}$: $q_t^{(1)} = 0.881$, $q_t^{(2)} = 0.916$, $q_t^{(3)} = 0.913$, $q_t^{(4)} = 0.914$, $q_t^{(5)} = 0.91398$, $q_t^{(6)} = 0.91399 = q_t^{(7)}$. This value is used as a fixed point, at sufficient numerical accuracy.

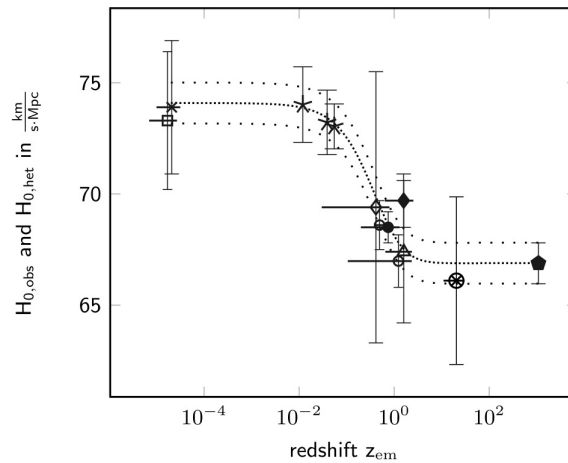


Figure 10. Empirical data $H_{0,obs}$ as well as deduced results $H_{0,het}$ for H_0 depending on z_{em} . Empirical methods or probes, from early to late universe. In principle, symbols in the figure correspond to symbols in the figure caption: filled pentagon, CMB [22]. \otimes , old galaxies or stars [100], (Table 1). Δ , strong gravitational lensing [101] \blacklozenge , starburst galaxies [102]. \circ , baryonic acoustic oscillations, BAO [103,104]. \bullet , weak gravitational lensing and galaxy clustering [105]. \diamond , gravitational wave [106]. \star , supernovae of type Ia (using a distance ladder) [13,107], Ref. [108] ([most precise evaluation]). \times , megamaser [109]. \square , surface brightness [110]. Values based on deduction based on derived physically adequate VD, see Figure 5: Densely dotted (t_{H_0} utilized as calendar date, which is particular and not generally deducible). Loosely dotted: measurement errors based on CMB. Empirical and deduced data are in accurate concordance, according to measurement errors.

With it, the idealized value $\zeta_{CMB} = 1.5$ is improved to the realistic value of ζ , see Equations (239) and (240):

$$\zeta_{late} = 1.532 \tag{246}$$

Therefore, the deduction provides this H_0 result:

$$H_{0,het}(z_{near}) = H_{0,\Lambda CDM} \sqrt{\frac{1}{3} + \frac{2}{3} \cdot 1.1842^{1.532}} \tag{247}$$

$$= 73.174 \pm 1.08 \frac{\text{km}}{\text{s} \cdot \text{Mpc}} \tag{248}$$

As a consequence, the derived value is in accurate concordance with empirical data in Equation (14):

$$H_{0,obs}(z_{late}) = 73.04 (\pm 1.01) \frac{\text{km}}{\text{s} \cdot \text{Mpc}} \text{ at } \langle z \rangle = 0.055 \quad (249)$$

The above is named baseline result [13] ([Sections 5.1 and 5.2]).

Empirical and deduced data have the fractional difference shown below:

$$\Delta_{obs, theo} = \frac{H_{0,obs}(z_{late}) - H_{0,het}(z_{late})}{H_{0,obs}(z_{late})} = \frac{73.174 - 73.04}{73.04} = 0.18\% \quad (250)$$

The fractional difference is very small. This provides evidence for the present theory.

13. Conclusions

In the present paper, the hypothetic deductive method has been used, see Section 1.1. Achieved results are presented progressively in respective short paragraphs:

- (1) In a first step of that method, very reliable observations are characterized as a basis.

13.1. Deduced Results

As a second step in the hypothetic deductive method, results are derived.

- (2) From the above basic facts in step (1), the following results have been deduced:
 - (2.1) The quantum postulates have been deduced, see Section 9.
 - (2.2) Laws of gravity and curved space near a mass have been deduced, see Section 6.
 - (2.3) For the case of the homogeneous universe, the energy density of dark energy has been derived, u_{DE} , this value is also called u_{vol} .
 - (2.4) For values of the redshift z ranging from the redshift z_{CMB} of the emission of the Cosmic Microwave Background (CMB) until to the present-day redshift $z_0 = 0$, the function $H_0(z)$ of the Hubble constant as a function of the redshift z is deduced. This function explains the Hubble tension.

13.2. Comparison with Empirical Findings

As a third step in the hypothetic deductive method, the deduced results are compared with respective empirical data.

- (3) In order to complete the hypothetic deductive method, the deduced results are compared with respective empirical findings:
 - (3.1) The quantum postulates are in accordance with many experimental data. This is shown in standard text books of quantum physics.
 - (3.2) The deduced laws of gravity and curved space near a mass are confirmed by many empirical findings. This is shown in standard text books of classical mechanics, gravity and relativity.
 - (3.3) For the case of the homogeneous universe, the deduced value of the energy density of dark energy u_{DE} or u_{vol} is in precise accordance with empirical data within the errors of measurement, see Section 10.3.5 and the respective Equations (178)–(180).
 - (3.4) The deduced function $H_0(z)$ of the Hubble constant as a function of the redshift z is in accurate concordance with empirical data within the errors of measurement, see Section 12.3, Figure 10 and Equations (243) and (248)–(250). This deduced function explains the Hubble tension.

Moreover, this function predicts the values $H_0(z)$ of the Hubble constant for those values of the redshift z , for which a measurement of the Hubble constant is not yet available.

13.3. Hypothetic Deductive Method II

The hypothetic deductive method and the used basis are described in Section 1.1. On that basis, results are deduced, and especially essential deduced results that are summarized in Section 13.1. These deduced results are compared with respective empirical data in Section 13.2. Thereby, a precise accordance with empirical data is achieved within the errors of measurement. Hereby, no fit is executed, and no unfounded hypothesis is proposed. Accordingly, as a special conclusion, a highly convincing evidence for the derived function $H_0(z)$ and for the derived explanation of the Hubble tension is achieved. As a consequence of the precise accordance elaborated above, this conclusion is supported by the deduced results.

Additionally, this precise accordance elaborated above completes the used hypothetic deductive method. Altogether, the used method is described in very high detail, especially essential results are presented in an especially clear and detailed manner, and the respective conclusions (including their support by these results) are worked out step by step in an especially detailed manner.

14. Discussion

14.1. The Problem Is Solved with Derived Indivisible Portions of Space

The problem of the Hubble-tension has been addressed and solved. Thereby, a critically discussed method is used, and an explanation is derived. The Hubble-tension is the following finding: Significantly different values have been measured for H_0 .

In order to solve that problem, essential fundamental properties of space have been used: The energy density u_{DE} of space is important, as it shows that space has a real energy. Moreover, the space has no rest mass. On that basis, a very enlightening and momentous result has been derived: A space paradox and its solution are derived: Space is not a single entity, but space is a stochastic average of volume portions propagating at $v = c$.

As a consequence, for the case of homogeneous space, by using a local isotropy, the indivisibility of volume portions with $v = c$ is derived. Additionally, empirical evidence has been provided for it. Therefore, these results are very founded.

14.2. Portions of Space Imply a Momentous Unification

The derived volume portions have many insightful and momentous implications: For mathematical reasons, these volume portions obey a differential equation of volume dynamics. In particular for the case of an indivisible volume portion δV_j , this differential equation implies the Schrödinger equation and a generalization thereof. Thereby, the corresponding wave function Ψ is the time derivative of a rel. add. vol. $\varepsilon_{L,rr,j}$ multiplied by a normalization constant t_n . According to the Higgs [48] mechanism, this derived Schrödinger equation includes the case of matter, as matter is formed from space via a phase transition.

Furthermore, the volume dynamics implies gravity. Moreover, on the basis of that implied gravity, the volume dynamics implies the quantum postulates. Altogether, this shows that the volume dynamics implies the deeply founded unification of quanta (including quantum postulates), gravitation (including exact fields and potentials related to volume portions), and relativity (including curvature explained by VPs). That foundation of the unification is very fundamental, as gravity is needed for the derivation of the quantum postulates. This provides the clarifying insight that quantum physics can hardly be understood without gravity at a fundamental level. Accordingly, the more general

volume dynamics of indivisible volume portions is a fundamental unification of quanta and gravitation (quantum gravity). An additional consequence is the local formation of volume (LFV).

14.3. The Unification Implies Values for Homogeneous Space

On the basis of that unification, a homogeneous universe is analyzed first. In that ideal case, many basic and ideal results have been deduced: The GFV (global formation of volume) in the universe, from its start until today. The result is $u_{DE,hom} = u_{vol}$, and its value. These results are in accurate concordance with the corresponding empirical values, values of the very early universe, which was very homogeneous. The Hubble constant $H_{0,hom}$ represents a calendar date $t_0 \approx t_{H_{0,hom}} = \frac{1}{H_{0,hom}}$, therefore, $H_{0,hom}$ cannot be derived from fundamental physical constants only.

14.4. The Unification Implies Values for Heterogeneous Space

The heterogeneity in the universe increased gradually in the course of time. That time can be described in an especially robust manner depending on the cosmological redshift: The present-day universe has $z = 0$, and the emission of the CMB in a very early universe occurred near $z = 1090.3$.

On this basis founded by the above unification in the case of homogeneity, the results in Section 14.3 have been generalized by including heterogeneity. In this manner, the following results have been derived as a function of the redshift: the GFV (global formation of volume), the density of volume u_{DE} and the Hubble constant $H_0(z)$. These results are in accurate concordance with the corresponding observed values in Figure 10. Moreover, the derived Hubble constant $H_0(z)$ as a function of z includes many values that have not yet been observed. These values are predicted.

14.5. Very Convincing Evidence Is Achieved

In this paper, all results have been derived without using any unfounded hypothesis, without proposing any postulate, and without executing any fit. Thereby, an accurate concordance with empirical data is achieved within measurement errors.

Therefore, the comparison of theory and observations provides a very convincing evidence for the developed and derived theory. That theory includes the following essential results: indivisible volume portions, volume portions, the volume dynamics, the derivation of the quantum postulates, the derivation of exact gravity, the derived unification of quantum physics, relativity and gravity, u_{DE} , $u_{DE,hom} = u_{vol}$ as an insightful ideal value, deduction of the Hubble tension by a gradual increase in heterogeneity, from the early universe until today.

14.6. Structure of the Derived Innovative Theory

The Hubble tension represents a fundamental problem about the dynamics of space in the universe. This assessment is affirmed by other hardly understood problems about space and time:

- (1) the International Astronomical Union (IAU) proclaimed the problem of finding an adequate coordinate system (ACS), see [14,24],
- (2) the unexplained nature and value of the energy density of dark energy, see [9,10,16,111],
- (3) the incompatibility of general relativity theory and quantum theory, see [68,112–114].
- (4) and the identification of the source of the Hubble tension, see [13].

The fundamental role of these problems is emphasized by the fact of the Nobel Prizes in Physics in 2006, see [16], in 2011, see [9,15], and in 2022, see [68,115,116].

Accordingly, an innovative and novel theory has been derived from founded observations, see the cognitive map in Figure 5:

As a first step, the problem of finding the ACS and its velocity $\vec{v}_{ACS,CS}$ relative to an arbitrary reference coordinate system (CS) has been solved. While the coordinate systems proposed by relativity theory are insufficient for space navigation, see [14,117], so that present-day relativity theory is incomplete, the derived ACS is in precise concordance with observation, see [23,24]. Together with the ACS, relativity theory can now be used in space flight: If a clock C is described in the ACS, then relativity theory can predict the time of the clock correctly, even under the circumstances of the precise measurements in space navigation. Moreover, the present fundamental derived unification of gravity, relativity and quanta can improve the precision of space navigation, this will be presented in a forthcoming paper. Furthermore, in the ACS, the velocity in the energy velocity relation and in the energy momentum relation is in accordance with a clock in the ACS. Accordingly, these relations are based on the Equation of time dilation and on the ACS in Figure 5. Therefore, the derived theory solves the first of the above problems and enables high precision space navigation.

In a second step, the space paradox is derived, which shows that space cannot be a single object ranging from one end of the light horizon to the other, and beyond, as it is modeled in relativity theory, see [3,5,6,20]. In contrast, the solution of the space paradox shows that homogeneous and isotropic space consists of indivisible volume portions, see Figure 5.

Thirdly, this raises the question, what the dynamics of these volume portions is. That dynamics has been derived without any additional assumption on a completely mathematical basis. As a consequence, that dynamics is very founded, it is the volume dynamics (VD), a differential equation, see Figure 5.

Fourthly, this VD explains and implies three fundamental physical dynamics: the local formation of volume (LFV), exact gravity, and the deterministic and stochastic dynamics of quanta.

Fifthly, this shows that gravity, an ACS-based relativity theory, and quantum physics are derived from the same dynamics, the VD. As a consequence, in this derived theory, the terms of these theories can be transformed to each other, and they can be used correctly in combination. For instance, the wave function in the Schrödinger equation is proportional to the time derivative of the relative additional volume. Consequently, the wave function has a physical meaning.

Hereby, the local formation of the relative additional volume explains and implies the correct value of the energy density u_{DE} of dark energy. This value has neither been derived from relativity theory, nor from quantum theory. Another correctly combined application is the derivation of the Hubble constant H_0 as a function of the redshift z .

Therefore, the theory derived here essentially solves the problem (3) in the above list, the incompatibility of relativity theory and quanta. Moreover, the derived theory solves problem (4), the identification of the source of the Hubble tension. Furthermore, the presented theory provides the process of formation and the value of the dark energy density u_{DE} , so that the theory essentially solves problem (2) of the above list. Altogether, this shows that the equations in this theory have a new and innovative additional meaning, as they describe derived indivisible volume portions, and as they unify quanta with an ACS-based relativity.

Sixthly, the generality of the theory derived here is emphasized by the fact that the Dirac theory as well as quantum field theory can be developed on the basis of the Schrödinger equation, which has been developed here, see [61,65].

Seventh, based on the theory derived here, Hamilton’s principle and the principle of gauge invariance have been successfully used in order to solve problems in the physics of fundamental interactions and elementary particles, see [72]. This shows that the present theory is compatible with very valuable and insightful principles in physics.

Altogether, the theory presented here is derived from founded observations as well as from the equation of time dilation. As a consequence, the derived theory is a physically adequate unification. Moreover, that theory essentially solves the four problems presented above.

14.7. Used Cosmological Parameters

In the present derivation of the Hubble constant $H_0(z)$ as a function of the redshift z , the following parameters and measurement procedures are used and explained progressively in respective paragraphs:

- (1) The Λ CDM-model is valid in a homogeneous universe. Moreover, at the Cosmic Microwave background (CMB), the universe was very homogeneous. Consequently, measurements based on the CMB can be evaluated with the Λ CDM-model in a precise and reliable manner.
- (2) The value $H_0(z_{CMB})$ of the Hubble constant at the redshift z_{CMB} of the CMB is used. In general, one value for the Hubble constant must be measured, as the Hubble constant represents a calendar date, $t_{H_0} = \frac{1}{H_0}$. As a calendar date is a specific value, it cannot be derived from general physical constants or laws.

Moreover, that value $H_0(z_{CMB})$ is used, that is measured on the basis of the CMB and that is evaluated with the Λ CDM-model. As a consequence of item (1), that value $H_0(z_{CMB})$ is precise and reliable.

- (3) The value Ω_m of the density parameter of matter is used. Thereby, that value is used here, that has been measured with help of CMB data that have been evaluated by application of the Λ CDM-model. As a consequence of item (1), that value of $\Omega_m(z_{CMB})$ is precise and reliable in the homogeneous universe, characterized by $0 \leq \sigma_8(z) \ll 1$. In addition, the value of $\Omega_m = \frac{1}{3}$ has been derived for the case of the completely homogeneous universe. This is in accordance with the CMB—based measured value $\Omega_m = 0.321 \pm 0.013$.

In general, at a redshift z , in a heterogeneous universe, characterized by $0 \leq \sigma_8(z)$, the value of $\Omega_m(z)$ differs slightly from $\Omega_m(z_{CMB})$. The difference can be expressed as a function of $\sigma_8(z)$, similarly as elaborated in the present theory for the case of H_0 , see Figure 10. This example shows that the Λ CDM-model can be a useful effective theory for the parameter estimation.

- (4) The value σ_8 of the standard deviation of matter fluctuations is used. Thereby, that value is used here, that has been measured with help of CMB data that have been evaluated by application of the Λ CDM-model.

Similarly as in item (3), also in this case, the Λ CDM-model can be a useful effective theory for the parameter estimation. Altogether, these examples show, how the Λ CDM-model can be a useful effective theory for the parameter estimation.

14.8. Dynamical Effects of the Breaking of Translation Symmetry

In general, the breaking of translation symmetry has immense dynamical effects. These effects are elaborated progressively in respective paragraphs:

- (1) A breaking of translation symmetry changes time: A completely empty space could have the property of translation invariance. When a gravitational field \vec{G}^* enters that space, this has momentous geometrical and dynamical consequences: \vec{G}^* breaks translation invariance. Based on \vec{G}^* , each clock C in that space obtains a determined

velocity \vec{v}_{C,\vec{G}^*} relative to \vec{G}^* , in an unscreenable manner. As a consequence, each such clock C has the kinematic fractional time difference $\delta t_{kin,frac,C} = -\frac{\vec{v}_{C,\vec{G}^*}^2}{2c^2}$. This has been confirmed by observation, and predictions for future observations are provided. Consequently, a coordinate system is an ACS, iff its velocity relative to \vec{G}^* is zero, $\vec{v}_{ACS,\vec{G}^*} = \vec{0}$. Therefore, \vec{G}^* breaks the principle of relativity by causing local special coordinate systems, the Adequate Coordinate Systems (ACS).

- (2) A breaking of translation symmetry changes the Hubble rate H_0 of the expansion of the universe. A completely homogeneous universe could have the property of translation invariance. At the time t_{CMB} of the formation of the CMB, the heterogeneity of our universe was very small. Without heterogeneity, space expanded according to the Λ CDM model. During the time evolution of our universe, gravity caused an increase in heterogeneity, described by the standard deviation of matter fluctuations $\sigma_8(t)$.

The Λ CDM model describes the dynamical effect of homogeneous matter, but the dynamical effect of $\sigma_8(t)$ is not included. More generally, the present theory derives and includes the dynamical effect of $\sigma_8(t)$. As a consequence, the function $H_0(z)$ is derived, the function $H_0(z)$ is in precise accordance with observation (see Figure 10, hereby, no fit is executed, and no unfounded hypothesis is proposed), the function $H_0(z)$ predicts future observations, and the Hubble tension is explained. This provides convincing evidence for including heterogeneity in the dynamics.

In both examples (1) and (2), translation symmetry is broken by a heterogeneity of matter density or of the gravitational field \vec{G}^* . In both cases, this has an immense effect upon the dynamics. Especially in (1), this causes a breaking of the principle of relativity, which causes a change in time, localized at the field \vec{G}^* .

In general, the similar paradigms of translation symmetry, of homogeneity, and of the principle of relativity can cause an immense idealization. This idealization can be overcome by a paradigm shift, which includes the dynamical effects of translation symmetry breaking, of heterogeneity, and of principle of relativity breaking. Here, the dynamical effect of heterogeneity in nature is described with help of the volume dynamics. It provides the formation of volume in nature, the energy density u_{DE} of volume, the function $H_0(z)$, and the explanation of the Hubble tension. Moreover, the dynamical effect of local breaking of the principle of relativity is described with the Adequate Coordinate System (ACS), which provides improved space navigation. Furthermore, for the first time, the ACS also provides the proof that at each point of the universe, there exists an ACS, which guarantees the validity of the relativistic kinematic time difference.

Additionally, the finding of moving regions of an ACS and of time opens the question: What are the smallest moving portions of space. The answer is provided with help of the space paradox: space consists of stochastically moving indivisible volume portions. These imply a volume dynamics, the quantum postulates, emergent gravity, and emergent curvature of space. In this manner, that question opens the path to the founded and impartible unification of cosmological volume, including adequate coordinate systems, of curved space and time, of quanta and of gravity.

Altogether, the derived Fundamental Solution overcomes the idealized principle of relativity by accepting the omnipresent breaking of translation invariance in our world, and by deriving the immense dynamical consequences of that breaking of translation symmetry. This represents an important paradigm shift from a description restricted to translation symmetry to a new description including realistic and dynamically essential breaking of translation symmetry. Thereby, the equations of the Fundamental Solution include localized structures that are not included in the principle of relativity, and these equations of the Fundamental Solution are generally applicable everywhere in the universe.

Funding: This research received no external funding.

Data Availability Statement: The original data presented in the study are openly available in [ResearchGate] since 13 November 2025 at [https://www.researchgate.net/publication/397562186-Supplementary_Material_for_the_Paper_A_Fundamental_Solution_of_the_Hubble_Tension].

Conflicts of Interest: The author declares no conflicts of interest.

Appendix A

Appendix A.1

In this appendix, for each energy portion, that can be described by a wave, and that propagates with the speed c , the energy circular frequency relation is derived.

In relativity, for a portion of energy E that propagates at the velocity c of light, the following relation between energy E and momentum p holds, see [20,118], §5.7:

$$E/p = c \tag{A1}$$

In wave theory, for a portion of energy E that propagates at the speed c of light, the following relation between circular frequency ω and wave vector \vec{k} holds, see [67]:

$$\omega/|\vec{k}| = c \tag{A2}$$

Consequently, the fractions in the above two equations are equal:

$$E/p = \omega/|\vec{k}| \tag{A3}$$

The above Equation is multiplied by p/ω . Therefore, the following the energy circular frequency relation is derived:

$$\frac{E}{\omega} = \frac{p}{|\vec{k}|} \tag{A4}$$

Appendix A.2

In this appendix, on the basis of observation, see e.g., [66,67], Section 3-3, for each circular frequency, for the case of an energy portion with the minimal energy E_{min} , the value of the fractions in Equation (A4) is presented.

As a result of observation, for the case of E_{min} , the value of the fractions in Equation (A4) does not depend on the circular frequency. Consequently, that value does not depend on the wave vector, see Equation (A2). As a further consequence, the corresponding momentum has its minimal value $p_{min} = E_{min}/c$, see Equation (A1). The observed value is the reduced Planck constant

$$\hbar = \frac{h}{2\pi}, \tag{A5}$$

with the Planck constant

$$h = 6.626\ 070\ 15 \cdot 10^{-34} \text{ J} \cdot \text{s}, \tag{A6}$$

consequently, the fractions in Equation (A4) are as follows:

$$\frac{E_{min}}{\omega} = \frac{p_{min}}{|\vec{k}|} = \hbar \tag{A7}$$

Therefore, E_{min} and p_{min} are functions of ω .

In particular, a volume portion (VP), that is indivisible, propagates at $v = c$, and it has the minimal energy, since it is indivisible. Consequently, Equation (A7) holds for the case of indivisible volume portions:

$$\frac{E_{min}}{\omega} = \frac{E_{indivisible VP}}{\omega} = \frac{p_{indivisible VP}}{|\vec{k}|} = \hbar \tag{A8}$$

Appendix A.3

In this appendix, the momentum operator is derived from the mathematically based differential equation of volume dynamics in Equation (45):

$$i\hbar \cdot \frac{\partial}{\partial \tau} \dot{\epsilon}_{L,jj} = c \cdot \vec{e}_v \cdot \left[-i\hbar \cdot \frac{\partial}{\partial \vec{L}} \right] \dot{\epsilon}_{L,jj} \tag{A9}$$

This Equation has the following wave solution, with an amplitude $\hat{\epsilon}_{L,jj}$:

$$\dot{\epsilon}_{L,jj} = \hat{\epsilon}_{L,jj} \cdot \exp[-i\omega \cdot \tau + \vec{k} \cdot \vec{L}] \tag{A10}$$

The differential Equation in (A9) is multiplied by \vec{e}_v/c , the solution in Equation (A10) is inserted, and the time derivative is executed. Consequently, the following Equation holds:

$$\vec{e}_v \cdot i\hbar \cdot (-i\omega/c) \dot{\epsilon}_{L,jj} = \left[-i\hbar \cdot \frac{\partial}{\partial \vec{L}} \right] \dot{\epsilon}_{L,jj} \tag{A11}$$

In particular, this Equation holds for each indivisible VP. Consequently, $\hbar\omega$ is equal to $E_{indivisible VP}$, see Equation (A8). As a consequence, the following relation holds:

$$\vec{e}_v \cdot E_{indivisible VP} / c \cdot \dot{\epsilon}_{L,jj} = \left[-i\hbar \cdot \frac{\partial}{\partial \vec{L}} \right] \dot{\epsilon}_{L,jj} \tag{A12}$$

As the VP has the speed c , its energy is equal to the momentum multiplied by c . Moreover, the absolute value of the momentum multiplied by the unit vector \vec{e}_v is the momentum vector. Consequently, the following relation holds:

$$\vec{p}_{indivisible VP} \cdot \dot{\epsilon}_{L,jj} = \left[-i\hbar \cdot \frac{\partial}{\partial \vec{L}} \right] \dot{\epsilon}_{L,jj} \tag{A13}$$

This equation is identified with an eigenvalue equation, with the eigenvector $\dot{\epsilon}_{L,jj}$ in the space of solutions of the linear differential equation in Equation (A9) of the volume dynamics, with the eigenvalue $\vec{p}_{indivisible VP}$, and with the operator $\left[-i\hbar \cdot \frac{\partial}{\partial \vec{L}} \right]$.

Therefore, the operator $\left[-i\hbar \cdot \frac{\partial}{\partial \vec{L}} \right]$ is the operator of the momentum as the eigenvalue. Traditionally, in physics, such an operator is called with respect to its eigenvalue, i.e., it is called momentum operator. It is emphasized that this is only a naming of the derived operator $\left[-i\hbar \cdot \frac{\partial}{\partial \vec{L}} \right]$ with the momentum as its eigenvector. The respective traditional naming can be found in the literature, see e.g., [61,62,76,88].

Appendix A.4. Explanation of the Observed Gigaparsec Structures

In the universe, there are Gigaparsec structures. For instance, the Hercules-Corona Borealis Great Wall, is at an observed redshift $z_{GW} \in [1.6; 2.1]$ or $z_{GW} = \frac{1.6+2.1}{2} = 1.85$, and it has a radius $R_{GW} \in [1000 \text{ Mpc}; 1500 \text{ Mpc}]$ or $R_{GW} = \frac{1000 \text{ Mpc} + 1500 \text{ Mpc}}{2} = 1250 \text{ Mpc} = 3.87 \cdot 10^{25} \text{ m}$, see [119]. For an estimation, the Great Wall as modeled a ball. Consequently, its volume is $V_{GW} = 2.40 \cdot 10^{77} \text{ m}^3$.

The mass of that Great Wall has not been measured. An essential mass m_{ess} can be estimated with help of densities as follows: The critical density of the Λ CDM model is $\rho_{cr} = 8.66 \cdot 10^{-27} \frac{\text{kg}}{\text{m}^3}$, see [40]. Consequently, the homogeneous density of matter is $\rho_{hom} = \rho_{cr} \cdot \Omega_m \cdot (1 + z_{GW})^3 = 6.68 \cdot 10^{-26} \frac{\text{kg}}{\text{m}^3}$, with $\Omega_m = 1/3$.

In that Great Wall, there is the overdensity $\rho_{het} = \rho_{hom} \cdot \sigma_8 / (1 + z_{GW}) = 1.90 \cdot 10^{-26} \frac{\text{kg}}{\text{m}^3}$. Outside that Great Wall, there is the typical overdensity of a void $\rho_{void} = -0.45 \cdot \rho_{hom}$, see [120]. Thus, $\rho_{void} = -3.01 \cdot 10^{-26} \frac{\text{kg}}{\text{m}^3}$. As a consequence, that Great Wall has the additional density relative to its surroundings $\rho_{add} = \rho_{het} - \rho_{void} = 4.91 \cdot 10^{-26} \frac{\text{kg}}{\text{m}^3}$.

The product of the volume V_{GW} and the additional density ρ_{add} represents an additional mass Δm , which causes the local gravitational field, and the respective potential difference $\Delta\Phi$. Consequently, $\Delta m = V_{GW} \cdot \rho_{add} = \rho_{het} - \rho_{void} = 1.18 \cdot 10^{52} \text{ kg}$. The corresponding gravitational potential is $\Delta\Phi_{gr} = -\frac{G \cdot \Delta m}{R_{GW}} = -2.04 \cdot 10^{16} \frac{\text{J}}{\text{kg}}$.

The Hubble flow is described with help the time derivative of the scale radius \dot{R} . Its square is equal to the Hubble parameter H multiplied by R^2 . $\dot{R}^2 = H^2 \cdot R^2$. The corresponding kinetic energy per mass represents a kinetic potential difference, $\Delta\Phi_{kin} = \dot{R}^2 / 2 = H^2 \cdot R_{GW}^2 / 2$. According to the virial theorem, see [34], the Hercules-Corona Borealis Great Wall can bind mass, if the sum of $\Delta\Phi_{gr} / 2$ and $\Delta\Phi_{kin}$ is negative:

$$\Delta\Phi = \Delta\Phi_{gr} / 2 + \Delta\Phi_{kin} = -\frac{G \cdot \Delta m}{2R_{GW}} + H^2 \cdot R_{GW}^2 / 2 \tag{A14}$$

According to the Friedmann Lemaître equation, the Hubble parameter is as follows:

$$H = \sqrt{\frac{8\pi G}{3} \cdot \rho_{hom}} = 3.74 \cdot 10^{-18} \frac{1}{\text{s}} \tag{A15}$$

The ratio of the resulting potential difference $\Delta\Phi$ and the potential difference $\Delta\Phi_{kin}$ is as follows:

$$\frac{\Delta\Phi}{\Delta\Phi_{kin}} = 0.02 \tag{A16}$$

Therefore, the estimated potential $\Delta\Phi$ is positive, so that the Great Wall cannot bind mass. Consequently, the Great Wall is an accidental pattern of galaxy clusters. However, the Great Wall can almost bind masses.

Accordingly, the effect of the Hubble constant variation is analyzed: At $z = 1.85$, the Hubble constant is increased by the factor 1.0075. As a consequence, the above ratio becomes slightly larger:

$$\frac{\Delta\Phi}{\Delta\Phi_{kin}} = 0.035 \tag{A17}$$

This example shows: In Gigaparsec clusters that can almost bind mass, the change in the Hubble constant could become decisive or significant for the ability to bind mass.

The absolute value of that potential difference is very small. As a consequence, a small error of estimation of the observed values can cause the estimation that the Great Wall could bind mass. For instance, if the overdensity in the vicinity of the Great wall would be $\rho_{void} = -0.48 \cdot \rho_{hom}$ instead of $\rho_{void} = -0.45 \cdot \rho_{hom}$, then the above ratio of potential differences would be negative,

$$\frac{\Delta\Phi}{\Delta\Phi_{kin}} = -0.00047, \text{ if } \rho_{void} = -0.48 \cdot \rho_{hom} \tag{A18}$$

In that case, the Great Wall could bind mass, so it would be bound by gravity. In fact, the Great Wall is the largest known Gigaparsec structure, and it is almost bound by gravity.

Slightly smaller large structures are bound by gravity, such as Laniakea with a diameter of 0.16 Gpc, see [121].

How essential is the heterogeneity described by $\sigma_8(z)$? In this theory, the standard deviation of matter fluctuations is the following function of the redshifts see Figure A1:

$$\sigma_8(z) = \frac{\sigma_8(z=0)}{z+1} = \frac{0.8118}{1+z}. \tag{A19}$$

At the redshift $z_{GW} = 1.85$, at which a present-day observation at Earth records the Great Wall, that standard deviation of matter fluctuations is $\sigma_8(1.85) = 0.2848$. According to errors of measurement, that observed redshift is in the interval $z_{GW} \in [1.6; 2.1]$. Based on the minimum of that interval, $z_{GW,min} = 1.6$, the standard deviation is $\sigma_8(1.6) = 0.3122$. As a consequence, the ratio of potentials is negative,

$$\frac{\Delta\Phi}{\Delta\Phi_{kin}} = -0.00123, \text{ if } z = 1.6. \tag{A20}$$

Therefore, a decrease in the redshift from 1.85 to 1.6 would enable the Hercules-Corona Borealis Great Wall to bind masses. This example shows, that the matter fluctuations or heterogeneity are already essential stabilizers at the redshift $z = 1.6$.

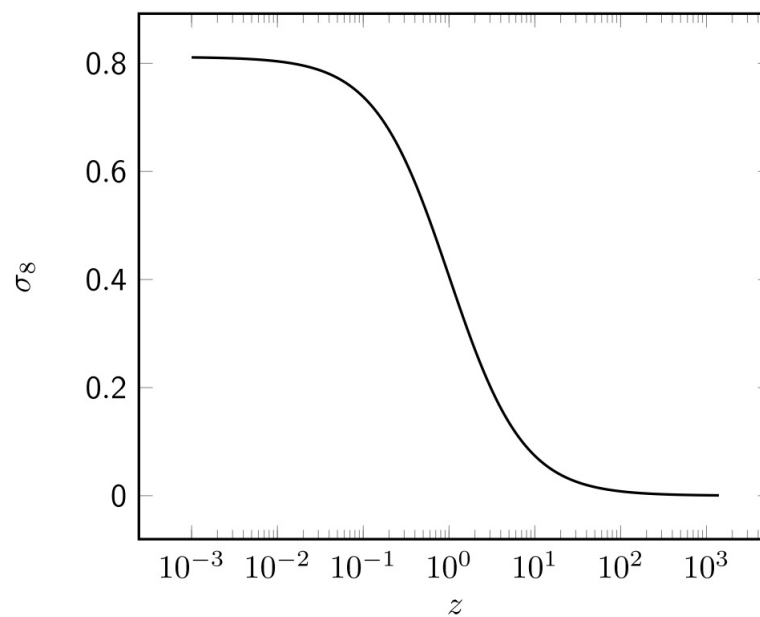


Figure A1. The standard deviation $\sigma_8(z)$ of matter fluctuations as a function of the redshift z .

Interpretation of the near-balance gravitational stability of the Great Wall: The Hercules-Corona Borealis Great Wall is the largest observed structure in the universe. Consequently, the Great Wall heterogeneity grows until the point of near-balance gravitational stability. At the present-day observation from Earth, the Great Wall is recorded at minimal possible redshift $z_{GW,min} = 1.6$, causing the standard deviation of matter fluctuations $\sigma_8(1.6) = 0.3122$, which causes the negative potential, see Equation (A14):

$$\Delta\Phi = \Delta\Phi_{gr}/2 + \Delta\Phi_{kin} = -\frac{G \cdot \Delta m}{2R_{GW}} + \frac{H^2}{2} \cdot R_{GW}^2 = -9.9 \cdot 10^{12} \frac{\text{J}}{\text{kg}} \tag{A21}$$

The relation $\Delta m = \frac{4\pi}{3} R_{GW}^3 \rho_{add}$ is inserted:

$$\Delta\Phi = \left(-\frac{2\pi G \cdot \rho_{add}}{3} + \frac{H^2}{2} \right) \cdot R_{GW}^2 = -9.9 \cdot 10^{12} \frac{\text{J}}{\text{kg}} \tag{A22}$$

This shows, that $z = 1.6$ is an essential or critical redshift with its essential or critical heterogeneity $\sigma_8(1.6) = 0.3122$: At a larger redshift or an earlier time, $z > 1.6$, the clusters with the mass determined by the additional heterogeneity ρ_{add} , as outlined above, cannot attract mass, so that mass attracting clusters must have even larger mass, such as Laniakea, see [121]. At a smaller redshift or a later time, $z < 1.6$, the clusters with the mass determined by the additional heterogeneity ρ_{add} , as outlined above, can attract mass, so that these clusters can grow even independent of their radius, as the radius is outside the bracket in Equation (A22).

Appendix A.5. Consistency of the Measures of Heterogeneity

In cosmology, the measures of heterogeneity are the density ρ_{het} and the standard deviation σ_8 . Both need the boxes in Figure 9, or similar basic regions, with a length $L = \frac{8\text{Mpc}}{\left(\frac{H}{\frac{100\text{km/s}}{\text{Mpc}}}\right)}$. These boxes cause a discretization error, that can be interpreted as

follows: In order to provide a relatively constant discretization error, the basic length 8 Mpc is divided by the Hubble parameter H over a roughly estimated Hubble constant $\frac{100\text{km/s}}{\text{Mpc}}$. As the Hubble constant H_0 varies with time, the discretization error is not constant. Moreover, as the heterogeneity causes an increase in the Hubble constant H_0 , regions with relatively high heterogeneity could exhibit an enhanced increase in the Hubble constant, so that the discretization error could vary in time and space. Furthermore, the kinematic relativistic time difference depends on the ACS, which may have slightly different effects in different discretization boxes. Of course, these effects are probably minor effects. Besides these discretization effects, the density ρ_{het} and the standard deviation σ_8 are well defined statistical quantities with a very robust mathematical basis. Nevertheless, it could be a slight innovation to improve the above denominator $\frac{100\text{km/s}}{\text{Mpc}}$.

Appendix A.6. The CMB-Frame as a Rest Frame

According to the principle of relativity, see [3], and to the principle of general covariance, see [122], there should be no special frame that is adequate for the description of nature. However, the Foucault pendulum showed, that at Earth’s north pole, a frame that describes nature adequately should rotate relative to Earth at 360° in 24 h. Similarly, the D1-Spacelab mission showed, that the clocks at Earth’s north pole describe nature and its kinematic time difference adequately, whereas a frame onboard the Spacelab does not describe the kinematic time difference adequately. Therefore, the IAU proclaimed the problem of finding an adequate coordinate system (ACS).

This problem has been solved, see [23,24]. Accordingly, the following two important questions arise:

- (1) Is the CMB-Frame a useful rest frame?
- (2) Is the CMB-Frame an ACS?

Answer to question (1): The state $state_{CMB}$ of the universe, from which the CMB has been emitted, had the following thermal property: Firstly, the state $state_{CMB}$ is essentially the state inside the light horizon. The state $state_{CMB}$ is a result of the era, in which the universe increased distances in a very rapid manner, the so-called era of cosmic inflation, see [40,123].

As a result of that era, the state $state_{CMB}$ was in thermal equilibrium as has been shown by the solution of the so-called horizon problem, see [40], Section 2.20.3. As a consequence, a region 1, and each region j of the state $state_{CMB}$ had the same average of the velocities \vec{v}_i of its contained objects:

$$\langle \vec{v}_i \rangle_{region\ 1} = \langle \vec{v}_i \rangle_{region\ j}. \tag{A23}$$

That is, for each region j of the state $state_{CMB}$, the average of the velocities \vec{v}_i is $\langle \vec{v}_i \rangle_{region\ 1}$. Therefore, the regions of the state $state_{CMB}$ have the common averaged velocity $\langle \vec{v}_i \rangle_{region\ 1}$. As a consequence, at the state $state_{CMB}$, the averaged velocity $\langle \vec{v}_i \rangle_{region\ 1}$ describes the common averaged velocity of the regions inside the light horizon. Consequently, at the state $state_{CMB}$, the averaged velocity $\langle \vec{v}_i \rangle_{region\ 1}$ represents a common frame of the regions inside the light horizon. As this state $state_{CMB}$ can essentially be observed in the present-day CMB, the CMB-Frame represents a common frame of states inside the light horizon. Therefore, this observable state represents an important reference frame.

Here is an answer to question (2): An ACS is a frame that is at rest to the local gravitational field. The velocity $\vec{v}_{C,ACS}$ of a clock C relative to the ACS describes the kinematic time difference of that clock $\delta_{kin,frac} = -\frac{\vec{v}_{C,ACS}^2}{2c^2}$, and a clock at rest in the ACS is at the universal zero of the kinematic time difference, $\vec{v}_{C,ACS} = 0 \rightarrow \delta_{kin,frac} = -\frac{\vec{v}_{C,ACS}^2}{2c^2} = 0$.

The state $state_{CMB}$ contains many density maxima, that have a dominant gravitational field in their vicinity, and that form a local ACS. Therefore, the frame of the CMB is not an ACS.

As long as you are not interested in the kinematic time differences, you can ignore the fact that the CMB-Frame is not an ACS. Similarly, in the fundamental derived theory here, the ACS can be ignored, as long as you are not interested in a kinematic time difference. In fact, the derivation does not need the kinematic time difference. But an important application of the derived theory is space navigation, see e.g., [23]. Therefore, the ACS is presented in Section 1.1.5.

Appendix A.7. Energy Conservation in the Expansion of the Universe

The expansion of the universe since the Big Bang is caused by the formation of indivisible VPs. Fundamentally, each indivisible VP δV_j has two basic energy terms. Further energy terms might be caused by additional interactions or structures, for instance. As a consequence, in a homogeneous region of space, each indivisible VP has only the two basic energy terms:

- (1) the energy density of the gravitational field $u_{f,j} = -\frac{(\vec{G}_j^*)^2}{8\pi G}$ in Equation (122),
- (2) the energy density $u_{indivisible\ VP,j} = \frac{c^2 \cdot \epsilon_{L,rr,indivisible\ VP}^2}{8\pi G}$ of relative additional volume $\epsilon_{L,rr,indivisible\ VP}$ of the indivisible VP δV_j in Equation (125).

Thereby, the sum of the two basic energy terms, that is the complete energy of an indivisible VP $u_{complete,indivisible\ VP,j}$, is zero, see Equation (124):

$$u_{complete,indivisible\ VP,j} := u_{indivisible\ VP,j} + u_{f,j} \text{ consequently, } u_{complete,indivisible\ VP,j} = 0. \tag{A24}$$

Therefore, the formation of space since the Big Bang does not violate the law of energy conservation, though the space has the energy density u_{DE} or u_{vol} in a homogeneous region of space.

In general, a physical quantity can be measured with an appropriate measurement device, which corresponds to the respective linear operator in the Hilbert space of the considered physical system. In the present case, there are several measurement methods and devices for the observation of an averaged version of $u_{indivisible\ VP,j}$, which corresponds to the observed dark energy density u_{DE} , see Figure 10. An averaged version of the energy density $u_{f,j}$ can be observed in the vicinity of a mass, see Figure 7.

Thereby, this result is derived on the basis of founded observation, see Figure 5. Especially, the essential differential equation of volume dynamics is derived on the basis of founded observation, see Figure 5. In particular, thereby no unfounded hypothesis is

utilized, no fit is executed, no wave equation has been guessed, and no result has been used as an assumption, see Figure 5.

References

1. Newton, I. *Philosophiæ Naturalis Principia Mathematica*; Jussu Societatis Regiæ ac typis Josephi Streater: London, UK, 1687.
2. Maxwell, J.C. A dynamical theory of the electromagnetic field. *Phil. Trans. R. Soc.* **1865**, *155*, 459–512. [[CrossRef](#)]
3. Einstein, A. Zur Elektrodynamik bewegter Körper. *Ann. Phys.* **1905**, *17*, 891–921. [[CrossRef](#)]
4. Minkowski, H. Raum und Zeit. *Jahresber. Dtsch.-Math.-Ver.* **1908**, *18*, 75–88.
5. Einstein, A. *Die Feldgleichungen der Gravitation*; Sitzungsberichte der Königlich Preußischen Akademie der Wissenschaften: Berlin, Germany, 1915; pp. 844–847.
6. Hilbert, D. Die Grundlagen der Physik. *Nachrichten von der Königlichen Gesellschaft der Wissenschaften zu Göttingen, Math-Physik. Klasse, November.* **1915**, 1–30.
7. Einstein, A. *Kosmologische Betrachtungen zur Allgemeinen Relativitätstheorie*; Sitzungsberichte der Königlich Preußischen Akademie der Wissenschaften: Berlin, Germany, 1917; pp. 142–152.
8. Hubble, E. A relation between distance and radial velocity among extra-galactic nebulae. *Proc. Natl. Acad. Sci. USA* **1929**, *15*, 168–173. [[CrossRef](#)]
9. Perlmutter, S.; Aldering, G.; Della Valle, M.; Deustua, S.; Ellis, R.S.; Fabbro, S.; Goldhaber, G.; Groom, D.E.; Hook, I.M.; Kim, A.G.; et al. Discovery of a Supernova Explosion at Half the Age of the Universe. *Nature* **1998**, *391*, 51–54. [[CrossRef](#)]
10. Zeldovich, Y.B. The cosmological constant and the theory of elementary particles. *Sov. Astron. A. J.* **1968**, *11*, 381–393.
11. Lamb, W.E.; Retherford, R.C. Fine Structure of the Hydrogen Atom by a Microwave Method. *Phys. Rev.* **1947**, *72*, 241–243. [[CrossRef](#)]
12. Casimir, H. On the attraction between two perfectly conducting plates. *Proc. Sect. Sci. K. Ned. Akad. Van Wet.* **1948**, *51*, 793–795.
13. Riess, A.G.; Yuan, W.; Macri, L.M.; Scolnic, D.; Brout, D.; Casertano, S.; Jones, D.O.; Murakami, Y.; Anand, G.S.; Breuval, L.; et al. A Comprehensive Measurement of the Local Value of the Hubble Constant with 1 km s⁻¹ Mpc⁻¹ Uncertainty from the Hubble Space Telescope and the SHOES Team. *Astrophys. J. Lett.* **2022**, *934*, L7. [[CrossRef](#)]
14. Soffel, M.; Klioner, S.A.; Petit, G.; Wolf, P.; Kopeikin, S.M.; Bretagnon, P.; Brumberg, V.A.; Capitaine, N.; Damour, T.; Fukushima, T.; et al. The IAU 2000 Resolutions for Astrometry, Celestial Mechanics, and Metrology in the relativistic Framework: Explanatory Supplement. *Astron. J.* **2003**, *126*, 2687–2706. [[CrossRef](#)]
15. Riess, A.G.; Filippenko, A.V.; Liu, M.C.; Challis, P.; Clocchiatti, A.; Diercks, A.; Garnavich, P.M.; Hogan, C.J.; Jha, S.; Kirshner, R.P.; et al. Tests of the Accelerating Universe with Near-Infrared Observations of a High-Redshift Type Ia Supernova. *Astrophys. J.* **2000**, *536*, 62–67. [[CrossRef](#)]
16. Smoot, G.F. Nobel Lecture: Cosmic microwave background radiation anisotropies: Their discovery and utilization. *Rev. Mod. Phys.* **2007**, *79*, 1347–1379. [[CrossRef](#)]
17. Friedmann, A. Über die Krümmung des Raumes. *Z. Phys.* **1922**, *10*, 377–386. [[CrossRef](#)]
18. Wirtz, C. Radialbewegung der Gasnebel. *Astron. Nachrichten* **1922**, *215*, 281–286. [[CrossRef](#)]
19. Lemaître, G. Un Univers homogène de masse constante et de rayon croissant rendant compte de la vitesse radiale des nébuleuses extra-galactiques. *Ann. Soc. Sci. Brux.* **1927**, *A47*, 49–59.
20. Hobson, M.P.; Efstathiou, G.P.; Lasenby, A.N. *General Relativity*; Cambridge University Press: Cambridge, UK, 2006.
21. Workman, R.L.; Burkert, V.D.; Crede, V.; Klempt, E.; Thoma, U.; Tiator, L.; Agashe, K.; Aielli, G.; Allanach, B.C.; Amsler, C.; et al. Review of Particle Physics (by Particle Data Group). *Progr. Theor. Exp. Phys.* **2022**, *2022*, 083C01.
22. Planck Collaboration; Aghanim, N.; Akrami, Y.; Ashdown, M.; Aumont, J.; Baccigalupi, C.; Ballardini, M.; Banday, A.J.; Barreiro, R.B.; Bartolo, N.; et al. Planck-Collaboration Planck 2018 results. VI. Cosmological parameters. *Astron. Astrophys.* **2020**, *641*, A6.
23. Carmesin, H.-O. *Universe: Unified from Microcosm to Macrocosm*; Carmesin, H.-O., Ed.; Verlag Dr. Köster: Berlin, Germany, 2025; Volume 12, pp. 1–231.
24. Carmesin, H.-O. Derivation of a Physically Adequate Coordinate System from an Observation on Earth's Ground. *J. Geosci. Earth Planet. Syst.* **2025**, *accepted for publication*.
25. Popper, K. *Logik der Forschung*, 1st ed.; Julius Springer: Wien, Austria, 1935.
26. Popper, K. *Objektive Erkenntnis*, 2nd ed.; Hoffmann und Campe: Hamburg, Germany, 1974.
27. Niiniluoto, I.; Sintonen, M.; Wolenski, J. *Handbook of Epistemology*; Springer: Dordrecht, The Netherlands, 2004.
28. Schwarzschild, K. *Über das Gravitationsfeld eines Massenpunktes nach der Einstein'schen Theorie*; Sitzungsberichte der Königlich Preußischen Akademie der Wissenschaften: Berlin, Germany, 1916; pp. 186–196.
29. Dyson, F.W.; Eddington, A.S.; Davidson, C. A Determination of the Deflection of Light by the Sun's Gravitational Field, from Observations Made at the Total Eclipse of May 29, 1919. *Philos. Trans. R. Soc. Lond.* **1920**, *A220*, 291–333.
30. Pound, R.V.; Rebka, G.A. Apparent weight of photons. *PRL* **1960**, *4*, 337–341. [[CrossRef](#)]

31. Zeldovich, Y.B.; Einasto, J.; Shandarin, S.F. Giant Voids in the Universe. *Nature* **1982**, *300*, 407–413. [[CrossRef](#)]
32. Contarini, S.; Pisani, A.; Hamaus, N.; Marulli, F.; Moscardini, L.; Baldi, M. The perspective of voids on rising cosmology tensions. *Astron. Astrophys.* **2024**, *682*, A20. [[CrossRef](#)]
33. Abbott, B.; Abbott, R.; Abbott, T.D.; Abernathy, M.R.; Acernese, F.; Ackley, K.; Adams, C.; Adams, T.; Addesso, P.; Adhikari, R.X.; et al. Observation of Gravitational Waves from a Binary Black Hole Merger. *Phys. Rev. Lett.* **2016**, *116*, 061102. [[CrossRef](#)] [[PubMed](#)]
34. Landau, L.; Lifschitz, J. *Course of Theoretical Physics I—Mechanics*, 3rd ed.; Pergamon Press: Oxford, UK, 1976.
35. Zogg, J.-M. *GPS Essentials of Satellite Navigation*; u-blox-AG: Chemnitz, Germany, 2009.
36. Carmesin, H.-O. *Universe: Unified from Microcosm to Macrocosm*; Carmesin, H.-O., Ed.; Verlag Dr. Köster: Berlin, Germany, 2021; Volume 4, pp. 1–2743.
37. Will, C.M. The Confrontation between General Relativity and Experiment. *Living Revies Relativ.* **2014**, *17*, 4. [[CrossRef](#)]
38. Hacking, I. *Representing and Intervening*; Cambridge University Press: Cambridge, UK, 1983.
39. Carmesin, H.-O. *Derivation of a Physically Adequate Coordinate System from an Observation at Space*; Elsevier SSRN library: Amsterdam, The Netherlands, 2025.
40. Carmesin, H.-O. *Universe: Unified from Microcosm to Macrocosm*; Carmesin, H.-O., Ed.; Verlag Dr. Köster: Berlin, 2019; Volume 1, pp. 1–226.
41. Huterer, D.; Turner, M.S. Prospects for probing the dark energy via supernova distance measurements. *Phys. Rev. D* **1999**, *60*, 081301. [[CrossRef](#)]
42. Penzias, A.; Wilson, R.W. A measurement of excess antenna temperature at 4080 Mc/s. *Astrophys. J. Lett.* **1965**, *142*, 419–421. [[CrossRef](#)]
43. Shech, E. *Idealizations in Physics*; Cambridge University Press: Cambridge, UK, 2023.
44. Song, J.; Park, J.; Kwon, S.; Chung, B. *Physics Teacher Education Beyond 2000*; Pinto, R., Surinach, S., Eds.; Elsevier: Amsterdam, The Netherlands, 2002.
45. Peebles, P.J.E. Statistical analysis of catalogs of extragalactic objects. I. Theory. *Astrophys. J.* **1973**, *185*, 413–440.
46. Mandal, A.; Nadkarni-Ghosh, S. One-point probability distribution function from spherical collapse: Early dark energy versus Λ CDM. *Mon. Not. R. Astron. Soc.* **2020**, *498*, 355–372. [[CrossRef](#)]
47. Brockhaus, T. *Brockhaus, die Enzyklopädie*, 20th ed.; Brockhaus GmbH: Leipzig, Germany; Mannheim, Germany, 1998.
48. Higgs, P.W. Broken Symmetries, Massless Particles and Gauge Fields. *Phys. Lett.* **1964**, *12*, 132–133. [[CrossRef](#)]
49. Carmesin, H.-O. *Vom Big Bang bis Heute Mit Gravitation: Model for the Dynamics of Space*; Verlag Dr. Köster: Berlin, Germany, 2017.
50. Carmesin, H.-O. *Universe: Unified from Microcosm to Macrocosm*; Carmesin, H.-O., Ed.; Verlag Dr. Köster: Berlin, Germany, 2021; Volume 5, pp. 1–198.
51. Peebles, P.J.E.; Bharat, R. Cosmology with a Time-Variable Cosmological ‘Constant’. *Astrophys. J.* **1988**, *325*, L17–L20. [[CrossRef](#)]
52. Carmesin, H.-O. *Entstehung der Raumzeit durch Quantengravitation—Theory for the Emergence of Space, Dark Matter, Dark Energy and Space-Time*; Verlag Dr. Köster: Berlin, Germany, 2018.
53. Landau, L.; Lifschitz, J. *Course of Theoretical Physics II—The Classical Theory of Fields*, 3rd ed.; Pergamon Press: Oxford, UK, 1971.
54. Heisenberg, W. Über den anschaulichen Inhalt der quantentheoretischen Kinematik und Mechanik. *Z. Phys.* **1927**, *43*, 172–198. [[CrossRef](#)]
55. Bandhi, T.N. A Comprehensive Overview of Atomic clocks and their Applications. *BEMS Rep.* **2023**, *92*, 1–10. [[CrossRef](#)]
56. Formichella, V.; Galleani, L.; Signorile, G.; Sesia, I. *GPS SOLUTIONS*; Springer: Heidelberg, Germany, 2021; p. 423.
57. Olofsson, P.; Andersson, M. *Probability, Statistics, and Stochastic Processes*; Wiley: New York, NY, USA, 2012.
58. Hinkley, N.; Lemke, N. Anatomic clock with 10^{-18} Instability. *Science* **2013**, *341*, 1215–1218. [[CrossRef](#)] [[PubMed](#)]
59. Redlich, O. Intensive and extensive properties. *J. Chem. Educ.* **1970**, *2*, 154. [[CrossRef](#)]
60. Hilbert, D.; Nordheim, L.; Neumann, J.v. Über die Grundlagen der Quantenmechanik. *Math. Ann.* **1928**, *98*, 395–407. [[CrossRef](#)]
61. Sakurai, J.J.; Napolitano, J. *Modern Quantum Mechanics*; Addison-Wesley: New York, NY, USA; London, UK; Delhi, India, 1994.
62. Ballentine, L.E. *Quantum Mechanics*; World Scientific Publishing: London, UK; Singapore, 1998.
63. Blokhintsev, D.I.; Galperin, F.M. Neutrino hypothesis and conservation of energy. *Pod Znam. Marx.* **1934**, *6*, 147–157.
64. Lee, J.M. *Riemannian Manifolds: An Introduction to Curvature*; Springer: New York, NY, USA, 1997.
65. Carmesin, H.-O. *Universe: Unified from Microcosm to Macrocosm*; Carmesin, H.-O., Ed.; Verlag Dr. Köster: Berlin, Germany, 2024; Volume 11, pp. 1–320.
66. Planck, M. On the Theory of the Energy Distribution Law of the Normal Spectrum. *Verhandl. Dtsch. Phys. Ges.* **1900**, *2*, 237–245.
67. Tipler, P.A.; Llewellyn, R.A. *Modern Physics*, 5th ed.; Freeman: New York, NY, USA, 2008.
68. Aspect, A.; Grangier, P.; Roger, G. Experimental Realization of the Einstein-Podolski-Rosen-Bohm Gedankenexperiment: A new Violation of Bell’s Inequalities. *Phys. Rev. Lett.* **1982**, *1*, 91–94. [[CrossRef](#)]
69. Schrödinger, E. Quantisierung als Eigenwertproblem IV. *Ann. Phys.* **1926**, *81*, 109–139. [[CrossRef](#)]

70. Aad, G.; Abajyan, T.; Abbott, B.; Abdallah, J.; Khalek, S.A.; Abdelalim, A.A.; Abdinov, O.; Aben, R.; Abi, B.; Abolins, M.; et al. Observation of a new particle in the search for the Standard Model Higgs boson with the ATLAS detector at the LHC. *Phys. Lett. B* **2012**, *716*, 1. [[CrossRef](#)]
71. Chatrchyan, S.; Khachatryan, V.; Sirunyan, A.M.; Tumasyan, A.; Adam, W.; Aguilo, E.; Bergauer, T.; Dragicevic, M.; Erö, M.; Fabjan, C.; et al. Observation of a new boson at a mass of 125 GeV with the CMS experiment at the LHC. *Phys. Lett. B* **2012**, *716*, 30. [[CrossRef](#)]
72. Carmesin, H.-O. *Universe: Unified from Microcosm to Macrocosm*; Carmesin, H.-O., Ed.; Verlag Dr. Köster: Berlin, Germany, 2022; Volume 8, pp. 1–168.
73. Guericke, O.v. *Experimenta Nova (ut Vocantur) Magdeburgica de Vacuo Spatio*; Jansson a Waesberge: Amsterdam, The Netherlands, 1672.
74. Van der Waals, J.D. *Over de Continuïteit van den gas- en Vloeistofoestand*; Sijthoff: Leiden, The Netherlands, 1873.
75. Landau, L.; Lifschitz, J. *Course of Theoretical Physics V-Statistical Physics I*, 3rd ed.; Pergamon Press: Oxford, UK, 1980
76. Landau, L.; Lifschitz, J. *Course of Theoretical Physics III-Quantum Mechanics*, 2nd ed.; Pergamon Press: Oxford, UK, 1965.
77. Carmesin, H.-O. Students Learn to Derive Universal Properties of Gravitons. *PhyDid B Internet J.* **2024**, *15*, 413–421.
78. Bose, S. Plancks Gesetz und Lichtquantenhypothese. *Z. Phys.* **1924**, *26*, 178–181. [[CrossRef](#)]
79. Stephani, H. *Allgemeine Relativitätstheorie*, 2nd ed.; VEB Deutscher Verlag der Wissenschaften: Berlin, Germany, 1980.
80. Blanchet, L. Post-Newtonian theory for gravitational waves. *Living Rev. Relativ.* **2024**, *27*, 4. [[CrossRef](#)]
81. Yang, Z. The Equations of Motion of the Post-Newtonian Compact Binary Inspirals as Gravitational Radiation Sources Under the Effective Field Theory Formalism. Ph.D. Thesis, University of Pittsburg, Pittsburg, PA, USA, 2014.
82. Condon, J.J.; Mathews, A.M. Λ CDM Cosmology for Astronomers. *Publ. Astron. Soc. Pac.* **2018**, *130*, 073001. [[CrossRef](#)]
83. Moore, T.A. *A General Relativity Workbook*; University Science Books: Mill Valley, CA, USA, 2013.
84. Carmesin, H.-O. *Universe: Unified from Microcosm to Macrocosm*; Carmesin, H.-O., Ed.; Verlag Dr. Köster: Berlin, Germany, 2023; Volume 10, pp. 1–320.
85. Peters, P.C. Where is the energy stored in the gravitational field? *Am. J. Phys.* **1981**, *49*, 564–569. [[CrossRef](#)]
86. Kumar, A. *Fundamentals of Quantum Mechanics*; Cambridge University Press: Cambridge, UK, 2018.
87. Griffiths, D.J. *Introduction to Quantum Mechanics*; Prentice Hall: Upper Saddle River, NJ, USA, 1994.
88. Scheck, F. *Quantum Physics*, 2nd ed.; Springer: Berlin/Heidelberg, Germany; New York, NY, USA; Dordrecht, The Netherlands; London, UK, 2013.
89. Teschl, G. *Mathematical Methods in Quantum Mechanics*, 2nd ed.; American Mathematical Society: Providence, RI, USA, 2014.
90. Carmesin, H.-O. *Universe: Unified from Microcosm to Macrocosm*; Carmesin, H.-O., Ed.; Verlag Dr. Köster: Berlin, Germany, 2022; Volume 7, pp. 1–148.
91. Carmesin, H.-O. Explanation of Quantum Physics by Gravity and Relativity. *PhyDid B Internet J.* **2022**, *13*, 425–438.
92. Carmesin, H.-O. Students Derive an Exact Solution of the Flatness Problem. *PhyDid B Internet J.* **2023**, *14*, 23–30.
93. Kravtsov, A.V.; Borgani, S. Formation of Galaxy Clusters. *Annu. Rev. Astr. Astrophys.* **2012**, *50*, 353–409. [[CrossRef](#)]
94. Haude, S.; Salehi, S.; Vidal, S.; Maturi, M.; Bartelmann, M. Model-independent determination of the cosmic growth factor. *Scipost Astron.* **2022**, *2*, 1–22. [[CrossRef](#)]
95. White, S.D.M.; Efstathiou, G.; Frenk, C.S. The amplitude of mass fluctuations in the universe. *Mon. Not. R. Astron. Soc.* **1993**, *262*, 1023–1028. [[CrossRef](#)]
96. Carmesin, H.-O. Students Learn to Solve the Cosmological Constant Problem. *PhyDid B Internet J.* **2024**, *15*, 341–348.
97. Carmesin, H.-O. Students Analyze the Impact of the H_0 Tension on the Worldview. *PhyDid B Internet J.* **2024**, *15*, 405–412.
98. Karttunen, H.; Kröger, P.; Oja, H.; Poutanen, M.; Donner, K. *Fundamental Astronomy*, 5th ed.; Springer: Berlin, Germany, 2007
99. Carmesin, H.-O.; Emse, A.; Piehler, M.; Pröhl, I.K.; Salzmann, W.; Witte, L. *Universum Physik Sekundarstufe II Niedersachsen Qualifikationsphase*; Cornelsen Verlag: Berlin, Germany, 2020.
100. Cimatti, A.; Moresco, M. Revisiting oldest stars as cosmological probes: New constraints on the Hubble constant. *Astrophys. J.* **2023**, *953*, 149. [[CrossRef](#)]
101. Birrer, S.; Shajib, A.J.; Galan, M.; Million, M.; Treu, T.; Agnello, A.; Auger, M.; Chen, G.C.-F.; Christensen, L.; Collet, T.; et al. TDCOSMO: IV. Hierarchical time-delay cosmography-joint inference of the Hubble constant and galaxy density profiles. *Astr. Astroph.* **2020**, *643*, A165. [[CrossRef](#)]
102. Cao, S.; Ryan, J.; Ratra, B. Cosmological constraints from H II starburst galaxy, quasar angular size, and other measurements. *Mon. Not. R. Astron. Soc.* **2021**, *509*, 4745–4757. [[CrossRef](#)]
103. Philcox, O.H.E.; Ivanov, M.; Mikhail; Simonovic, M.; Zaldarriaga, M. Combining Full-Shape and BAO Analyses of Galaxy Power Spectra: A 1.6% CMB-Independent Constraint on H_0 . *J. Cosmol. Astropart. Phys.* **2020**, *2020*, 1–42. [[CrossRef](#)]
104. Addison, G.E.; Watts, D.J.; Bennett, C.L.; Halperin, M.; Hinshaw, G.; Weiland, J.L. Elucidating Λ CDM: Impact of Baryon Acoustic Oscillation Measurements on the Hubble Constant Discrepancy. *Astrophys. J.* **2018**, *853*, 119. [[CrossRef](#)]

105. Abbott, T.M.C.; Abdalla, F.B.; Alarcon, A.; Aleksić, J.; Allam, S.; Allen, S.; Amara, A.; Annis, J.; Asorey, J.; Avila, S.; et al. Dark Energy Survey Year 1 Results: Cosmological Constraints from Galaxy Clustering and Weak Lensing. *Phys. Rev. D* **2018**, *98*, 043526. [[CrossRef](#)]
106. Escamilla-Rivera, C.; Najera, A. Dynamical Dark Energy Models in the Light of Gravitational-Wave Transient Catalogues. *J. Cosmol. Astropart. Phys.* **2022**, *2022*, 60–85. [[CrossRef](#)]
107. Galbany, L.; de Jaeger, T.; Riess, A.G.; Müller-Bravo, T.E.; Dhawan, S.; Phan, K.; Stritzinger, M.D.; Karamahmetoglu, E.; Leibundgut, B.; Burns, C.; et al. An updated measurement of the Hubble constant from near-infrared observations of type Ia supernovae. *Astr. Astrophys.* **2023**, *679*, A95. [[CrossRef](#)]
108. Uddin, S.A.; Burns, C.R.; Phillips, M.M.; Suntzeff, M.; Freedman, W.L.; Brown, P.J.; Morrell, N.; Hamuy, M.; Krisciunas, K.; Wang, L.; et al. Carnegie Supernova Project I and II: Measurement of H_0 using Cepheid, TRGB and SBF Distance Calibration to Type Ia Supernovae. *Astrophys. J.* **2024**, *970*, 72. [[CrossRef](#)]
109. Pesce, D.W.; Braatz, J.A.; Reid, M.J.; Riess, A.G.; Scolnic, D.; Condon, J.J.; Gao, F.; Henkel, C.; Impellizzeri, C.M.V.; Kuo, C.Y.; et al. The Megamaser Cosmology Project: XIII. Combined Hubble Constant Constraints. *Astrophys. J. Lett.* **2020**, *891*, L1. [[CrossRef](#)]
110. Blakeslee, J.P.; Jensen, J.B.; Ma, C.; Milne, P.A.; Greene, J.E. The Hubble Constant from Infrared Surface Brightness Fluctuation Distances. *Astrophys. J.* **2021**, *911*, 65. [[CrossRef](#)]
111. Cugnon, J. On the Einstein-Podolski-Rosen paradox. *Physics* **1964**, *1*, 195–200.
112. Bell, J. The Casimir Effect and the Vacuum Energy: Duality in the Physical Interpretation. *Few-Body Systems* **2012**, *53*, 181–188.
113. Einstein, A. Can the quantum-mechanical description of physical reality be considered complete? *Phys. Rev.* **1916**, *47*, 777–780. [[CrossRef](#)]
114. Einstein, A. Quanten-Mechanik und Wirklichkeit-Quantum Mechanics and Reality. *Dialectica* **1948**, *2*, 320–324. [[CrossRef](#)]
115. Clauser, J.F.; Horne, M. A Experimental consequences of objective local theories. *Phys. Rev. D* **1974**, *10*, 526–535. [[CrossRef](#)]
116. Zeilinger, A.; Gähler, R.; Shull, G.C.; Treimer, W.; Mampe, W. On the Einstein-Podolski-Rosen paradox. *Rev. Mod. Phys.* **1988**, *60*, 1067–1073. [[CrossRef](#)]
117. Starker, S.; Nau, H.; Hammesfahr, J. The Shuttle Experiment Navex Completed on Spacelab Mission D1. In Proceedings of the Seventeenth Annual Precise Time and Time Interval Applications and Planning Meeting, Washington DC, USA, 29 November–2 December 1985; pp. 405–412.
118. Einstein, A. Über das Relativitätssprinzip und die aus demselben gezogenen Folgerungen. *Jahrb. Radioakt. Und Elektron.* **1907**, *4*, 411–462.
119. Horvath, I.; Bagoly, Z.; Hakkila, J.; Toth, L.V. New data support the existence of the Hercules-Corona Borealis Great Wall. *Astron. Astrophys.* **2015**, *584*, A48. [[CrossRef](#)]
120. Böhringer, H.; Chon, G.; Collins, C.A. Observational evidence for a local underdensity in the Universe and its effect on the measurement of the Hubble constant. *Astron. Astrophys.* **2020**, *633*, A19. [[CrossRef](#)]
121. Tully, B.R.; Courtoise, H.; Hoffmann, Y.; Pomeroy, D. The Laniakea supercluster of galaxies. *Nature* **2014**, *513*, 71–74. [[CrossRef](#)]
122. Einstein, A. Grundlage der allgemeinen Relativitätstheorie. *Ann. Phys.* **1916**, *49*, 769–822. [[CrossRef](#)]
123. Guth, A.H. Inflationary universe: A possible solution to the horizon and flatness problems. *Phys. Rev. D* **1981**, *23*, 347–356. [[CrossRef](#)]

Disclaimer/Publisher’s Note: The statements, opinions and data contained in all publications are solely those of the individual author(s) and contributor(s) and not of MDPI and/or the editor(s). MDPI and/or the editor(s) disclaim responsibility for any injury to people or property resulting from any ideas, methods, instructions or products referred to in the content.